

UCLA

UCLA Electronic Theses and Dissertations

Title

Reelin signaling in the basal ganglia: comparative neuroanatomy and implications for vocal behavior

Permalink

<https://escholarship.org/uc/item/8h15t96g>

Author

Fraley, Elizabeth Ross

Publication Date

2017

Peer reviewed|Thesis/dissertation

UNIVERSITY OF CALIFORNIA

Los Angeles

Reelin signaling in the basal ganglia: comparative neuroanatomy and implications for
vocal behavior

A dissertation submitted in partial satisfaction of the requirements for the degree Doctor
of Philosophy in Molecular, Cellular & Integrative Physiology

by

Elizabeth Ross Fraley

2017

© Copyright by

Elizabeth Ross Fraley

2017

ABSTRACT OF THE DISSERTATION

Reelin signaling in the basal ganglia: comparative neuroanatomy and implications for
vocal behavior

by

Elizabeth Ross Fraley

Doctor of Philosophy in Molecular, Cellular & Integrative Physiology

University of California, 2017

Professor Stephanie Ann White, Chair

Vocal learning is a complex motor activity that relies on the coordination of different brain regions including the basal ganglia. By studying the vocal learning zebra finch, this work has uncovered a novel pathway that is regulated by singing behavior. The Reelin-signaling pathway like the human language transcription factor, FoxP2, is regulated in a basal ganglia region, Area X. The pathway was found to be regulated during the sensorimotor phase of song learning in finches as well as in adults. Injections of recombinant Reelin into Area X during sensorimotor learning showed that Reelin injected pupils to learn their tutors' songs better than controls. These results indicated

that 1) Reelin signaling is important to sensorimotor learning phase of vocal learning 2) Like FoxP2, oscillations of the level of Reelin signaling are likely to subserve vocal learning. This pathway is implicated in the etiology of autism spectrum disorders (ASD), of which social communication deficits are key diagnostic criteria. Mice insufficient or completely lacking Reelin signaling components (*Dab1*, *Apoer2*, and *Vldlr*) exhibited reduced number of vocalizations and abnormal vocalization repertoires. Reelin-secreting cell types and Reelin-sensitive cell types were identified across both mouse and zebra finch species. A common theme was uncovered, whereby Reelin is secreted in the striatum, and *Dab1* is expressed in the pallidum. I therefore hypothesize that Reelin signaling occurs in the basal ganglia in a striato-pallidal manner across different species and may reflect a general mechanism of signaling in the basal ganglia. Some features of Reelin signaling that are unique to the zebra finch Area X were uncovered including: Reelin secretion by calretinin and somatostatin interneurons. Additionally, *Dab1* expression was observed in cholinergic interneurons of Area X. Contrasts between the zebra finch and mouse highlight differences that could be a result of unique qualities of Area X or could reflect differences between vocal learning and non-vocal learning basal ganglia. This work identifies, confirms, and defines the novel involvement of an established pathway, the Reelin-signaling pathway, in vocal behavior of multiple species.

The dissertation of Elizabeth Ross Fraley is approved.

Patricia E. Phelps

Arthur P. Arnold

William X. Yang

Stephanie Ann White, Committee Chair

University of California, Los Angeles

2017

Dedicated to my grandfather, Dr. Harlan Douglas, who has always supported and inspired my academic endeavors.

Table of Contents

Chapter 1: Introduction.....	1
Birdsong as a model for human speech and language.....	2
Critical periods for vocal learning.....	2
Neurocircuitry underlying vocal learning.....	4
Neuromolecular mechanisms underlying vocal learning.....	5
FoxP2 in zebra finches.....	7
Targets of FoxP2.....	8
Reelin-signaling and the basal ganglia.....	9
Reelin-signaling and communication deficits	10
Reelin-signaling in songbirds.....	11
Figures.....	13
References.....	20
Chapter 2: Insights from a Nonvocal Learner on Social Communication.....	27
References.....	34
Chapter 3: Mice with <i>Dab1</i> or <i>Vldlr</i> insufficiency exhibit abnormal neonatal	
 vocalization patterns	35
Abstract.....	36
Introduction.....	37
Methods.....	42
Results.....	46
Discussion.....	53
Figures.....	58

References.....	69
Chapter 4: Reelin signaling in the basal ganglia: Comparative neuroanatomy and implications for vocal behavior.....	75
Abstract.....	76
Introduction.....	77
Methods.....	81
Results.....	86
Discussion.....	95
Figures	100
References.....	124
Chapter 5: Conclusion.....	130
References.....	141
Appendix: Molecular microcircuitry underlies functional specification in a basal ganglia circuit dedicated to vocal learning.....	144
Statement of contribution.....	145
Abstract.....	146
Introduction.....	147
Experimental procedures.....	150
Results.....	156
Discussion.....	175
Figures.....	178
References.....	194

List of Tables

4-1. Area X cell types and markers.....	108
4-2. Primary antibodies	109

List of Figures

Figure 1-1: Evolutionary timelines and emergences of vocal learning.....	13
Figure 1-2: Critical periods for various songbird species including: Sparrows, Zebra finches, and Canaries.....	14
Figure 1-3: Developmental timeline for critical periods in language learning.....	15
Figure 1-4: Comparative neuroanatomy of circuits underlying vocalization.....	16
Figure 1-5: Singing and social context regulates FoxP2 levels in Area X.	17
Figure 1-6: Network analysis revealed that <i>FoxP2</i> and <i>Vldlr</i> had high topological overlap.....	18
Figure 1-7: Reelin-signaling regulates multiple pathways.....	19
Figure 3-1: <i>Dab1</i> genotype and postnatal age affect pup isolation call amounts.....	58
Figure 3-2: <i>Dab1</i> genotype affects P7 call repertoire.....	59
Figure 3-3: <i>Dab1</i> genotype does not affect P14 call repertoire.....	61
Figure 3-4: <i>Vldlr</i> and <i>Vldlr/Apoer2</i> insufficient pups have altered developmental trajectories in calling amount.....	62
Figure 3-5: P7 call repertoire is influenced by <i>Vldlr/Apoer2</i> genotype.....	64
Figure 3-6: P14 call repertoire is influenced by <i>Vldlr/Apoer2</i> genotype.....	65
Figure 3-7: <i>Dab1</i> and <i>Vldlr/Apoer2</i> pups exhibit a gene-dose dependent increase in repertoire correlation at P7.....	66

Figure 3-8: *Dab1*^{+/*lacZ*} and *Vldlr*^{-/-}/*Apoer2*^{+/+} pups have high syntax similarity scores.....68

Figure 4-1: Behavioral regulation of Reelin-signaling is specific to males and to song
nucleus Area X in juvenile zebra finches.....100

Figure 4-2: Reelin supplementation acutely enhances song learning.....102

Figure 4-3: Reelin and Dab1 expression and distribution in the basal ganglia of mouse
and zebra finch.....104

Figure 4-4: Reelin and Darpp-32 co-expression patterns in mouse and zebra finch basal
ganglia.....107

Figure 4-5: Reelin and FoxP2 co-expression patterns in mouse and zebra finch basal
ganglia.....109

Figure 4-6: Reelin is expressed in two populations of interneurons in zebra finch
Area X.....111

Figure 4-7: Dab1 and Nkx2.1 co-localize in zebra finch Area X but not in mouse globus
pallidus.....113

Figure 4-8: Dab1 is expressed in cholinergic cells in zebra finch Area X but not in
mouse.....115

Figure 4-9: Both cholinergic and indirect pallidal-like neurons express Dab1 in zebra
finch Area X.....117

Figure 4-10: Dab1 and Lant6 co-localize in pallidal cells of both mouse zebra finch
Area X.....118

Figure 4-S1: Apoer2 immunostaining across species.....120

Figure 4-S2: Some but not all Nkx2.1 expressing cells are cholinergic in Area X.....122

Figure 4-S3: Doublecortin and Dab1 co-stain cells in zebra finch.....123

Figure 5-1: Cell types expressing Reelin and Dab1 in the zebra finch Area X.....139

Figure 5-2: Cell types expressing Reelin and Dab1 in the mouse basal ganglia.....140

Figure A-1: Neuroanatomical overview.....178

Figure A-2: Song patterns that emerged from the behavioral paradigm.....180

Figure A-3: Relationships between network modules and behavioral traits.....181

Figure A-4: Module membership predicts relationship to singing in area X.....183

Figure A-5: Gene co-expression levels, rather than individual expression levels,
distinguish area X song modules.....185

Figure A-6: Behavioral regulation of gene expression coupled with WGCNA captures
genes co-regulated with FOXP2.....186

Figure A-7: Application of WGCNA to identify novel pathways in learned
vocalization189

Figure A-8: Behavioral regulation of hub genes and pathways in area X.....191

Acknowledgements

Thank you to my advisor, Dr. Stephanie White for her support and guidance. Also thanks to my committee members Drs. Phelps, Yang, and Arnold for their contributions toward the success of this dissertation.

Chapter 2 is a version of a review article that appeared in the Journal of Neuroscience: Day N.F. & Fraley E.R. The authors thank Stephanie White for her helpful discussion.

Chapter 3 is a version of a manuscript published in Scientific Reports: Fraley, E.R., Burkett, Z.B., Day, N.F, Schwartz, B.A., Phelps, P.E., White, S.A. The authors thank Ava DeLu for help in processing USVs, and Aly Mulji for assistance with mouse breeding and care. This work was supported by the NIH T32 HD07228 (ERF), NIH R01 MH070712 (SAW), NSF IOB-0924143 (PEP).

Chapter 4 is a version of a manuscript currently being edited for submission. Fraley, E.R., Gu, Y., DeLu, A, Phelps, P.E., White, S.A. The authors thank Zack Burkett and Nancy Day for critical feedback on song and statistical analyses.

The **Appendix** is a version of a manuscript published in Neuron. Hilliard, A.T., Miller, J.E., Fraley, E.R., Horvath, S, White, S.A. The authors thank Peter Langfelder and Michael Oldham for advice on microarray pre-processing and network analysis, Jason Howard and Erich Jarvis for the arrays through a partnership with Agilent Technologies, Patty Phelps, Sarah Bottjer and Erica Sloan for material support, Felix Schweizer and

Grace Xiao for statistical advice, and 4 anonymous reviewers for insightful commentary.
Supported by NIH grants F31 MH082533 (ATH) and R01 MH070712 (SAW).

The work presented in this dissertation was supported by the Laboratory of
Neuroendocrinology Training Grant NIH T32 HD07228 (ERF), NSF IOB-0924143
(PEP), and NIH R01 MH070712 (SAW).

VITA

- 2008
B.S. Biology, Psychology
Virginia Commonwealth University
Richmond, Virginia
- 2008
Teaching Assistant
“Biology of the Seed Plant”
Dr. Wan-Ching Liu
Virginia Commonwealth University
Richmond, Virginia
- 2007-2009
Laboratory Technician
Laboratory of Wan-Ching Liu
Virginia Commonwealth University
Richmond, Virginia
- 2013-2016
Laboratory of Neuroendocrinology Fellowship
University of California, Los Angeles
- 2014- 2015
Teaching Assistant
“Neuroethology”
Drs. Stephanie White, Peter Narins, Walter Metzner
University of California, Los Angeles

Publications and Presentations

- Khamar, H.J. et al., 2010. Multiple roles of soluble sugars in the establishment of Gunnera-Nostoc endosymbiosis. *Plant physiology*, 154(3), pp.1381–1389.
- Hilliard, A.T. et al., 2012. Molecular microcircuitry underlies functional specification in a basal ganglia circuit dedicated to vocal learning. *Neuron*, 73(3), pp.537–552.
- Day, N.F. & Fraley, E.R., 2013. Insights from a nonvocal learner on social communication. *The Journal of neuroscience : the official journal of the Society for Neuroscience*, 33(31), pp.12553–12554.
- Fraley, E.R. et al., 2016. Mice with Dab1 or Vldlr insufficiency exhibit abnormal neonatal vocalization patterns. *Scientific reports*, 6, p.25807.

Chapter 1: Introduction

Birdsong as a model for human speech and language

For centuries, humans have been fascinated with the ability of songbirds to imitate sounds. The modern neurobiological study of songbirds has revealed that, in fact, similar brain mechanisms underlie both speech and song learning (Doupe & Kuhl 1999; Bolhuis et al. 2010). Vocal learning is a process whereby sounds that are heard can be imitated. Vocal learning is distinct from language learning, which is more complex and unique to humans. Parallels between language and song learning include; 1) a reliance on developmentally sensitive periods for learning (critical periods), 2) similar neurocircuitry 3) similar neurogenetic mechanisms including a dependency on the FoxP2 transcription factor, 4) a reliance on hearing, 5) occur spontaneously as part of the organisms' species-specific behavior. I will discuss the first three parallels in further detail below. Vocal learning is observed in three clades of birds: hummingbirds, songbirds, and parrots; as well as in bats, elephants, whales, dolphins, and humans (Jarvis 2004). This indicates that vocal learning evolved independently multiple times. Similarities between evolutionarily distant species would thus reflect robust mechanisms essential for vocal learning.

Critical periods for vocal learning

In songbirds, sensory acquisition is the encoding of the auditory information of the tutor song template. Exposure to a tutor during this phase is critical, and failure to be exposed to a tutor during the critical period can result in poor song quality (Marler 1997). The sensorimotor phase of learning is when actual motor practice begins and birds, much like babies learning to talk, babble and produce what is known as subsong

(Johnson et al. 2002; Aronov et al. 2008). This is when the pupil explores vocal motor space and learns to coordinate movements in order to replicate sounds of the tutor. Interestingly, the ability to incorporate variability is essential to many different types of motor learning, including vocal learning (Graybiel 2005).

After a period of sensorimotor exploration and practice, certain songbirds such as the zebra finch species studied here, converge on their mature song, a process referred to as crystallization. There are many different species of songbirds (~5,000), and many different learning paradigms (Brainard & Doupe 2002). Some songbird species, such as the canary, are open-ended learners. These birds can continue learning new songs throughout their lives because they cycle through sensorimotor and sensory acquisition phases with the changing of seasons (Nottebohm et al. 1986). These changes are critically reliant on hormonal factors (Arnold 1992; Nottebohm 1981). Other species, like the white-crowned sparrow, have a wide separation between the sensory acquisition and sensorimotor phases of learning. This means that a young bird can hear its father's song during the summer, then in fall, migrate to a different territory where it only enters sensorimotor learning and begins to practice its song in spring, referencing a template that was learned two seasons before. The zebra finch has a sensory acquisition phase that begins at ~20d and continues until ~65d. The sensorimotor phase begins ~35d and continues until ~90d when song becomes stereotyped and crystallized. Here, the sensory acquisition and sensorimotor phases partially overlap. Critical periods also underlie human speech, and early exposure to language is essential (Figure 3; Kuhl 2004). In some cases of isolation or extreme neglect, lack of exposure to language

(~before 2 years of age) resulted in aphasias (Windsor et al. 2011; Windsor et al. 2013). Thus, both song learning and language learning share a reliance on critical periods.

Neurocircuitry underlying vocal learning

Similar neurocircuitry underlies language and oscine song learning. Both are types of motor learning that rely on the basal ganglia for the integration and coordination of movement. In the songbird, as with mammalian motor learning, there is a homologous organizational feedback loop that consists of the cortex, striatum, and thalamus (Figure 4; Vates et al. 1997; Bottjer & Johnson 1997; Arriaga et al. 2012). In the songbird, specific areas of the brain have evolved to support the function of singing and are known as the song control nuclei (Nottebohm et al. 1976). Song control nuclei represent a privileged network in the songbird brain dedicated solely to the process of song learning and maintenance (anterior forebrain pathway, AFP) or acquisition, production and performance (posterior descending pathway, PDP). The AFP is made up of a subset of neurons within the cortical nucleus known as HVC that project to the cortical nucleus lateral magnocellular nucleus of the nidopallium (LMAN), the striato-pallidal nucleus Area X, and the dorsolateral thalamus (DLM) (Figure 4, white arrows). The PDP consists of a separate set of neurons in HVC that send their projections to the robust nucleus of the arcopallium (RA) which synapses directly onto motor neurons in the XII cranial nerve which innervates the syrinx (Figure 4, red arrows). The HVC is simultaneously upstream of both the AFP and PDP, and integrates auditory and motor activities (McCasland & Konishi 1981). Based on genetic expression profiles and functional studies, HVC has been identified as homologous to Wernicke's and Broca's

areas in the human brain; RA was identified as homologous to precentral gyrus and central sulcus of the motor cortex (Pfenning et al. 2014; Long & Fee 2008; Long et al. 2016). HVC and Broca's area share a function essential for timing and sequencing of voiced elements. RA and the central sulcus/precentral gyrus of the motor cortex are important for articulation (Long & Fee 2008; Long et al. 2016). Genetic parallels underlie homologies between many of the other song nuclei and human brain regions involved in language as well. Area X has been identified as highly homologous to human anterior striatum (Pfenning et al. 2014).

Neuromolecular mechanisms underlying vocal learning

Both birdsong and human language rely on the function of FoxP2/FOXP2 in the basal ganglia (Scharff & White 2004). FOXP2 is a transcriptional factor essential for human speech and language (Lai et al. 2001). Study of the KE family revealed that a point mutation, resulting in the substitution of an arginine to histidine in the DNA binding domain of *FOXP2*, disrupted function and resulted in verbal dyspraxia (Lai et al. 2001; Alcock et al. 2000; Vargha-Khadem et al. 1995). Affected members of the KE family also have problems with language comprehension, word inflection, and exhibited syntactical errors (Watkins, Dronkers, et al. 2002; Vargha-Khadem et al. 1995). Affected members have non-verbal IQs that are within the normal population range, signifying that the deficits are specific to verbal skills. Interestingly, functional and structural analysis of the brains of KE affected members highlighted changes in the basal ganglia (Liégeois et al. 2003; Watkins, Vargha-Khadem, et al. 2002; Belton et al. 2003; Vargha-Khadem et al. 1998). Voxel based morphometry revealed that the grey matter of the

caudate nucleus (a subdivision of human striatum) was reduced significantly in affected KE family members; size of the caudate nucleus was also highly correlated with verbal praxia scores (Watkins, Dronkers, et al. 2002). Functional magnetic resonance imaging (fMRI) showed that affected KE family members had under-activation of the putamen region during speech tasks (subdivision of the human striatum) (Liégeois et al. 2003). Therefore, multiple lines of evidence highlighted the striatum as affected by the KE mutation. Because FOXP2 is a transcription factor, elucidation of transcriptional targets in human brain was essential to understanding its function (Vernes et al. 2007; Spiteri et al. 2007). Human targets relevant to our research laboratory's work include the autism risk gene *CNTNAP2* and the Reelin receptor *VLDLR*.

Further studies in the mouse have uncovered more about the function of *Foxp2* in the basal ganglia. Mice heterozygous for a point mutation of *Foxp2* like that of KE family (*Foxp2-R552H*) exhibited cortico-striatal synaptic abnormalities (decrease in long term depression, LTD) and motor learning deficits (Groszer et al. 2008; French et al. 2012). Genetic substitutions to create a “humanized” version of *Foxp2* (T303N, N325S) resulted in increased plasticity at the cortico-striatal synapse (increase in LTD) and an increase in the number of dendrites in the medium spiny neurons (Enard et al. 2009). Insertion of the humanized *Foxp2* version in mice also resulted in enhanced motor learning (Schreiweis et al. 2014). These findings suggest *Foxp2* in the basal ganglia regulates striatal plasticity, dendritic morphology, and plays an important role in motor learning.

Insertion of humanized *Foxp2* did not alter mouse vocalizations significantly (Hammerschmidt et al. 2015; Enard et al. 2009). Mice with a heterozygous KE-like

mutation (*Foxp2-R552H*) had subtle vocal changes in adult male vocalization patterns but not in acoustic parameters (Chabout et al. 2016). These mice exhibited shorter vocalization bouts, and lacked more complex syntactical structures in their ultra-sonic vocalizations (USVs). Mice however, are not vocal learners (Kikusui et al. 2011; Mahrt et al. 2013). *Foxp2* may not influence the vocal ability of mice because of inherent differences to the neurocircuitry underlying vocalization (Arriaga et al. 2012). Thus, to further probe the role *Foxp2* has in learned vocalizations, one must look to a vocal learning model such as the zebra finch.

FoxP2 in zebra finches

FoxP2 mRNA sequence in zebra finches is 98% identical to that of mouse and human forms (Haesler et al. 2004). The expression pattern of *FoxP2* in zebra finch is strikingly similar to that of the developing human brain (Teramitsu et al. 2004). Since both human and mouse studies focused on how *FOXP2*/*Foxp2* influences basal ganglia, a locus of interest in studying *FoxP2* function in zebra finches has been the striato-pallidal nucleus Area X. Area X function is essential for song learning (Scharff & Nottebohm 1991; Sohrabji et al. 1990). *FoxP2* is expressed throughout the zebra finch basal ganglia; levels in Area X of canary appear to qualitatively increase preceding an increase in vocal variability as part of the sensorimotor phase of learning (Haesler et al. 2004). Data from our lab showed that *FoxP2* levels in Area X were regulated by singing behavior in adults (Figure 5; Teramitsu & White 2006)). *FoxP2* was observed to be higher during vocal motor practice (undirected singing, UD) when compared to a period of non-singing (NS) or female-directed singing (FD). Vocal variability is higher in periods of UD, further suggesting a relationship between vocal motor variability and *FoxP2*.

Similarly, juvenile finches were found to regulate *FoxP2* levels in Area X by UD singing (Miller et al. 2008; Teramitsu et al. 2010). Knock-down or overexpression of *FoxP2* during song learning results in poor song quality (Haesler et al. 2007; Heston & White 2015). Knock-down of *FoxP2* in Area X resulted in aberrant dendritic spine morphology of the medium spiny neurons, reminiscent of results in the murine striatum (Schulz et al. 2010). These findings suggest that in Area X, the behavior-linked oscillations of *FoxP2* levels are critical for regulating variability thereby impacting vocal motor learning.

Targets of FoxP2

In order to understand the broad effects that *FoxP2* has on genetic expression, I focused my work on behaviorally regulated gene networks within Area X (Appendix A; Hilliard et al. 2012). Network analyses revealed that many genes were regulated by singing (~2000 genes), including many putative *FoxP2* targets. To validate the network analyses, biological confirmation was essential and prompted this exploration into the role of Reelin-signaling pathway in vocalization. Very-low density lipoprotein receptor, *Vldlr* was identified as behaviorally regulated in Area X; transcriptional network analyses revealed that *Vldlr* had co-expression patterns highly interconnected with that of *FoxP2* (Figure 6; Hilliard et al. 2012). *VLDLR* is a *FOXP2* transcriptional target in human (Vernes et al. 2007) and in zebra finch brain (Adam et al. 2016). *FoxP2* acts to transcriptionally enhance *Vldlr* expression. Therefore, a functional relationship between the Reelin-signaling pathway and *FoxP2* appears across both human and zebra finch.

Reelin-signaling and the basal ganglia

Reelin is a large secreted glycoprotein famous for its role in coordinating neuronal migration during development (D'Arcangelo et al. 1995). *Reeler* mutants, mice lacking Reelin expression (*Reln*^{-/-}) were generated from a spontaneous mutation (Falconer 1951). These mice had striking phenotypes including severe ataxia or a “reeling” gait. Examination of their brains showed that they had inverted cerebral cortical layers, a disorganized hippocampal formation and a rudimentary cerebellum. Reelin signals through two receptors Vldlr, and apolipoprotein receptor 2 (Apoer2) (Trommsdorff et al. 1999). Reelin binding facilitates phosphorylation of Dab1 by Src-family kinases which then relay the signal to numerous downstream targets (Figure 7; Hiesberger et al. 1999; Bock & Herz 2003; Herz & Chen 2006). Reelin-signaling has roles in learning and memory, and can modulate plasticity and dendritic morphology in the hippocampus (Rogers & Weeber 2008; Qiu et al. 2006; Qiu & Weeber 2007; Beffert et al. 2005). Maturation of the NMDAR subunit composition is also influenced by Reelin (Chen et al. 2005). Because the basal ganglia are not laminated structures, many Reelin-signaling investigations have largely ignored this brain region.

An interesting finding in *reeler* mice shows that these mice have abnormal cortico-striatal plasticity (Marrone et al. 2006). *Reeler* mice have a cortico-striatal synapse that is hyperexcitable, possibly adding to their motor coordination difficulties. Additional studies have investigated the role Reelin plays in the development of the basal ganglia. When the rat striatum is developing, there is transient concentrated expression of Reelin in a patchwork of small developing striosomes (Nishikawa et al. 1999). In mice, development of the substantia nigra is dependent on Reelin (Nishikawa et

al. 2003). In *reeler* mice, dopaminergic neurons of the substantia nigra exhibit migrational deficits, they fail to migrate out of the ventral tegmental area (VTA). However, these neurons still form appropriate axonal connections with their target cells in the striatum. Reelin is expressed in the striatum and is able to reach targets in the VTA; so this work provides evidence that trans-axonal delivery of Reelin-signal is possible (Lein et al. 2007; Niskikawa et al. 2003).

Further investigation into cell types involved in Reelin-signaling in the mouse striatum have revealed that in adults, Reelin was secreted by calbindin-28-positive cells, and Dab1 was localized to a non-specified type of GABA-ergic cells (Sharaf et al. 2015). Vldlr signal was reported only in oligodendrocytes, and Apoer2 is not expressed at all in the murine striatum. Surprisingly, there was a brief time point during development (P15) when expression of Dab1 and Apoer2 was reported to be high in a population of GAD-67 cells (GABAergic), of the striatum (Sharaf et al. 2015). This could indicate that Reelin-signaling in the basal ganglia at P15 serves a different function than in the mature brain.

Reelin-signaling and communication deficits

Autism spectrum disorders (ASD) are diagnosed on the criteria of 1) repetitive behaviors or restricted interests 2) social and/or communication deficits. Lowered Reelin expression is observed in patients with autism (Fatemi et al. 2002; Fatemi et al. 2005). Additionally, epigenetic mechanisms whereby Reelin is downregulated are associated with ASD (Lintas et al. 2016; Zhubi et al. 2014). Single nucleotide polymorphism (SNP) linkage studies have had mixed results (Lammert & Howell 2016). Studies of murine

behavior with reduced or no Reelin-signaling have revealed ASD-like communicative phenotypes including: reduced pup ultrasonic vocalization (USV) and abnormal vocal repertoires (Chapter 3; Ognibene et al. 2007; Laviola et al. 2009; Mullen et al. 2013). This is in line with what has been reported for other genetic mouse models of autism, where reduced number of vocalizations and simplification of repertoire are observed (Takahashi et al. 2015; Ey et al. 2011; Scattoni et al. 2008; Young et al. 2010; Burkett et al. 2015). The work presented here emphasizes a link between unlearned vocal communication and Reelin-signaling. While informative, this does not help us to understand mechanisms unique to vocal learning. Thus, I return focus to Reelin-signaling in the songbird.

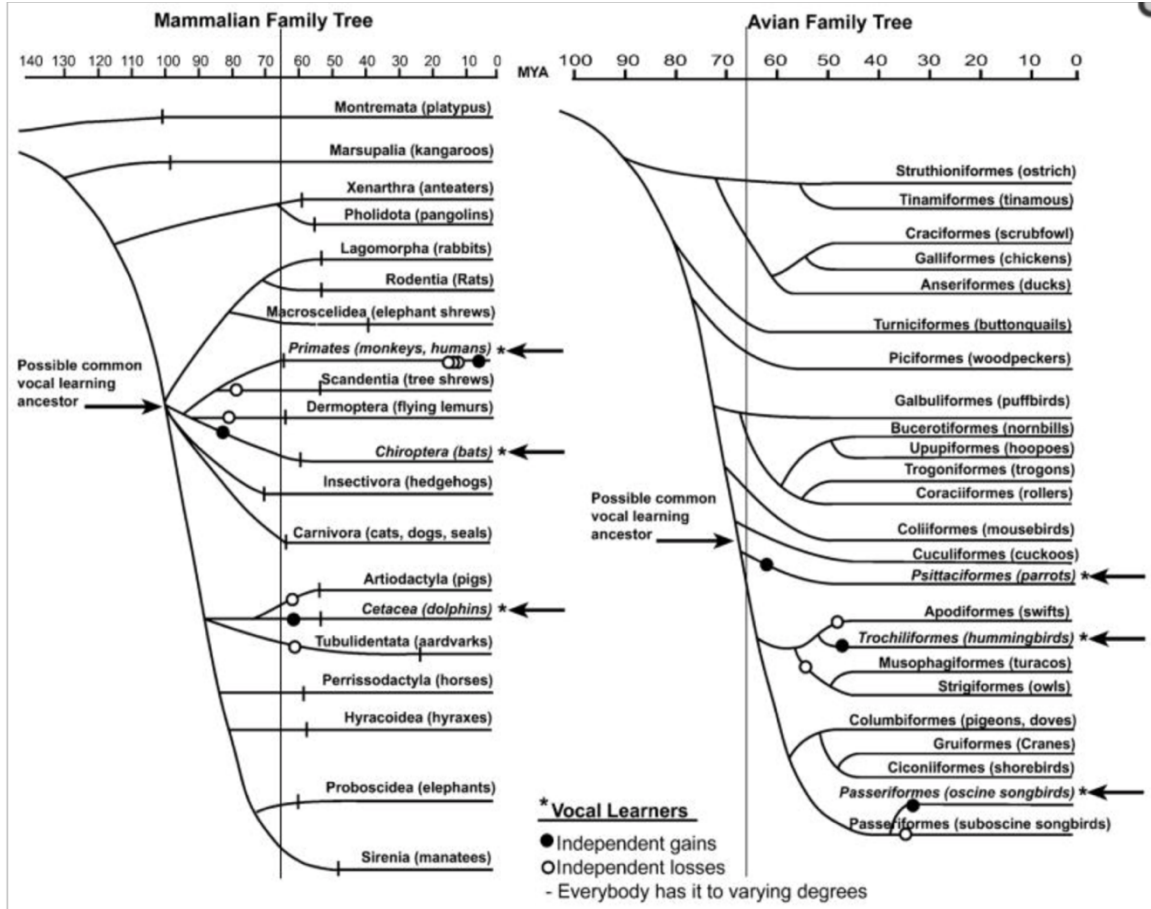
Reelin-signaling in songbirds

A previous report in canary provided information on mRNA expression of Reelin-signaling components across all song control nuclei (Balthazart et al. 2008). *Reelin* mRNA and Reelin immunoreactive cells were found to be concentrated in Area X. Other song control nuclei did not show the same high level of expression, including HVC, which is puzzling considering both nuclei exhibit neurogenesis in adulthood (Alvarez-Buylla & Kirn 1997). *Vldlr*, *Apoer*, and *Dab1* were also expressed in Area X of canary. In the zebra finch, another study examined the identity of *Vldlr* and *Dab1* expressing cells (Adam et al. 2016). The authors found that a subset of medium spiny neurons co-stained for *Vldlr*, *Dab1*, and *FoxP2*. Another subset of medium spiny neurons only stained for *FoxP2* and *Vldlr* but lacked *Dab1*; and another unidentified cell type co-stained for *Vldlr* and *Dab1* lacked *FoxP2*. Thus, there appears to be substantial

heterogeneity of cells in Area X with respect to Reelin-signaling. This is not surprising considering that Area X has both striatal and pallidal characteristics and contains multiple interneuron species (Person et al. 2008; Carrillo & Doupe 2004; Goldberg & Fee 2010; Farries et al. 2005). It was thus important to clearly identify the signal sender (Reelin – secreting) and signal receiver (Dab1 – containing) cell populations.

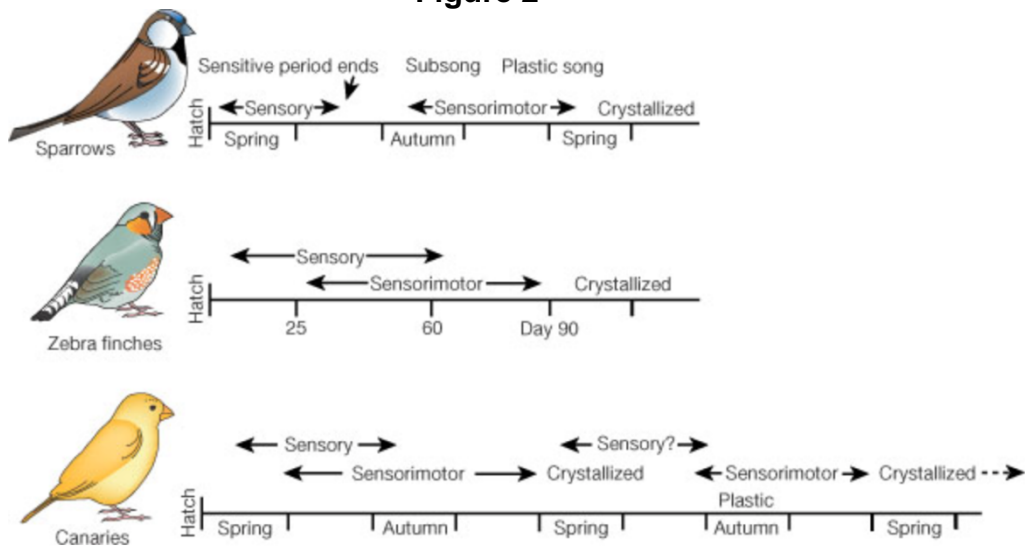
Determination of these cellular phenotypes is essential to hypothesize the function of behavioral regulation in the songbird basal ganglia (Chapter 4). Further comparison with murine basal ganglia cell types could delineate unique vocal learning mechanisms.

Figure 1



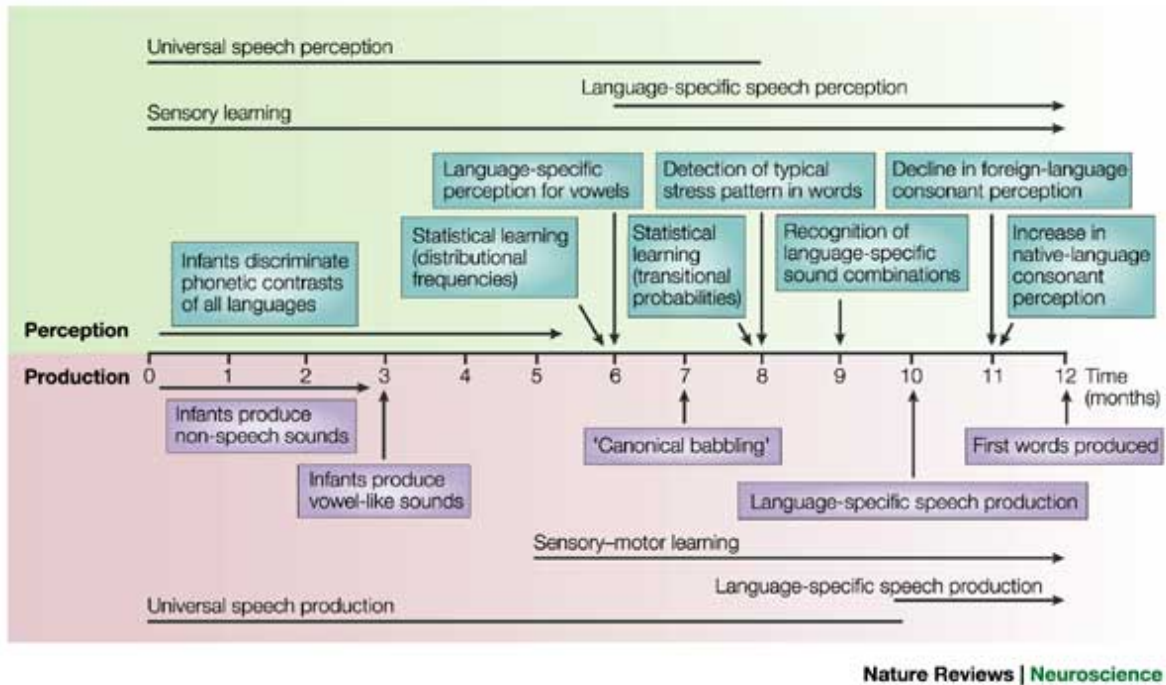
Evolutionary timelines and emergences of vocal learning. Adapted from (Jarvis 2004). Arrows indicate species capable of vocal learning. Filled circle indicate independent gain of function, and empty circles indicate loss of function. Top scaling indicates millions of years ago (MYA).

Figure 2



Critical periods for various songbird species including: Sparrows, Zebra finches, and Canaries. Adapted from (Brainard & Doupe 2002). Critical periods for sensory acquisition and sensorimotor learning leading to crystallization are illustrated for the different songbird species. Scaling is in days.

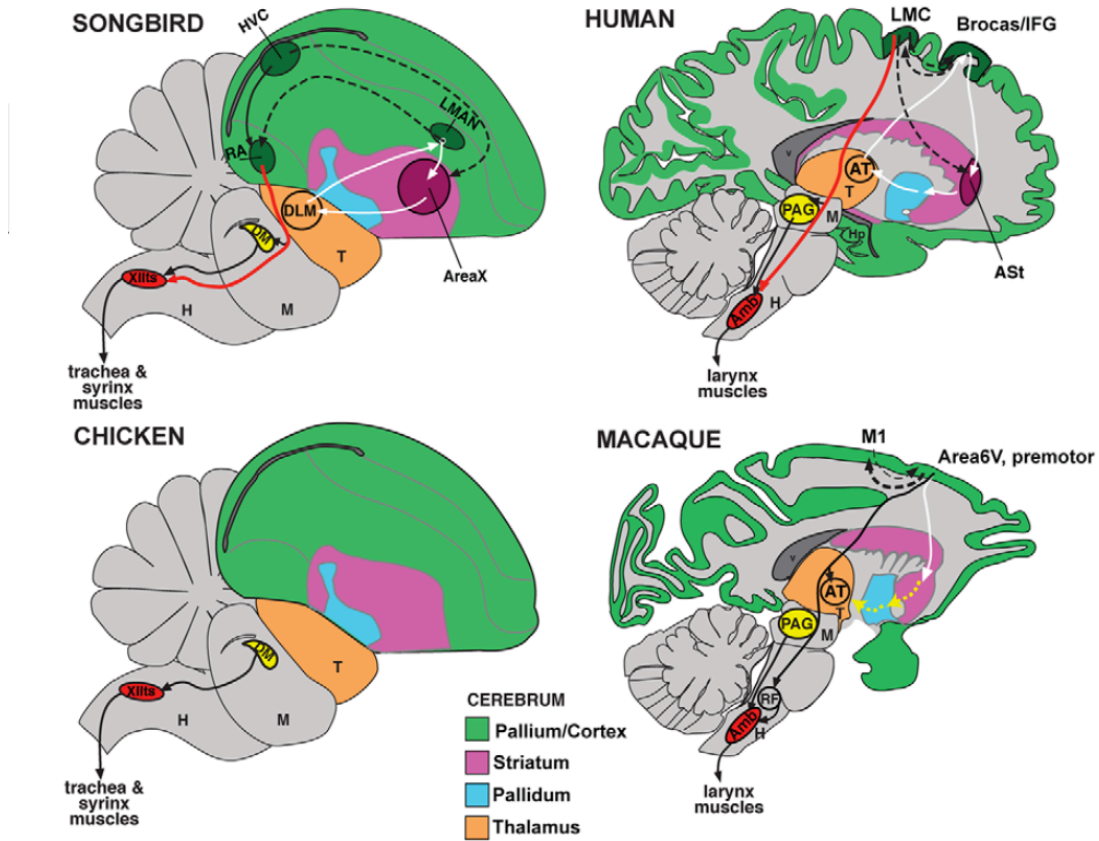
Figure 3



Nature Reviews | Neuroscience

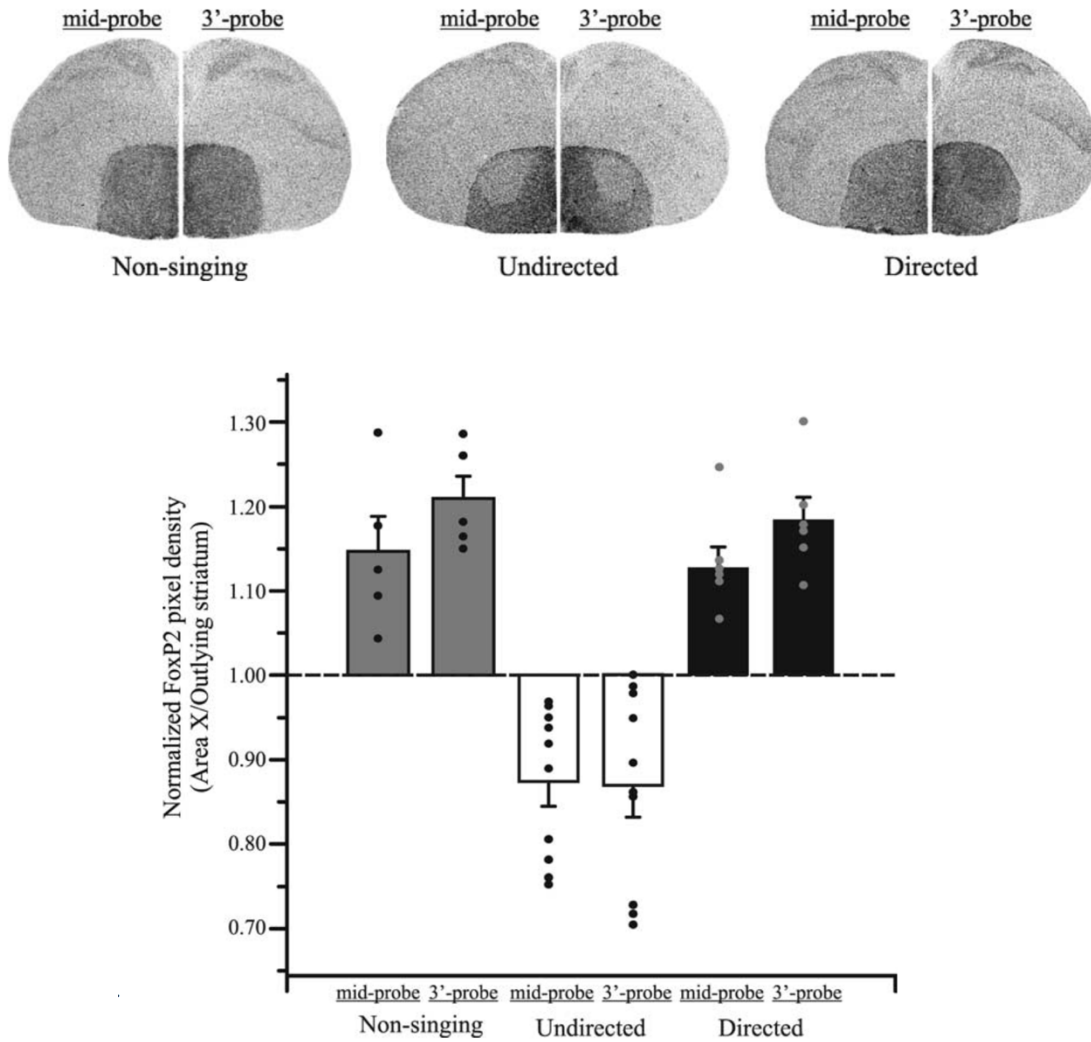
Developmental timeline for critical periods in language learning. Adapted from (Kuhl 2004). Critical periods for sensory acquisition and sensorimotor are defined. Scaling is in months.

Figure 4



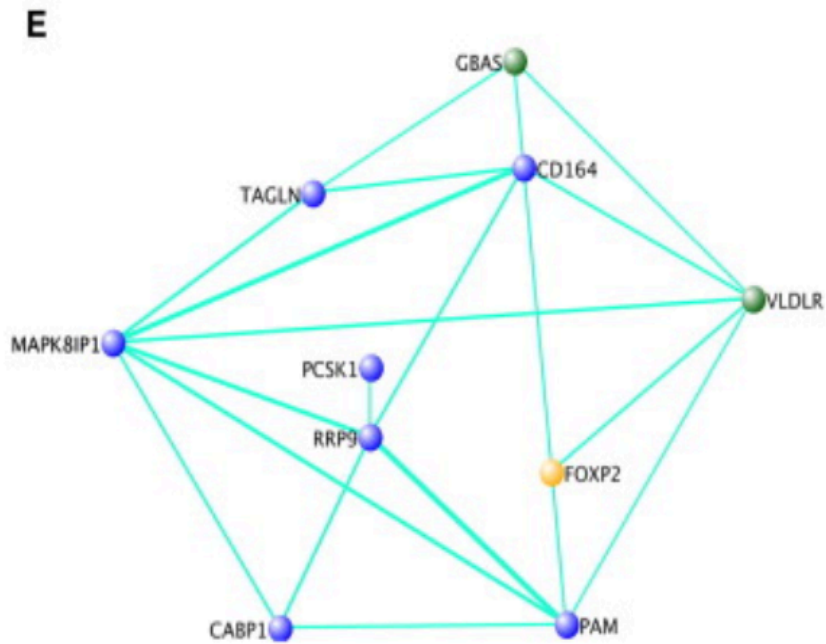
Comparative neuroanatomy of circuits underlying vocalization. Adapted from (Arriaga et al. 2012). Sagittal sections through the brains of different species including the vocal learning human and songbird, and the non-vocal learning macaque and chicken. Colors indicate brain region.

Figure 5



Singing and social context regulates FoxP2 levels in Area X. Adapted from (Teramitsu & White 2006). Adult songbirds' in situ hybridization for *FoxP2* shown in coronal section. High levels of *FoxP2* are observed when the bird is quiet, or singing directed song, but not while practicing undirected song. Below: quantification of mRNA *insitu* results.

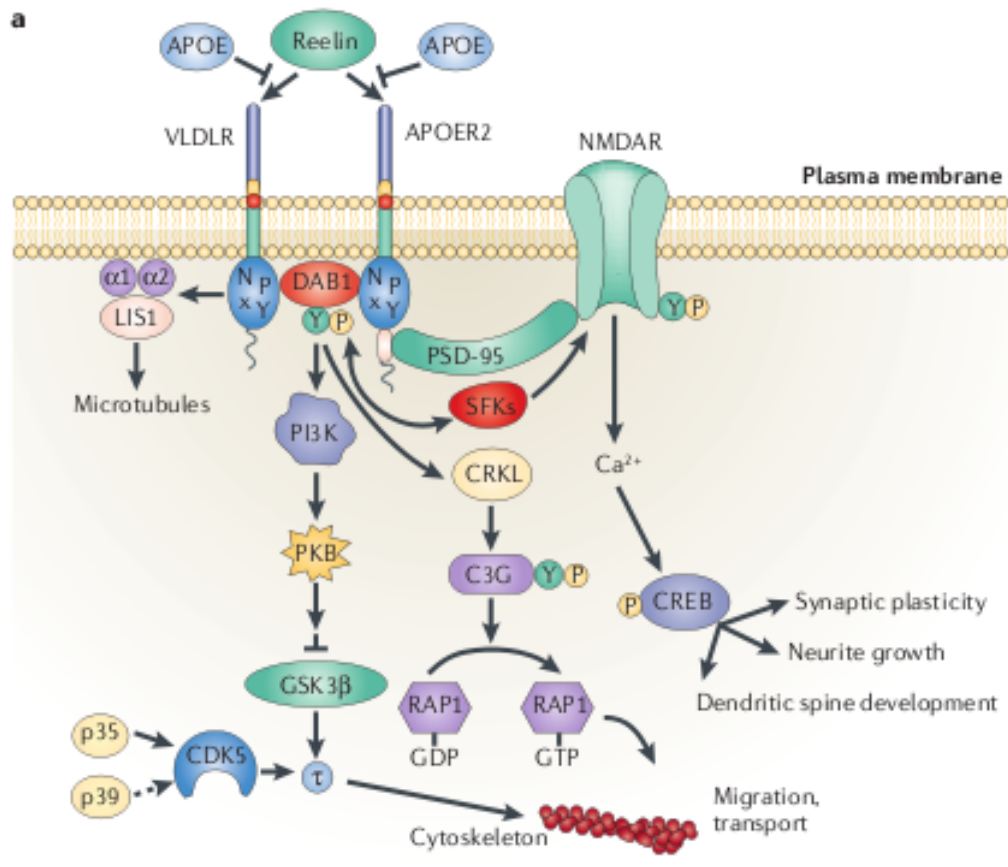
Figure 6



Network analysis revealed that FoxP2 and Vldlr had high topological overlap.

Adapted from (Hilliard et al. 2012). Weighted gene co-expression network analysis revealed networks of genes regulated by singing. FoxP2 and Vldlr had high topological overlap, and were among the genes that were regulated in human brain(Vernes et al. 2007). This predicted a functional connection that was later confirmed.

Figure 7



Reelin-signaling regulates multiple pathways. Adapted from (Herz & Chen 2006).

Reelin signals through either Vldlr or Apoer2 to initiate Dab1 phosphorylation and activate downstream targets. PSD-95 mediated enhancement of NMDA synaptic plasticity only occurs when Apoer2 is present (Rogers & Weeber 2008).

References

- Adam, I. et al., 2016. FoxP2 directly regulates the reelin receptor VLDLR developmentally and by singing. *Molecular and cellular neurosciences*.
- Alcock, K.J. et al., 2000. Oral dyspraxia in inherited speech and language impairment and acquired dysphasia. *Brain and language*, 75(1), pp.17–33.
- Alvarez-Buylla, A. & Kirn, J.R., 1997. Birth, migration, incorporation, and death of vocal control neurons in adult songbirds. *Journal of neurobiology*, 33(5), pp.585–601.
- Arnold, A.P., 1992. Developmental plasticity in neural circuits controlling birdsong: sexual differentiation and the neural basis of learning. *Journal of neurobiology*, 23(10), pp.1506–1528.
- Aronov, D., Andalman, A.S. & Fee, M.S., 2008. A specialized forebrain circuit for vocal babbling in the juvenile songbird. *Science (New York, N.Y.)*, 320(5876), pp.630–634.
- Arriaga, G., Zhou, E.P. & Jarvis, E.D., 2012. Of mice, birds, and men: the mouse ultrasonic song system has some features similar to humans and song-learning birds. C. R. Larson, ed. *PloS one*, 7(10), p.e46610.
- Balthazart, J. et al., 2008. Expression of reelin, its receptors and its intracellular signaling protein, Disabled1 in the canary brain: relationships with the song control system. *Neuroscience*, 153(4), pp.944–962.
- Beffert, U. et al., 2005. Modulation of synaptic plasticity and memory by Reelin involves differential splicing of the lipoprotein receptor Apoer2. *Neuron*, 47(4), pp.567–579.
- Belton, E. et al., 2003. Bilateral brain abnormalities associated with dominantly inherited verbal and orofacial dyspraxia. *Human brain mapping*, 18(3), pp.194–200.
- Bock, H.H. & Herz, J., 2003. Reelin activates SRC family tyrosine kinases in neurons. *Current biology : CB*, 13(1), pp.18–26.
- Bolhuis, J.J., Okanoya, K. & Scharff, C., 2010. Twitter evolution: converging mechanisms in birdsong and human speech. *Nature reviews. Neuroscience*, 11(11), pp.747–759.
- Bottjer, S.W. & Johnson, F., 1997. Circuits, hormones, and learning: vocal behavior in songbirds. *Journal of neurobiology*, 33(5), pp.602–618.
- Brainard, M.S. & Doupe, A.J., 2002. What songbirds teach us about learning. *Nature*, 417(6886), pp.351–358.

- Burkett, Z.D. et al., 2015. VoICE: A semi-automated pipeline for standardizing vocal analysis across models. *Scientific reports*, 5, p.10237.
- Carrillo, G.D. & Doupe, A.J., 2004. Is the songbird Area X striatal, pallidal, or both? An anatomical study. *The Journal of comparative neurology*, 473(3), pp.415–437.
- Chabout, J. et al., 2016. A Foxp2 Mutation Implicated in Human Speech Deficits Alters Sequencing of Ultrasonic Vocalizations in Adult Male Mice. *Frontiers in behavioral neuroscience*, 10(76), p.197.
- Chen, Y. et al., 2005. Reelin modulates NMDA receptor activity in cortical neurons. *The Journal of neuroscience : the official journal of the Society for Neuroscience*, 25(36), pp.8209–8216.
- D'Arcangelo, G. et al., 1995. A protein related to extracellular matrix proteins deleted in the mouse mutant reeler. *Nature*, 374(6524), pp.719–723.
- Doupe, A.J. & Kuhl, P.K., 1999. Birdsong and human speech: common themes and mechanisms. *Annual review of neuroscience*, 22(1), pp.567–631.
- Enard, W. et al., 2009. A humanized version of Foxp2 affects cortico-basal ganglia circuits in mice. *Cell*, 137(5), pp.961–971.
- Ey, E., Leblond, C.S. & Bourgeron, T., 2011. Behavioral profiles of mouse models for autism spectrum disorders. J. Crawley, E. DiCicco-Bloom, & A. J. Bailey, eds. *Autism research : official journal of the International Society for Autism Research*, 4(1), pp.5–16.
- Falconer, D.S., 1951. Two new mutants, 'trembler' and "reeler," with neurological actions in the house mouse (*Mus musculus* L.). *Journal of genetics*, 50(2), pp.192–201.
- Farries, M.A., Ding, L. & Perkel, D.J., 2005. Evidence for "direct" and "indirect" pathways through the song system basal ganglia. *The Journal of comparative neurology*, 484(1), pp.93–104.
- Fatemi, S.H. et al., 2005. Reelin signaling is impaired in autism. *Biological psychiatry*, 57(7), pp.777–787.
- Fatemi, S.H., Stary, J.M. & Egan, E.A., 2002. Reduced blood levels of reelin as a vulnerability factor in pathophysiology of autistic disorder. *Cellular and molecular neurobiology*, 22(2), pp.139–152.
- Fraleigh, E.R. et al., 2016. Mice with Dab1 or Vldlr insufficiency exhibit abnormal neonatal vocalization patterns. *Scientific reports*, 6, p.25807.
- French, C.A. et al., 2012. An aetiological Foxp2 mutation causes aberrant striatal activity and alters plasticity during skill learning. *Molecular psychiatry*, 17(11),

pp.1077–1085.

- Goldberg, J.H. & Fee, M.S., 2010. Singing-related neural activity distinguishes four classes of putative striatal neurons in the songbird basal ganglia. *Journal of neurophysiology*, 103(4), pp.2002–2014.
- Graybiel, A.M., 2005. The basal ganglia: learning new tricks and loving it. *Current opinion in neurobiology*, 15(6), pp.638–644.
- Groszer, M. et al., 2008. Impaired synaptic plasticity and motor learning in mice with a point mutation implicated in human speech deficits. *Current biology : CB*, 18(5), pp.354–362.
- Haesler, S. et al., 2004. FoxP2 expression in avian vocal learners and non-learners. *The Journal of neuroscience : the official journal of the Society for Neuroscience*, 24(13), pp.3164–3175.
- Haesler, S. et al., 2007. Incomplete and inaccurate vocal imitation after knockdown of FoxP2 in songbird basal ganglia nucleus Area X. R. Mooney, ed. *PLoS biology*, 5(12), p.e321.
- Hammerschmidt, K. et al., 2015. A humanized version of Foxp2 does not affect ultrasonic vocalization in adult mice. *Genes, brain, and behavior*, 14(8), pp.n/a–n/a.
- Herz, J. & Chen, Y., 2006. Reelin, lipoprotein receptors and synaptic plasticity. *Nature reviews. Neuroscience*, 7(11), pp.850–859.
- Heston, J.B. & White, S.A., 2015. Behavior-linked FoxP2 regulation enables zebra finch vocal learning. *The Journal of neuroscience : the official journal of the Society for Neuroscience*, 35(7), pp.2885–2894.
- Hiesberger, T. et al., 1999. Direct binding of Reelin to VLDL receptor and ApoE receptor 2 induces tyrosine phosphorylation of disabled-1 and modulates tau phosphorylation. *Neuron*, 24(2), pp.481–489.
- Hilliard, A.T. et al., 2012. Molecular microcircuitry underlies functional specification in a basal ganglia circuit dedicated to vocal learning. *Neuron*, 73(3), pp.537–552.
- Jarvis, E.D., 2004. Learned birdsong and the neurobiology of human language. *Annals of the New York Academy of Sciences*, 1016(1), pp.749–777.
- Johnson, F., Soderstrom, K. & Whitney, O., 2002. Quantifying song bout production during zebra finch sensory-motor learning suggests a sensitive period for vocal practice. *Behavioural brain research*, 131(1-2), pp.57–65.
- Kikusui, T. et al., 2011. Cross fostering experiments suggest that mice songs are innate. B. Brembs, ed. *PloS one*, 6(3), p.e17721.

- Kuhl, P.K., 2004. Early language acquisition: cracking the speech code. *Nature reviews. Neuroscience*, 5(11), pp.831–843.
- Lai, C.S. et al., 2001. A forkhead-domain gene is mutated in a severe speech and language disorder. *Nature*, 413(6855), pp.519–523.
- Lammert, D.B. & Howell, B.W., 2016. RELN Mutations in Autism Spectrum Disorder. *Frontiers in cellular neuroscience*, 10, p.84.
- Laviola, G. et al., 2009. Gene-environment interaction during early development in the heterozygous reeler mouse: clues for modelling of major neurobehavioral syndromes. *Neuroscience and biobehavioral reviews*, 33(4), pp.560–572.
- Lein, E.S. et al., 2007. Genome-wide atlas of gene expression in the adult mouse brain. *Nature*, 445(7124), pp.168–176.
- Liégeois, F. et al., 2003. Language fMRI abnormalities associated with FOXP2 gene mutation. *Nature neuroscience*, 6(11), pp.1230–1237.
- Lintas, C., Sacco, R. & Persico, A.M., 2016. Differential methylation at the RELN gene promoter in temporal cortex from autistic and typically developing post-puberal subjects. *Journal of neurodevelopmental disorders*, 8(1), p.18.
- Long, M.A. & Fee, M.S., 2008. Using temperature to analyse temporal dynamics in the songbird motor pathway. *Nature*, 456(7219), pp.189–194.
- Long, M.A. et al., 2016. Functional Segregation of Cortical Regions Underlying Speech Timing and Articulation. *Neuron*, 89(6), pp.1187–1193.
- Mahrt, E.J. et al., 2013. Engineered deafness reveals that mouse courtship vocalizations do not require auditory experience. *The Journal of neuroscience : the official journal of the Society for Neuroscience*, 33(13), pp.5573–5583.
- Marler, P., 1997. Three models of song learning: evidence from behavior. *Journal of neurobiology*, 33(5), pp.501–516.
- Marrone, M.C. et al., 2006. Altered cortico-striatal synaptic plasticity and related behavioural impairments in reeler mice. *The European journal of neuroscience*, 24(7), pp.2061–2070.
- McCasland, J.S. & Konishi, M., 1981. Interaction between auditory and motor activities in an avian song control nucleus. *Proceedings of the National Academy of Sciences of the United States of America*, 78(12), pp.7815–7819.
- Miller, J.E. et al., 2008. Birdsong decreases protein levels of FoxP2, a molecule required for human speech. *Journal of neurophysiology*, 100(4), pp.2015–2025.
- Mullen, B.R. et al., 2013. Decreased reelin expression and organophosphate pesticide

- exposure alters mouse behaviour and brain morphology. *ASN neuro*, 5(1), p.e00106.
- Nishikawa, S. et al., 2003. Lack of Reelin causes malpositioning of nigral dopaminergic neurons: evidence from comparison of normal and *Reln(rl)* mutant mice. *The Journal of comparative neurology*, 461(2), pp.166–173.
- Nishikawa, S. et al., 1999. Transient and compartmental expression of the reeler gene product reelin in the developing rat striatum. *Brain research*, 850(1-2), pp.244–248.
- Nottebohm, F., 1981. A brain for all seasons: cyclical anatomical changes in song control nuclei of the canary brain. *Science (New York, N.Y.)*, 214(4527), pp.1368–1370.
- Nottebohm, F., Nottebohm, M.E. & Crane, L., 1986. Developmental and seasonal changes in canary song and their relation to changes in the anatomy of song-control nuclei. *Behavioral and neural biology*, 46(3), pp.445–471.
- Nottebohm, F., Stokes, T.M. & Leonard, C.M., 1976. Central control of song in the canary, *Serinus canarius*. *The Journal of comparative neurology*, 165(4), pp.457–486.
- Ognibene, E. et al., 2007. Neurobehavioural disorders in the infant reeler mouse model: interaction of genetic vulnerability and consequences of maternal separation. *Behavioural brain research*, 177(1), pp.142–149.
- Person, A.L. et al., 2008. Organization of the songbird basal ganglia, including area X. *The Journal of comparative neurology*, 508(5), pp.840–866.
- Pfenning, A.R. et al., 2014. Convergent transcriptional specializations in the brains of humans and song-learning birds. *Science (New York, N.Y.)*, 346(6215), pp.1256846–1256846.
- Qiu, S. & Weeber, E.J., 2007. Reelin signaling facilitates maturation of CA1 glutamatergic synapses. *Journal of neurophysiology*, 97(3), pp.2312–2321.
- Qiu, S. et al., 2006. Differential reelin-induced enhancement of NMDA and AMPA receptor activity in the adult hippocampus. *The Journal of neuroscience : the official journal of the Society for Neuroscience*, 26(50), pp.12943–12955.
- Rice, D.S. & Curran, T., 2001. Role of the reelin signaling pathway in central nervous system development. *Annual review of neuroscience*, 24(1), pp.1005–1039.
- Rogers, J.T. & Weeber, E.J., 2008. Reelin and apoE actions on signal transduction, synaptic function and memory formation. *Neuron glia biology*, 4(3), pp.259–270.
- Scattoni, M.L. et al., 2008. Reduced ultrasonic vocalizations in vasopressin 1b knockout mice. *Behavioural brain research*, 187(2), pp.371–378.

- Scharff, C. & Nottebohm, F., 1991. A comparative study of the behavioral deficits following lesions of various parts of the zebra finch song system: implications for vocal learning. *The Journal of neuroscience : the official journal of the Society for Neuroscience*, 11(9), pp.2896–2913.
- Scharff, C. & White, S.A., 2004. Genetic components of vocal learning. *Annals of the New York Academy of Sciences*, 1016(1), pp.325–347.
- Schreiweis, C. et al., 2014. Humanized Foxp2 accelerates learning by enhancing transitions from declarative to procedural performance. *Proceedings of the National Academy of Sciences of the United States of America*, 111(39), pp.14253–14258.
- Schulz, S.B. et al., 2010. Knockdown of FoxP2 alters spine density in Area X of the zebra finch. *Genes, brain, and behavior*, 9(7), pp.732–740.
- Sharaf, A. et al., 2015. Localization of reelin signaling pathway components in murine midbrain and striatum. *Cell and tissue research*, 359(2), pp.393–407.
- Sohrabji, F., Nordeen, E.J. & Nordeen, K.W., 1990. Selective impairment of song learning following lesions of a forebrain nucleus in the juvenile zebra finch. *Behavioral and neural biology*, 53(1), pp.51–63.
- Spiteri, E. et al., 2007. Identification of the transcriptional targets of FOXP2, a gene linked to speech and language, in developing human brain. *American journal of human genetics*, 81(6), pp.1144–1157.
- Takahashi, T. et al., 2015. Structure and function of neonatal social communication in a genetic mouse model of autism. *Molecular psychiatry*.
- Teramitsu, I. & White, S.A., 2006. FoxP2 regulation during undirected singing in adult songbirds. *The Journal of neuroscience : the official journal of the Society for Neuroscience*, 26(28), pp.7390–7394.
- Teramitsu, I. et al., 2004. Parallel FoxP1 and FoxP2 expression in songbird and human brain predicts functional interaction. *The Journal of neuroscience : the official journal of the Society for Neuroscience*, 24(13), pp.3152–3163.
- Teramitsu, I. et al., 2010. Striatal FoxP2 is actively regulated during songbird sensorimotor learning. H. Tanimoto, ed. *PloS one*, 5(1), p.e8548.
- Trommsdorff, M. et al., 1999. Reeler/Disabled-like disruption of neuronal migration in knockout mice lacking the VLDL receptor and ApoE receptor 2. *Cell*, 97(6), pp.689–701.
- Vargha-Khadem, F. et al., 1998. Neural basis of an inherited speech and language disorder. *Proceedings of the National Academy of Sciences of the United States of America*, 95(21), pp.12695–12700.

- Vargha-Khadem, F. et al., 1995. Praxic and nonverbal cognitive deficits in a large family with a genetically transmitted speech and language disorder. *Proceedings of the National Academy of Sciences of the United States of America*, 92(3), pp.930–933.
- Vates, G.E., Vicario, D.S. & Nottebohm, F., 1997. Reafferent thalamo- “cortical” loops in the song system of oscine songbirds. *The Journal of comparative neurology*, 380(2), pp.275–290.
- Vernes, S.C. et al., 2007. High-throughput analysis of promoter occupancy reveals direct neural targets of FOXP2, a gene mutated in speech and language disorders. *American journal of human genetics*, 81(6), pp.1232–1250.
- Watkins, K.E., Dronkers, N.F. & Vargha-Khadem, F., 2002. Behavioural analysis of an inherited speech and language disorder: comparison with acquired aphasia. *Brain : a journal of neurology*, 125(Pt 3), pp.452–464.
- Watkins, K.E., Vargha-Khadem, F., et al., 2002. MRI analysis of an inherited speech and language disorder: structural brain abnormalities. *Brain : a journal of neurology*, 125(Pt 3), pp.465–478.
- Windsor, J. et al., 2013. Effect of foster care on language learning at eight years: findings from the Bucharest Early Intervention Project. *Journal of child language*, 40(3), pp.605–627.
- Windsor, J. et al., 2011. Effect of foster care on young children's language learning. *Child development*, 82(4), pp.1040–1046.
- Young, D.M. et al., 2010. Altered ultrasonic vocalizations in a tuberous sclerosis mouse model of autism. *Proceedings of the National Academy of Sciences of the United States of America*, 107(24), pp.11074–11079.
- Zhubi, A. et al., 2014. Increased binding of MeCP2 to the GAD1 and RELN promoters may be mediated by an enrichment of 5-hmC in autism spectrum disorder (ASD) cerebellum. *Translational psychiatry*, 4(1), p.e349.

Chapter 2: Insights from a Nonvocal Learner on Social Communication

Nancy Day & Elizabeth Fraley

Language is unique to humans. As a result, the neurobiological underpinnings of language are difficult to study in animal models. Fortunately, components of language, such as vocal learning, occur in other animals, including cetaceans, pinnipeds, elephants, bats, and several classes of birds, including songbirds. Many of these animals are not amenable for laboratory study, however, and the ones that are well suited (e.g., birds) are difficult to genetically manipulate. Stereotactic injections of virus to alter songbird gene regulation are possible, but there is limited reach with this method, including the inability to interfere before hatching or early in development before song learning. Given these challenges, determining the capacity for vocal learning in traditional genetically tractable animal models, such as rodents, is important. Male mice emit quantifiable ultrasonic vocalizations (USVs; 30–125 kHz) throughout their lifespan; pups call to signal distress and adult males call during courtship. There is ongoing scientific debate as to whether mice learn these vocalizations and the relevance of rodent models to vocal learning. Mahrt et al. (2013) present rigorous data that suggest rodent vocalizations are innate, not learned, but that rodents can nonetheless be valuable for elucidating genetic control of the brain circuitry underlying vocal motor function.

There are three well known experimental paradigms that test for vocal learning in animal species. In social isolation experiments, animals are reared in the absence of tutors or auditory models. Vocalizations from isolated animals are compared with normally reared animals to determine whether vocalizations are innate, or rather require memorized templates. In juvenile zebra finches, isolation from a tutor song results in disordered and abnormal singing behavior in young birds that persists into adulthood

(Doupe and Kuhl, 1999). In many songbird species only the male sings, which allows young to be reared by females without exposure to song. Social isolation experiments in mice are difficult, if not impossible, to perform because both males and females emit USVs, and maternal care is critical for pup survival (Bowers et al., 2013).

A second test for vocal learning is cross-fostering. Vocal learning animals generate vocalizations that mimic the social environment in which they were raised, as opposed to vocalizations that characterize their genetic background. Cross-fostering experiments in mice suggest that mouse vocalizations are innate (Kikusui et al., 2011), because vocalizations of adult animals more closely resemble their genetic parentage than the vocalizations of the animals with whom they were raised. However, as Mahrt et al. (2013) indicate, cross-fostering studies in mice are confounded by restriction of high-frequency hearing in inbred mouse strains.

Perhaps the most compelling manipulation that can be used to determine the capacity for vocal learning is auditory deprivation during the sensory phase (a time period in which an animal is exposed to auditory stimuli from conspecifics to derive its later vocalizations; Konishi, 1965). Songbirds that are deafened before sensory acquisition (song memorization) never acquire or learn to sing a song. However, auditory deprivation studies have come to opposing conclusions regarding vocal learning in mice. First, Hammerschmidt et al. (2012) used Otoferlin knock-out mice to assess differences in USV acoustic structure between deaf and hearing mice. These knock-out mice model human deafness resulting from deficits in the inner hair cell synaptic vesicle protein otoferlin. No differences in USV spectral features from deaf and wild-type (WT; hearing) littermates were observed in either young or adult animals.

However, one potential limitation of this study is that calls were classified into 2–3 major categories, as opposed to the 10 categories that have been described and quantified by Scattoni et al. (2008). A second deafening study found “striking” alterations in USV structure of pup vocalizations in caspase 3 (*Casp3*) knock-out mice (Arriaga et al., 2012). *Casp3* mice are born congenitally deaf because of the loss of inner ear hair cells shortly after birth. This study sorted calls into 11 categories, quantified differences between hearing and deaf animals for each call type, and concluded that auditory experience is important for strain-typical vocal production in both mouse pups and in mice mechanically deafened as adults. One major caveat to these data is that *Casp3* knock-out mice have abnormal brain morphology that could result in altered vocalizations independent of hearing loss (see Mahrt et al., 2013).

In this most recent contribution to the debate about vocal learning in rodents, Mahrt et al. (2013) used conditional cell ablation to selectively kill all hair cells before the onset of hearing at postnatal d9 (P9), thereby avoiding any confounds present in previous studies (Kikusui et al., 2011; Arriaga et al., 2012). The mouse strain, CBA/CaJ, had human *DTR* (diphtheria toxin receptor) inserted into a gene (*Pou4f3*) found exclusively in hair cells. As a result, when diphtheria toxin was injected into P2 mice, all *Pou4f3*⁺/*DTR* mice were rendered deaf, and all WT littermates were spared hearing loss. All animals were raised within litters and subsequently lived within mixed-genotype colonies to control for exposure to the acoustic environment. Male USVs were recorded in the presence of a female for 15–20 min between 1 and 5 times between P60 and P70 to assess differences in adult courtship vocalizations between deaf-reared and control animals. After behavioral testing, auditory brainstem responses were recorded to verify

that injected *Pou4f3*^{+/-DTR} animals were functionally deaf, and that WT animals exhibited normal hearing (Mahrt et al., their Fig. 2). Additionally, intact cochleae were examined using immunohistochemistry to ensure that the manipulation eliminated hair cells from the inner ears of deafened animals only (Mahrt et al., their Fig. 3).

The authors analyzed USVs by categorizing calls into 12 different groups based on previously described criteria (Scattoni et al., 2008). Deaf and hearing animals emitted the same types of syllables and at approximately the same rate (Mahrt et al., their Fig. 4). Calls within each category were subjected to rigorous quantification (up to 50 parameters were used to quantify syllables within each class; Mahrt et al., their Tables 2–3). The described methodology permitted precise measurements of multiple aspects of each syllable, using software developed to semiautomatically categorize syllables. Importantly, no statistically significant differences between hearing and deaf animals in number, duration, frequency, spectral, or temporal aspects for calls within each USV category were observed (Mahrt et al., their Figs. 8–9), indicating that mouse vocalizations are innate and not learned.

Though the conclusions in this paper are well supported, replication of these results in another mouse strain will be critical, because different mouse strains exhibit different calling behavior (Kikusui et al., 2011). Furthermore, in songbirds, subtle differences in timing and variability of courtship song, which are difficult for humans to detect, greatly impact zebra finch female preference and partner choice. Therefore, it would be worth determining whether subtle changes to vocalizations from deaf mice detract from the overall reproductive success of the animal.

Overall, the study by Mahrt et al. (2013) provides strong support for the innate capacity for vocal production, yet clearly suggests that CBA/CaJ mice do not learn their vocalizations. Although the lack of vocal learning in mice may limit their use for studies pertaining to human speech learning, mice may still be useful for studying the general mechanisms of vocal communication, and perhaps more importantly, the molecules putatively involved in vocalization. For example, mouse pup isolation calling appears to be related to *FOXP2* function, a gene essential for language in humans (Lai et al., 2001) and song learning in zebra finches (Haesler et al., 2007). Male mouse pups call more than females, tend to be retrieved by their dams preferentially, and have higher *Foxp2* levels (Bowers et al., 2013). Expressing the human-like form of *FOXP2* in mouse pups resulted in changes to ultrasonic calling behavior (Enard et al., 2009). Despite the inability of rodents to acquire socially learned vocalizations, examining vocalizations in rodent models may underscore the relevance of *Foxp2* and other molecules that affect vocal output across both vocal learning and nonvocal learning animals.

Analyzing similarities between rodents, songbirds, and humans will elucidate shared neuromolecular mechanisms of vocal learning and social communication. The parallels between bird song and human speech learning include reliance upon corticobasal ganglia-thalamic loops, social interactions that occur early in life, and similar neuromolecular mechanisms. Where one model falls short (i.e., molecular manipulation in songbirds or innate courtship vocalizations in rodents), the other model can compensate. Effects of genes such as *FOXP2* on vocal behavior across species strengthen the case that it is essential to vocal communication. Because the evolution of language and vocal learning are likely to rely on genes and molecules already in place

in nonvocal learning species, a complementary panel of both songbird and rodent might best characterize a gene's contribution to vocalization. The findings of Mahrt et al. (2013) underscore a weakness in the established rodent model and open the door for cross-species comparisons in the future.

References

- Mahrt EJ, Perkel DJ, Tong L, Rubel EW, Portfors CV (2013). Engineered Deafness Reveals That Mouse Courtship Vocalizations Do Not Require Auditory Experience. *J Neurosci* **33**:5573–5583.
- Doupe AJ, Kuhl PK (1999). Birdsong and human speech: common themes and mechanisms. *Annu Rev Neurosci* **22**:567.
- Bowers JM, Perez-Pouchoulen M, Edwards NS, McCarthy MM (2013). Foxp2 mediates sex differences in ultrasonic vocalization by rat pups and directs order of maternal retrieval. *J Neurosci* **33**:3276–3283.
- Kikusui T, Nakanishi K, Nakagawa R, Nagasawa M, Mogi K, Okanoya K (2011). Cross fostering experiments suggest that mice songs are innate. *PLoS One* **6**:e17721.
- Konishi M (1965). The role of auditory feedback in the control of vocalization in the white-crowned sparrow. *Z Tierpsychol* **22**:770–783.
- Hammerschmidt K, Reisinger E, Westekemper K, Ehrenreich L, Strenzke N, Fischer J (2012). Mice do not require auditory input for the normal development of their ultrasonic vocalizations. *BMC Neurosci* **13**:40.
- Scattoni ML, Gandhi SU, Ricceri L, Crawley JN (2008). Unusual repertoire of vocalizations in the BTBR T+tf/J mouse model of autism. *PLoS One* **3**:e3067.
- Arriaga G, Zhou EP, Jarvis ED (2012). Of mice, birds, and men: the mouse ultrasonic song system has some features similar to humans and song-learning birds. *PLoS One* **7**:e46610.
- Lai CS, Fisher SE, Hurst JA, Vargha-Khadem F, Monaco AP (2001). A forkhead-domain gene is mutated in a severe speech and language disorder. *Nature* **413**:519–523.
- Haesler S, Rochefort C, Georgi B, Licznarski P, Osten P, Scharff C (2007). Incomplete and inaccurate vocal imitation after knockdown of FoxP2 in songbird basal ganglia nucleus Area X. *PLoS Biol* **5**:e321.
- Enard W, Gehre S, Hammerschmidt K, Hölter SM, Blass T, Somel M, Brückner MK, Schreiweis C, Winter C, Sohr R, Becker L, Wiebe V, Nickel B, Giger T, Müller U, Groszer M, Adler T, Aguilar A, Bolle I, Calzada-Wack J, et al. (2009). A humanized version of Foxp2 affects cortico-basal ganglia circuits in mice. *Cell* **137**:961–971.

Chapter 3: Mice with *Dab1* or *Vldlr* insufficiency exhibit abnormal neonatal vocalization patterns

Fraley, ER; Burkett ZD; Day NF, Schwartz BA, Phelps, PE, White, SA

Abstract

Genetic and epigenetic changes in components of the Reelin-signaling pathway (*RELN*, *DAB1*) are associated with autism spectrum disorder (ASD) risk. Social communication deficits are a key component of the ASD diagnostic criteria, but the underlying neurogenetic mechanisms remain unknown. *Reln* insufficient mice exhibit ASD-like behavioral phenotypes including altered neonatal vocalization patterns. Reelin affects multiple pathways including through the receptors, Very low-density lipoprotein receptor (Vldlr), Apolipoprotein receptor 2 (Apoer2), and intracellular signaling molecule Disabled-1 (Dab1). As Vldlr was previously implicated in avian vocalization, here we investigate vocalizations of neonatal mice with a reduction or absence of these components of the Reelin-signaling pathway. Mice with low or no Dab1 expression exhibited reduced calling rates, altered call-type usage, and differential vocal development trajectories. Mice lacking Vldlr expression, also had altered call repertoires, and this effect was exacerbated by deficiency in Apoer2. Together with previous findings, these observations 1) solidify a role for Reelin in vocal communication of multiple species, 2) point to the canonical Reelin-signaling pathway as critical for development of normal neonatal calling patterns in mice, and 3) suggest that mutants in this pathway could be used as murine models for Reelin-associated vocal deficits in humans.

Introduction

Reelin is a large secreted glycoprotein that has numerous nervous system functions including regulating neuronal migration, neuronal excitability, and dendritic morphology (D'Arcangelo et al. 1995; Weeber et al. 2002; Niu et al. 2004; Niu et al. 2008; Rice & Curran 2001; Herz & Chen 2006). Murine *reeler* mutants (*Reln*^{-/-}) do not express Reelin and exhibit a characteristic phenotype of a reeling gait, disorganization of laminated structures including the neocortex, cerebellum, and hippocampus, and a reduction in cerebellar volume (Goffinet et al. 1984; Caviness & Rakic 1978; Falconer 1951; D'Arcangelo et al. 1995; Tissir & Goffinet 2003). When Reelin binds to Very low-density lipoprotein receptor (Vldlr) and/or Apolipoprotein receptor 2 (Apoer2), this initiates binding of Disabled-1 (Dab1) to the internal domain of the receptors (D'Arcangelo et al. 1999; Howell et al. 1997). Dab1 is then phosphorylated at critical tyrosine residues by Src-family kinases to influence a wide array of downstream effectors (Hiesberger et al. 1999; Herz & Chen 2006; Bock & Herz 2003).

RELN has been identified as a risk allele for autism spectrum disorder (ASD) in multiple populations (Persico et al. 2001; Vorstman et al. 2006; Serajee et al. 2006; Skaar et al. 2005; Dutta et al. 2007; Kelemenova et al. 2010; H. Li et al. 2008; Holt et al. 2010; Ashley-Koch et al. 2007). Polymorphisms throughout *RELN* include variants in both coding and non-coding regions. Changes leading to an expansion in GGC repeats in the 5' region reduce *RELN* expression levels and confer ASD risk in some cases (Persico et al. 2006). Reelin protein (RELN) is low in post-mortem brain tissue of ASD patients compared to controls (Fatemi et al. 2005). Additionally, *RELN* mRNA is

low in the cerebellum and cortex of these patients (Fatemi et al. 2005). Epigenetic down regulation of *RELN* via increased methylation of its promoter is also linked to increased ASD risk (Zhubi et al. 2014). Intriguingly, *DAB1* polymorphisms are associated with ASD risk in the Chinese-Han population whereas *RELN* polymorphisms are not (J. Li et al. 2013). These results indicate that not only *RELN*, but the function of the downstream Reelin-signaling pathway could be involved in the etiology of ASD.

Social communication deficits are a key diagnostic feature of ASD. Autistic symptoms are generally undetected at birth, but instead appear over time and reflect differential developmental trajectories (Ozonoff et al. 2010). High risk infants, i.e. children with one or more ASD siblings, and infants later diagnosed with ASD, have altered acoustic features of their cries (Sheinkopf et al. 2012). At 6 months, their cries are more disordered and of higher pitch compared with those of typically developing children. High risk infants also exhibit abnormal pre-linguistic vocal behavior such as making fewer speech-like vocalizations and more non-speech vocalizations as well as producing fewer consonant types than typically developing peers (Paul et al. 2011). Given these observations, examination of the amount and acoustic parameters of infant cries could serve as a tool for early ASD detection.

Genetic causes are linked to 10-25% of ASD cases (Ey et al. 2011). Investigation of how these gene mutations alter behavioral phenotypes, and the underlying brain organization and function, are enabled by mouse models (Silverman et al. 2010). Neonatal mouse pups typically emit ultrasonic vocalizations (USVs) when isolated from the dam which act as a signal for the dam to retrieve and care for the pup (Crawley 2004). Pups are entirely reliant on the dam during this time (P0-P14), and thus

appropriate communication cues are critical to their survival. Isolation USVs first occur at ~postnatal day 4 (P4) and peak around P6-7, before gradually declining at P14 when the pup is able to self-retrieve (Noirot 1966). Dams preferentially retrieve pups that call more and prefer more elaborate call types (Bowers et al. 2013; Takahashi et al. 2015). Reductions in total calling, delays in the peak calling age, and an altered call repertoire occur in many mouse ASD models (Chadman et al. 2008; Scattoni, McFarlane, et al. 2008; Nakatani et al. 2009; Shu et al. 2005; Young et al. 2010; Searce-Levie et al. 2008; Winslow et al. 2000; Scattoni, Gandhi, et al. 2008). Murine neonatal isolation calls are considered to be more like human baby cries than early speech. Although laboratory mice are not robust vocal learners (Chapter2; Day & Fraley 2013), their vocal behavior can reflect sociability and mechanisms of communication that subserve both learned and unlearned vocalizations.

Because humans with ASD were reported to have low levels of Reelin, the *Reln*^{+/-} mouse was proposed as a model for ASD (Folsom & Fatemi 2013). *Reln*^{+/-} mice have a 50% reduction in Reelin protein and lack the typical neuronal migration deficits seen in *Reln*^{-/-} mice (Biamonte et al. 2009). *Reln*^{+/-} mice however, exhibit GAD67 down-regulation in the frontoparietal cortex (Liu et al. 2001), Purkinje cell loss and hypoplasia of the cerebellum (Marrone et al. 2006) and parvalbumin-positive cell loss in the striatum (Ammassari-Teule et al. 2009), resulting in changes to cortico-striatal plasticity (Marrone et al. 2006). These changes are parallel to those in human ASD cases which show the following abnormalities: low GAD67 across brain regions including the frontal cortex (Akbarian & Huang 2006); Purkinje cell loss and reduced cerebellar volume (Kemper & Bauman 1993; Courchesne et al. 1988), and altered connectivity and

function of the striatum (Di Martino et al. 2011; Sears et al. 1999). Genetic vulnerability can determine phenotype by interacting with the environment; other studies have examined multivariate conditions (separation, stress, drug/pesticide exposure) that interact with the reduced *Reln* expression to mirror ASD-like phenotypes (Ognibene, Adriani, Macrì, et al. 2007; Laviola et al. 2006; Ognibene, Adriani, Granstrem, et al. 2007; Mullen et al. 2013; Biamonte et al. 2014).

To investigate whether or not Reelin deficiency alone creates an ASD-like phenotype, the early vocal behavior of the *Reln*^{+/-} and *Reln*^{-/-} mice was characterized (Ognibene, Adriani, Macrì, et al. 2007; Romano et al. 2013). *Reln*^{+/-} mice show a delay in the age of peak isolation USV calling, whereas *Reln*^{-/-} mice have low calling rates at all measured time points (P2-P12), most likely due to gross motor deficits (Ognibene, Adriani, Macrì, et al. 2007). Repertoires of P6 pups are altered in a gene-dose dependent manner, with a particularly large expansion of two-syllable call types (see Methods below for call type classifications)(Romano et al. 2013). Differences in repertoire based on genotype disappear as pups mature (P8-12). These findings indicate a deficit in early vocal communication in *Reln*^{+/-} mice.

VLDLR is a known target of the language-associated transcription factor *FOXP2* in humans(Vernes et al. 2007). Moreover, vocally regulated gene networks in the zebra finch basal ganglia (Area X)(Hilliard et al. 2012) include *Vldlr*, *Dab1*, and *Reelin*; *Vldlr* is in the same gene module as *FoxP2*. These observations suggest that the Reelin-signaling pathway is essential for normal vocal development in multiple species.

Here, we examine the early vocal phenotypes of mice with reductions in *Vldlr*, *Apoer2* and *Dab1*. Findings are then compared with those from *Reln*^{+/-} and *Reln*^{-/-} mice

(Romano et al. 2013) in order to attribute changes in vocal development to the canonical Reelin-signaling pathway. Given the greater incidence of ASD in the male population (Developmental Disabilities Monitoring Network Surveillance Year 2010 Principal Investigators Centers for Disease Control and Prevention (CDC) 2014), sex as a contributing factor was also examined.

Methods

Mouse breeding and care. Experiments were approved by UCLA Office of Animal Research Oversight. All animal use was in accordance with the UCLA Institutional Animal Care and Use Committee and complied with American Veterinary Association standards for working with laboratory animals. Mice were maintained on a 12h light/dark cycle, with *ad libitum* food and water. *Dab1^{lacZ}* mice were a gift from Dr. Brian Howell (Upstate Medical University, SUNY). The mice have a truncation of *Dab1* at residue 22 and expression of a fusion of the *lacZ* reporter rendering the protein unable to initiate downstream signaling via phosphorylation at critical residues⁶⁶. These mice were generated as previously described (Pramatarova et al. 2008) by breeding *Dab1 cKlneo* mice with *Meox-Cre* germline deleter mice (B6.129S4-*Meox2^{tm1(cre)SOR}/J*, Jackson Laboratories, Bar Harbor, ME, USA) and selected progeny. The expression of beta-galactosidase is in line with established *Dab1* expression in cerebral cortex, cerebellum, and hippocampus (Abadesco et al. 2014; Pramatarova et al. 2008). *Vldlr^{tm1Her}* mice have a targeted complete deletion of the *Vldlr* gene. These were generated in B6.129S7/SvEvBrd mice by Dr. Joachim Herz. Double receptor mutants do not have *Apoer2* or *Vldlr* and resemble *Reln^{-/-}* mice (Hiesberger et al. 1999). *Dab1*, *Vldlr*, and *Apoer2* mice were genotyped using PCR as previously described (Pramatarova et al. 2008; Frykman et al. 1995; Trommsdorff et al. 1999).

Vocal Recording. To test isolation calls, mouse pups were removed from the nest, four at a time, and individually placed into sound attenuation chambers for recording. These

chambers were constructed from small coolers (Coleman) that were coated inside with soundproof foam (Soundcoat). An ultrasonic microphone (UltraSoundGate, Avisoft Bioacoustics) was suspended above the pup. Recordings were conducted at P7 and P14 for a total of 15 minutes at each time point. In order to not affect calling patterns of any remaining pups in a given litter, only four (the total number of recording chambers) from each litter were recorded. After recording at P7, pups were tailed for genotyping, and tattooed to enable identification for re-recording at P14. The initial distance between the microphones and the pups was equivalent across chambers at P7 when pups are fairly immobile. At P14, pups are ambulatory so their distance from the microphone varied. Because of this, amplitude measurements were not included in the acoustic analysis. Pups were recorded within the same 2-hour time window each day (light: 14:00-16:00hr) to avoid circadian effects. Temperature was maintained at 21-22°C.

Acoustic analysis, quantification and classification. Ultrasonic (20-125kHz) vocalizations were acquired using a sampling rate of 250kHz. In order to reduce background noise and focus on ultrasound, sounds with a frequency <40kHz were high-pass filtered and removed from analysis. Recorded vocalizations were segmented based on amplitude threshold to allow for recording of bouts (Avisoft-SASLab Pro Recorder). Bouts are a series of USVs that occur in rapid succession (≤ 40 ms between calls) and are surrounded by ≥ 1 second of silence. Recordings were transduced from amplitude traces into spectrograms using Fast Fourier Transform with a transform of 256 points and a time window overlap of 75% (Avisoft Bioacoustics; SASLab Pro). Bouts were then segmented into individual syllables and then processed using VoICE, a

semi-automated unbiased clustering mechanism, to classify these calls into categories (Burkett et al. 2015).

Call type categories from the work of Scattoni and colleagues (Scattoni, Gandhi, et al. 2008) were used and include 9 basic types: 'short' (duration $<10\text{ms}$), 'downward' (frequency sweeps downward of $\geq 10\text{kHz}$ and $>10\text{ms}$), 'upward' (frequency sweeps upward of $\geq 10\text{kHz}$, $>10\text{ms}$), 'flat' ($<10\text{kHz}$ of modulation, $>10\text{ms}$), 'complex' (wave shaped frequency sweep, $>10\text{ms}$) 'frequency step' (multiple jump containing calls), 'chevron' (inverted U shape frequency with $\geq 10\text{kHz}$ of modulation), 'harmonic' (multiple jump containing with harmonic stacking), and 'two-syllable' (one-jump containing). Composite call types (those containing no jumps but with harmonic stacking) were collapsed into the harmonic call category; unstructured call types (broadband of $\geq 40\text{kHz}$ with no clear single frequency) comprised $<1\%$ of the recordings and were not analyzed. Additional call categories of 'doubles', 'triples', and 'miscellaneous' were observed and included. Double and triple calls are comprised of various frequency sweeps that occur in rapid succession, being separated by $\leq 10\text{ms}$. These were rare and considered together as a single call type. Miscellaneous call types did not fit into any of the groups described previously, and may represent emerging novel types. The sequence of the calls, referred to here as 'syntax', was also assessed. Syntax similarity, syntax entropy and repertoire correlation analyses were performed as described previously (Burkett et al. 2015).

Statistical methods. Where possible, resampling statistical tests were used because this methodology makes no assumptions about the data distribution. Call counts were

quantified and analyzed using two-way ANOVA followed by individual 2-tailed t-tests with as follows: Once call classifications were determined, we noticed a high degree of variability between individual pups of the same genotype (Supplemental Fig. 1). To overcome this variability, we normalized each raw call count in each category to the total number of call counts per animal. These normalized values were used to create pie charts. In order to assess statistical differences in repertoire between groups, call count categories of each animal were rank transformed and then resampled 10,000 times to determine the median rank and 95% confidence interval (CI) for each genotype. Only measures with non-overlapping CIs were considered to differ. Syntax similarity scores, syntax entropy scores, and repertoire correlation were also subjected to one-way ANOVA followed by *post hoc* 2-tailed t-tests with Welch's correction.

Results

Amount of calling depends on *Dab1* genotype at P7 but not at P14. To test for an early social communication deficit, *Dab1* deficient mice pups were recorded (Fig. 1A). The number of calls produced by male and female *Dab1* pups of each of the 3 genotypes was quantified (*Dab1*^{+/+} N=21, *Dab1*^{+/*lacZ*} N=23, *Dab1*^{*lacZ*/*lacZ*} N=11). A significant effect of genotype on calling behavior was observed at P7, with no effect of sex (Fig. 1B; two-way ANOVA, sex effect $p=0.308$, genotype effect $p=0.005$, interaction $p=0.671$). As call number did not differ based on sex, data from both sexes were pooled (Supplemental Fig. 1A). At P7, *Dab1*^{+/+} mice called the most and their call counts were significantly greater than those of the *Dab1*^{*lacZ*/*lacZ*} mice (t-test; $p=0.0001$). The *Dab1*^{+/*lacZ*} mice called more than the *Dab1*^{*lacZ*/*lacZ*} mice (t-test, $p=0.004$). The *Dab1*^{*lacZ*/*lacZ*} mutants made the least number of calls at this time point, a result that may reflect their severe motor deficits. Thus, at P7, a *Dab1* gene-dose dependent effect on calling amount was evident, with no effect of sex.

At P14, the amount of calling was relatively low and similar across all three genotypes (Fig. 1C; *Dab1*^{+/+} N=17, *Dab1*^{+/*lacZ*} N=19, *Dab1*^{*lacZ*/*lacZ*} N=9; two-way ANOVA; genotype effect $p=0.545$, sex effect $p=0.400$, interaction $p=0.296$, NS). The amount of calling by *Dab1*^{+/+} mice did not differ from *Dab1*^{+/*lacZ*} mice (t-test, $p=0.206$, NS) or *Dab1*^{*lacZ*/*lacZ*} mice (t-test, $p=0.800$, NS). Interestingly, comparison of the total call counts between P7 and P14 time points by genotype reveals a differential rate of age-related decline (Fig. 1D; two-way ANOVA; age effect $p=0.0001$, genotype effect $p=0.006$, interaction $p=0.0143$). The *Dab1*^{+/+} mice exhibit a steep fall-off in calling amount

between P7 and P14 (t-test, $p < 0.0001$) in line with the normal developmental decline of isolation calling (Noirot 1966). Comparatively, in $Dab1^{+/lacZ}$ mice the decline from P7 to P14 was less significant (t-test, $p = 0.001$); and the $Dab1^{lacZ/lacZ}$ mice did not significantly differ in the amount of calling between P7 and P14 (t-test, $p = 0.275$). These findings indicate altered vocal developmental trajectories for the $Dab1$ reduced ($Dab1^{+/lacZ}$) and null ($Dab1^{lacZ/lacZ}$) mice.

***Dab1* genotype affects P7 call repertoires.** Next, the types of calls were analyzed to determine any genotype-dependent differences (Fig. 2A). In addition to an altered amount of calling, described above, the types of calls were also altered in a gene dose-dependent manner (Fig. 2B,C). As with call number, the call repertoire exhibited a great deal of variability between pups, even within the same genotype (Supplemental Fig. 2A,B). To enable comparison, data were normalized to create pie charts depicting the combined call repertoire for each genotype (See Methods; Fig. 2B). At P7, $Dab1^{+/+}$ mice (N=13,345 calls from 21 mice) had a relatively diverse repertoire. When comparing calls from $Dab1^{+/+}$ and $Dab1^{+/lacZ}$ pups (N=11,075 calls, from 22 mice), $Dab1^{+/lacZ}$ had significantly more upward call types. Otherwise, $Dab1^{+/lacZ}$ mice had an intermediate phenotype. Trends that placed the $Dab1^{+/lacZ}$ between the $Dab1^{+/+}$ and $Dab1^{lacZ/lacZ}$ mice include an intermediate level of the downward and frequency step call types. The $Dab1^{lacZ/lacZ}$ pups (N=1,317 calls, from 7 mice) exhibited a relatively restricted repertoire comprised of significantly more short and downward calls than found in the other genotypes. The $Dab1^{+/+}$ pups made significantly more complex and frequency step calls than did the $Dab1^{lacZ/lacZ}$ mice. $Dab1^{lacZ/lacZ}$ pups also had significantly more of an

unusual call type, the triple, than the other groups. Chevron, flat, harmonic, two-syllable, double, and miscellaneous call types did not differ significantly based on genotype. A few sex differences in repertoire at P7 were found for *Dab1^{lacZ/lacZ}* (Supplemental Fig. 1C). However, based on the lack of sex effect on repertoire in *Dab1^{+//lacZ}* (Supplemental Fig. 1B), call type data were pooled across sexes to provide greater power for further analysis. Notably, repertoire analysis of all wild-type mice across experiments pooled revealed no repertoire differences based on sex (Supplemental Fig. 3).

At P14, *Dab1^{+//+}* and *Dab1^{+//lacZ}* repertoires were fairly similar, while those of *Dab1^{lacZ/lacZ}* mice appeared more restricted than *Dab1^{+//+}* (Fig. 3A, Supplemental Fig. 2B). There were however, no statistically significant differences in call repertoires (Fig. 3B; syllables analyzed: *Dab1^{+//+}* N=1141 from 13 mice, *Dab1^{+//lacZ}* N=2,518 from 13 mice, *Dab1^{lacZ/lacZ}* N=684 from 7 mice). The lack of statistical significance is likely due to the relatively low numbers of calls made at this time point, especially by *Dab1^{lacZ/lacZ}* mice. In summary, at P7, *Dab1^{+//lacZ}* and *Dab1^{lacZ/lacZ}* mice exhibited partially and extremely restricted call repertoires, respectively, relative to the *Dab1^{+//+}* mice. *Dab1^{lacZ/lacZ}* repertoires included a decreasing level of some of the more elaborate call types and an increase in some of the simpler ones. Notably, despite gross motor deficits, *Dab1^{lacZ/lacZ}* pups were able to make a majority of the call types described. Thus, changes in their repertoires may not be fully attributable to global motor deficits.

Effect of *Vldlr* ablation on calling rates at P7 and P14. *Vldlr* and *Apoer2* are high-affinity Reelin receptors essential for transduction of the signal to *Dab1* (Fig. 4A). To further test that vocal deficits could be related to *Vldlr* insufficiency, we examined the

effect of *Vldlr* deletion with or without *Apoer2*. Wild-type (*Vldlr*^{+/+}/*Apoer2*^{+/+}; N=12), *Vldlr* single receptor mutants (*Vldlr*^{-/-}/*Apoer2*^{+/+}; N=18), and *Vldlr/Apoer2* double receptor mutants (*Vldlr*^{-/-}/*Apoer2*^{-/-}; N=4) were recorded at P7 and P14. At P7, there were no significant differences in the number of calls emitted by each group and no effect of sex (Fig. 4B, Supplemental Fig. 4A; two-way ANOVA, genotype effect $p=0.226$, sex effect $p=0.447$, interaction $p=0.700$, NS). This lack of genotype effect on call amount at P7 could be due to the low number of double mutants obtained for recording (N=4). Upon closer examination, the call counts of *Vldlr*^{-/-}/*Apoer2*^{-/-} mice (mean call count=736.5) were close to statistical significance as being lower than those of the *Vldlr*^{-/-}/*Apoer2*^{+/+} mice (mean call count=1504; t-test $p=0.057$).

At P14, there were no differences in calling amount based on the *Vldlr* or *Apoer2* genotype, but there was a sex difference (two-way ANOVA, genotype effect $p=0.325$, sex effect $p=0.010$, interaction $p=0.224$). The males appear to be more adversely affected and called less than the females (Supplemental Fig. 4A). Developmental trajectories of each group were then examined (two-way ANOVA; genotype effect $p=0.220$, age effect $p=0.001$, interaction $p=0.085$). There was a significant decrease in calling from P7 to P14 (Fig. 4D) by the *Vldlr*^{+/+}/*Apoer2*^{+/+} (t-test $p=0.0001$) and *Vldlr*^{-/-}/*Apoer2*^{+/+} mice (t-test $p<0.0001$). *Vldlr*^{-/-}/*Apoer2*^{-/-} mice, much like the *Dab1*^{lacZ/lacZ} mice, did not have a significant difference in call counts between P7 and P14 (t-test $p=0.459$, NS). The normal developmental decline in calling rate was observed for both *Vldlr*^{+/+}/*Apoer2*^{+/+} and *Vldlr*^{-/-}/*Apoer2*^{+/+} mice and but not for *Vldlr*^{-/-}/*Apoer2*^{-/-} mice.

***Vldlr/Apoer2* genotype affects call repertoires at P7 and P14.** The call repertoire based on presence of *Vldlr* was then assessed at P7 and P14 (Figs. 5,6). Despite the high degree of individual variability, there were significant differences in call usage that paralleled what was observed for *Dab1* mice (Fig. 5B; Supplemental Fig. 2C,D). To improve power, data were pooled across sex, as only minimal sex differences were observed (Supplemental Fig. 4B,C). Overall, the severity of receptor deficiency was inversely related to the call repertoire, with greater deficiencies corresponding to more restricted repertoires (Fig. 5A). At P7, the *Vldlr*^{+/+}/*Apoer2*^{+/+} pups (N=15046 calls) made more frequency step calls and fewer short calls compared to the other groups. There were significantly more short calls and fewer frequency step calls in both *Vldlr*^{-/-}/*Apoer2*^{+/+} (N=25522 calls) and *Vldlr*^{-/-}/*Apoer2*^{-/-} mice (N=2946 calls) compared to *Vldlr*^{+/+}/*Apoer2*^{+/+} mice (Fig. 5B). There was a significant increase in the upward call type in the P7 *Vldlr*^{-/-}/*Apoer2*^{+/+} group only, which parallels an increase in upward call type observed in *Dab1*^{+/*lacZ*} pups. No significant differences were found for the other call types. Thus, at P7 the *Vldlr*^{-/-}/*Apoer2*^{+/+} pups had altered calling behavior reminiscent of that observed in *Dab1*^{+/*lacZ*} heterozygotes; and extremely restricted repertoires were observed in both *Vldlr*^{-/-}/*Apoer2*^{-/-} and *Dab1*^{*lacZ*/*lacZ*} pups.

At P14, repertoire analysis revealed significant differences based on *Vldlr* genotype (Fig. 6; *Vldlr*^{+/+}/*Apoer2*^{+/+}, N=1021 calls, *Vldlr*^{-/-}/*Apoer2*^{+/+}, N=3360 calls, *Vldlr*^{-/-}/*Apoer2*^{-/-}, N=1554 calls). *Vldlr*^{+/+}/*Apoer2*^{+/+} mice emitted the double call type significantly less often than *Vldlr*^{-/-}/*Apoer2*^{+/+} and *Vldlr*^{-/-}/*Apoer2*^{-/-} mice, and the short call type less than *Vldlr*^{-/-}/*Apoer2*^{-/-} mice. Miscellaneous call types were significantly expanded in the *Vldlr*^{-/-}/*Apoer2*^{-/-} compared to the *Vldlr*^{-/-}/*Apoer2*^{+/+} pups. These findings

reflect an extremely restricted repertoire of the *Vldlr*^{-/-}/*Apoer2*^{-/-} at P14 as was shown in these animals at P7. This was also true of the single receptor mutants, albeit to a lesser degree. Thus, absence of *Vldlr*, and *Vldlr* with *Apoer2*, had a significant effect on calling repertoire at P7 and P14.

Parallel effects of Dab1 and Vldlr genotypes on repertoire correlation and syntax

similarity. Repertoire correlation analysis of all pups was performed at P7 (Fig. 7A,B) to provide a measure of how similar individual repertoires are within a given genotype. A high correlation between repertoires (positive correlation values, denoted by red) indicates convergence on similar call type usage, while a low correlation (negative correlation values, denoted in blue) are indicative of very different call usage between individuals (Fig. 7C,D). Overall, *Dab1* mice exhibited a gene-dose dependent effect on repertoire correlation (one-way ANOVA, $p < 0.001$). Pups with the *Dab1*^{+/+} genotype had the lowest repertoire correlation (average $\rho = 0.22$), followed by *Dab1*^{+/*lacZ*} (average $\rho = .33$, t-test $p < 0.001$), then *Dab1*^{*lacZ*/*lacZ*} with the highest (average $\rho = .50$, t-test, $p = 0.005$). The same was true for pups of the *Vldlr*/*Apoer2* genotype (one-way ANOVA, $p = 0.015$) with *Vldlr*^{+/+}/*Apoer2*^{+/+} having lowest correlation scores (average $\rho = 0.52$), followed by the *Vldlr*^{-/-}/*Apoer2*^{+/+} (average $\rho = 0.61$, t-test, $p = 0.013$); and then *Vldlr*^{-/-}/*Apoer2*^{-/-} (average $\rho = 0.74$, $p = 0.185$, not significant). Repertoire correlations of *Vldlr*^{-/-}/*Apoer2*^{-/-} pups were significantly lower than those of *Vldlr*^{+/+}/*Apoer2*^{+/+} pups (t-test $p = 0.038$). These findings indicate an association between highly similar repertoires within the groups of low or no Reelin-signaling pathway components, i.e. *Dab1*, *Vldlr*, and *Apoer2*. Convergence on similar call types within a genotype would explain

increasing repertoire correlation, and was most striking in the *Dab1^{lacZ/lacZ}* and *Vldlr^{-/-}/Apoer2^{-/-}* pups.

The effect of genotype on call sequence, or syntax, was then examined using syntax similarity analysis of isolation calls for P7 pups (Fig. 8). This type of analysis shows how alike call transitions are between animals within a given group. High syntax similarity indicates similar types of transitions within a group. There was a significant effect of *Dab1* genotype on syntax similarity (Fig. 8A, one-way ANOVA, $p=0.014$). Syntax similarity was highest for the *Dab1^{+ / lacZ}* mice (Syntax similarity average, SS =0.19) compared to *Dab1^{lacZ/lacZ}* (SS =0.17) and *Dab1^{+/+}* pups (SS =0.16). Surprisingly, the *Dab1^{lacZ/lacZ}* pups had SS scores that were almost identical to that of *Dab1^{+/+}* pups. There was an effect of *Vldlr* genotype on SS as well (Fig. 8B, one-way ANOVA $p=0.002$). *Vldlr^{-/-}/Apoer2^{+/+}* pups had higher similarity (SS =0.37) than *Vldlr^{+/+}/Apoer2^{+/+}* pups (SS =0.28) and *Vldlr^{-/-}/Apoer2^{-/-}* pups (SS =0.33). In summary, parallel patterns of syntax similarity were observed across both the *Dab1* and *Vldlr/Apoer2* mouse lines.

Discussion

Altered isolation vocalizations are a hallmark of ASD-like early phenotype in mice (Crawley 2004). In order to determine if *Dab1* or *Vldlr* insufficiency impacts patterns of early social communication, we characterized the age related calling patterns in *Dab1* and *Vldlr/Apoer2* deficient mice, generating novel findings. Additionally, we queried whether or not the canonical Reelin-signaling pathway may be responsible for the changes in vocalization seen in *Reln*^{+/-} and *Reln*^{-/-} pups (Ognibene, Adriani, Macrì, et al. 2007; Romano et al. 2013). Despite extreme inter-individual variation in calling, we found that the *Dab1* genotype profoundly affected the calling rate and repertoire of P7 pups in a gene dose dependent manner. The effect subsided at P14 in concert with the typical overall decrease in calling amount. Our findings reflect an ASD-like communicative pattern: reduced calling amount, reduced variety in syllable usage, and parallel changes seen in *Reln*^{+/-} and *Reln*^{-/-} pups.

We examined the effect of *Vldlr* deficiency on vocal phenotype, based on our previous findings which highlighted *Vldlr* as being vocally regulated in the basal ganglia of adult male zebra finches (Hilliard et al. 2012). Changes in other genes that are critical for birdsong learning, including *Cntnp2* and *FoxP2*, have produced abnormal vocal communication patterns in neonatal mice (Burkett et al. 2015; Shu et al. 2005; Enard et al. 2009; Peñagarikano et al. 2011; Condro & White 2014). These findings underscore shared mechanisms between vocal learning and non-learning species, and validate a cross-species approach. We found that *Vldlr*^{-/-} genotype alone did not affect calling rate in mice, but did significantly affect call repertoire at both time points. These

changes were observed in both *Vldlr*^{-/-}/*Apoer2*^{+/+} and *Vldlr*^{-/-}/*Apoer2*^{-/-} groups indicating that loss of *Vldlr* is sufficient to produce these changes to the vocal repertoire. This limited syllable usage reflects a subtle ASD-like phenotype. The early vocal behavior of *Vldlr* insufficient pups had not been previously characterized.

Both *Dab1* and *Vldlr* gene dose affected the diversity of call repertoires, resulting in simpler call types (no frequency modulation, short duration) with fewer elaborate calls (jump containing, harmonic stacking, long duration). Parallels between the two mouse lines are further underscored by similarities in both the repertoire correlation and the syntax similarity measures. The more repetitive or stereotyped sequencing in both the *Dab1*^{+//lacZ} and *Vldlr*^{-/-}/*Apoer2*^{+/+} lines may reflect a subtle vocal phenotype not uncovered by call count and repertoire analyses. The genetic changes in these lines are very different and thus convergence on a high degree of syntax similarity was not predicted. In auditory playback experiments, adult female mice prefer greater call complexity from both adult males and neonates (Chabout et al. 2015; Takahashi et al. 2015). It would therefore be advantageous for pups to emit more elaborate call types in order to be retrieved and thus survive. The restricted repertoire and convergence on simple syllable usage seen here in *Dab1* and *Vldlr* deficient pups would thus be maladaptive, as is the reduction in calling rate as dams prefer to retrieve pups that call more (Bowers et al. 2013).

Sex is another factor contributing to ASD etiology. Because ASD is more prevalent in males, we characterized early vocal phenotypes in each sex and compared them, expecting an exacerbated phenotype in males. To our surprise, when pooling across wild-type controls of both lines (C57BL/6J, B6), there was no sex difference in

calling rate or repertoire. Some minimal sex differences in repertoire were observed in *Dab1* and *Vldlr* deficient pups at P7, but none that suggested that one sex was more adversely affected by the gene loss of *Dab1* or *Vldlr* than the other. Thus, sex does not appear to interact with *Dab1* or *Vldlr/Apoer2* genotype to produce a more pronounced vocal phenotype. Prior studies provide conflicting reports regarding sex differences in the calling behavior of rodents with some indicating that male neonatal rats and mice call more, or that female mice do, or that there is no difference (Hahn & Lavooy 2005). These disparate findings indicate that each species and strain should be individually tested rather than generalizing between studies regarding the influence of sex on vocal communication.

Loss of neonatal call type diversity is associated with reduced Reelin signaling as demonstrated here and in prior work. *Reln*^{+/-} and *Reln*^{-/-} pups on a similar background as used here, Romano and colleagues (Romano et al. 2013) observed increased usage of two-syllable call type, and reduced numbers of short and flat call types with increasing *Reelin* insufficiency. In our study, we likewise observe an expansion of some call types and a reduction in others. While the exact call types differed, in both studies, increasingly restricted repertoires emerged in a gene-dose dependent manner. This similar gene-dose restriction across *Reelin*, *Dab1*, and *Vldlr/Apoer2* lines indicates a newly discovered function of the canonical Reelin-signaling pathway in shaping call-type usage.

ASD is a neurodevelopmental disorder in humans, and diagnosis is based, in part, on altered developmental trajectories and unusual social communication patterns (Ozonoff et al. 2010). *Reln*^{+/-} and *Reln*^{-/-} mouse pups exhibit differential vocal

developmental trajectories; *Reln*^{+/-} pups have a delayed peak in calling and *Reln*^{-/-} pups lack a peak in calling (Romano et al. 2013). We observed similarly altered trajectories for *Dab1*^{+/*lacZ*}, *Dab1*^{*lacZ*/*lacZ*} and *Vldlr*^{-/-} *Apoer2*^{-/-} mice. These findings also suggest that, like *Reln*^{+/-} mice (Folsom & Fatemi 2013), *Dab1* insufficient mice may serve as a good ASD-risk mouse model. Future studies could determine whether or not these mice exhibit additional ASD-like behavioral features including repetitive behavior, decreased sociability, or behavioral inflexibility as adults. Once more is understood about the cellular phenotypes underlying Reelin-signaling in the basal ganglia, targeted *Dab1* knock-out mice could be used to determine if a vocal phenotype is still present.

Building on previous work (Romano et al. 2013), our findings identify a new role for the Reelin-signaling pathway in early vocal phenotypes in mice. It is noteworthy that any differences at all were observed in calling phenotype considering the high degree of inter-individual differences, particularly in call repertoire, that typify these vocalizations. Moreover, mouse pups congenitally engineered to lack a neocortex and hippocampus have indistinguishable calling patterns from wild-type pups (Hammerschmidt et al. 2015), emphasizing the significance of the deficits observed here. Since the lack of a cortex does not lead to abnormal calling, the deficits observed here may arise from alterations in subcortical structures. Notably, the basal ganglia has an established role in vocal learning (Bolhuis et al. 2010), cortico-striatal plasticity is altered in Reelin insufficient mice (Marrone et al. 2006), and abnormal basal ganglia connectivity and excitability are associated with ASD (Di Martino et al. 2011; Sears et al. 1999). Together these observations provide a relevant yet understudied anatomical locus for future

determination of the Reelin-associated neurodevelopmental mechanisms behind early vocal phenotypes.

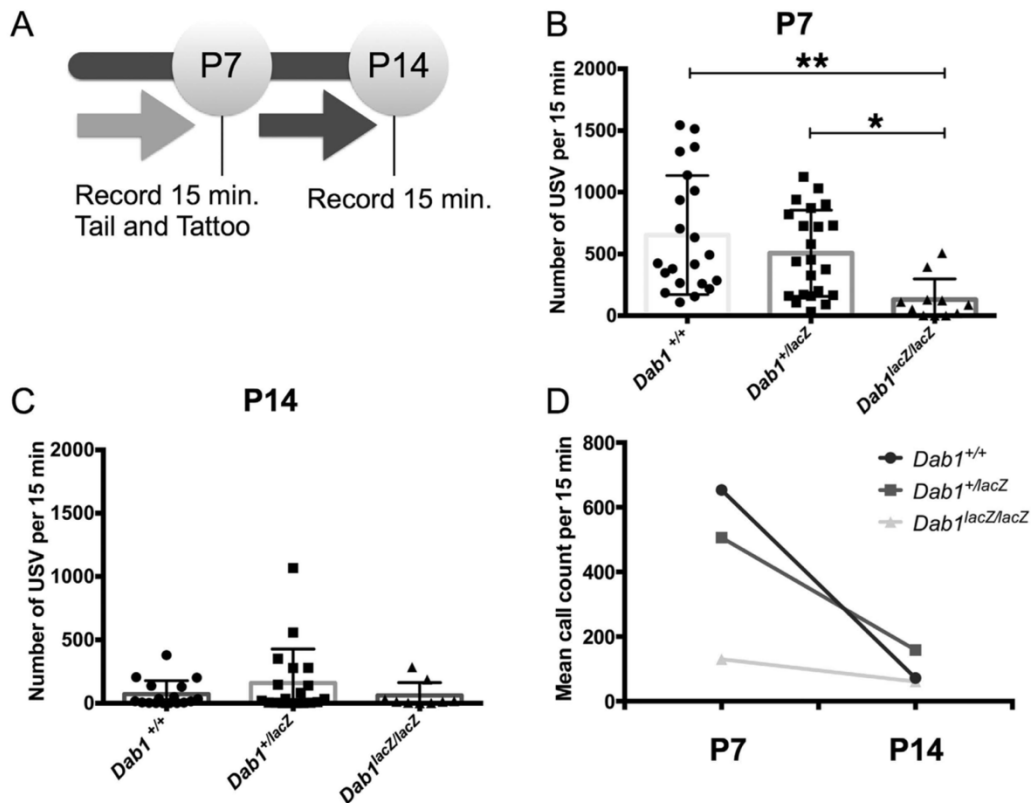


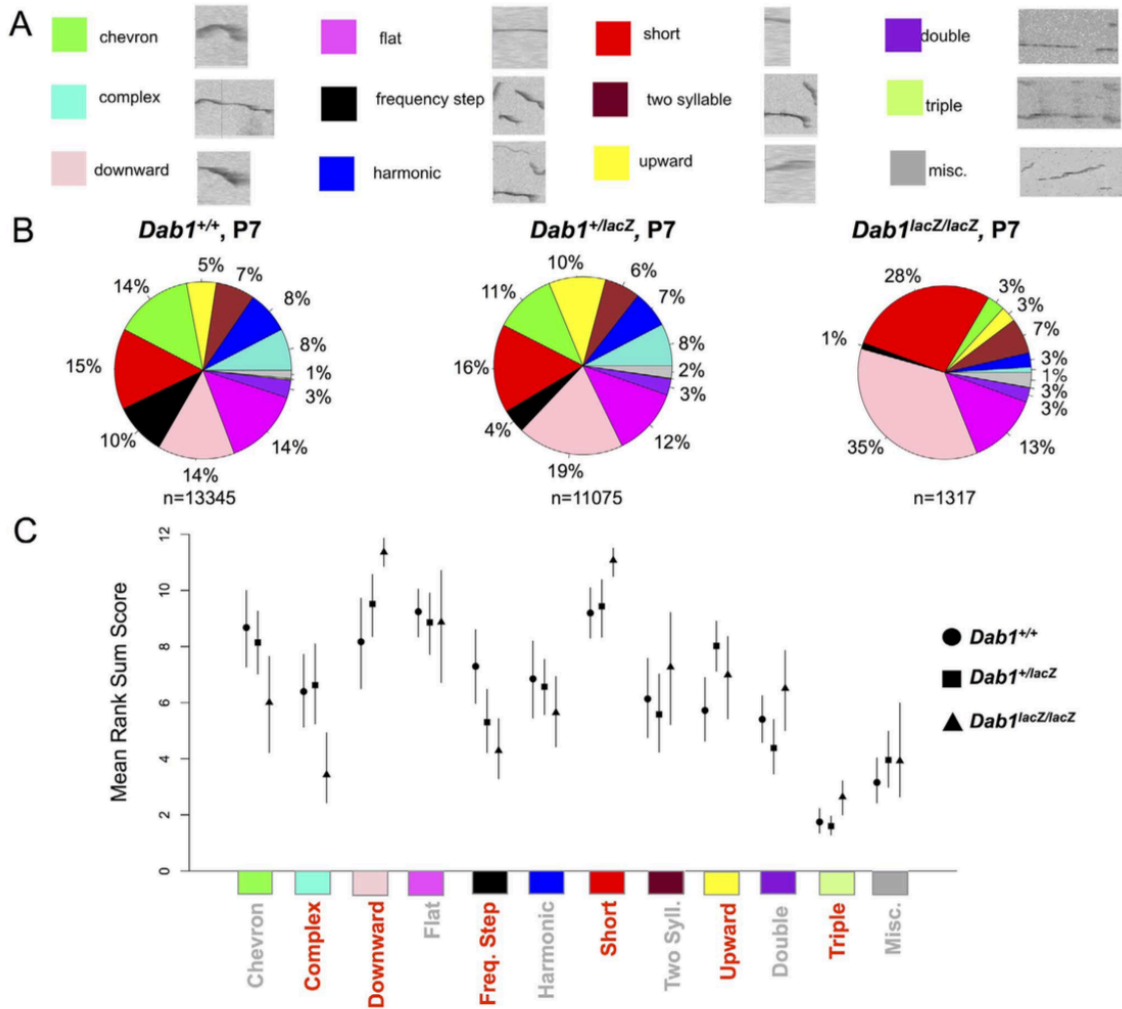
Figure 1

***Dab1* genotype and postnatal age affect pup isolation call amounts. (A)**

Experimental paradigm. (B) At P7, *Dab1* mice exhibit gene-dose dependent effects on call number: wild-type pups ($Dab1^{+/+}$) call the most, followed by heterozygote pups ($Dab1^{+/lacZ}$), while homozygous mutant pups ($Dab1^{lacZ/lacZ}$) call the least (**, $p=0.0001$; *, $p=0.0002$). (C) At P14, no differences between call rates are observed. (D)

Developmental trajectories in calling amount vary by genotype. Between P7 and P14, $Dab1^{+/+}$ pups exhibit the steepest decline (**, $p<0.0001$) followed by $Dab1^{+/lacZ}$ pups (*, $p=0.0007$). Call rate did not decline in $Dab1^{lacZ/lacZ}$ mice ($p=0.297$, NS).

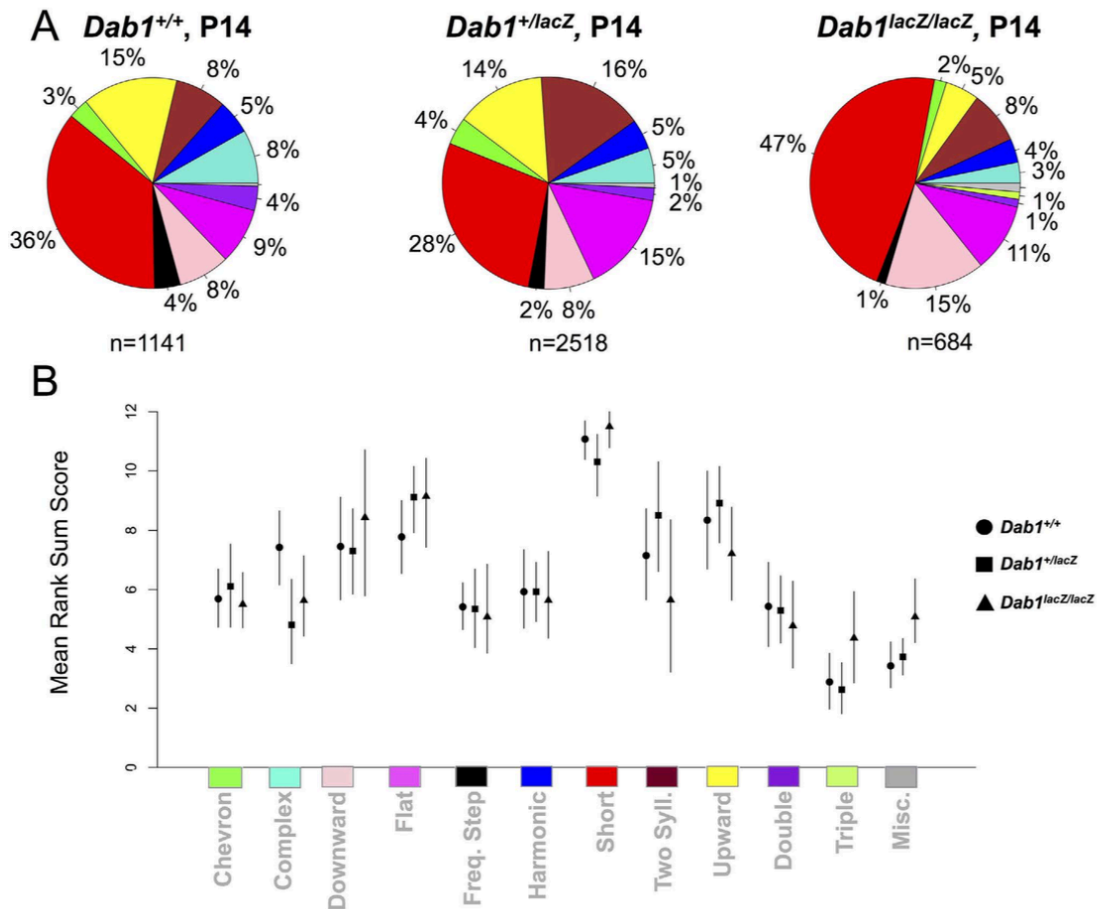
Figure 2



***Dab1* genotype affects P7 call repertoire.** (A) Representative syllables for each call cluster, known as eigen syllables, are shown with their classifications and representative colors. (The same colors are used in Figs. 3,5-6) (B) Pie charts depict P7 calling repertoires of *Dab1*^{+/+} (N=13,345 calls from 21 pups), *Dab1*^{+/lacZ} (N=11,075 calls from 22 pups), and *Dab1*^{lacZ/lacZ} mice (N=1,317 calls from 7 pups). (C) Quantitative repertoire analysis. Data are rank sum transformed such that 12 on the y axis denotes high call use probability and 1, low call use probability. Lines indicate 95% confidence intervals, shapes correspond to genotypes: Circle (*Dab1*^{+/+}), square (*Dab1*^{+/lacZ}), and

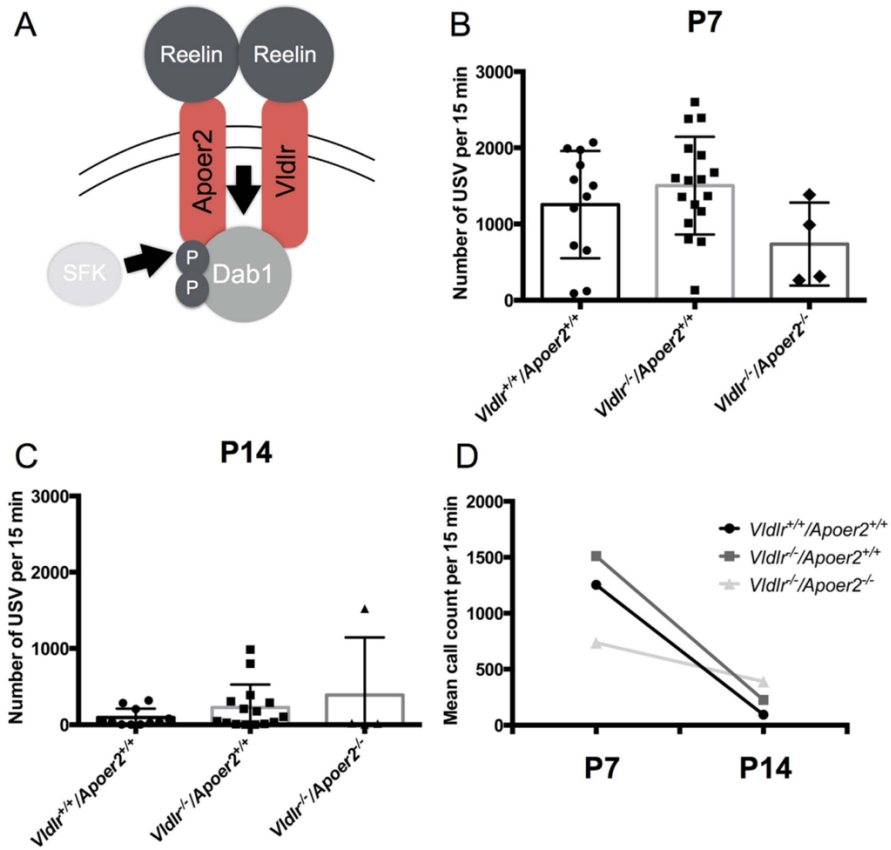
triangle (*Dab1^{lacZ/lacZ}*). Significant differences are indicated when call categories are highlighted in red on the x axis, and the 95% confidence intervals do not overlap between one or more genotypes. Differences are found for the following categories: complex, downward, frequency step, short, upward, and triple.

Figure 3



***Dab1* genotype does not affect P14 call repertoire.** (A) Call repertoires for wild-type (N=1,141 calls from 11 pups), heterozygous (N=2,518 calls from 19 pups), and homozygous mice (N=684 calls from 3 pups). (B) For each genotype, quantification shows 95% confidence intervals resampled about the median call usage. Shapes correspond to genotypes: circle (*Dab1*^{+/+}), square (*Dab1*^{+/*lacZ*}), and triangle (*Dab1*^{*lacZ*/*lacZ*}). There are no significant differences.

Figure 4



***Vldlr* and *Vldlr/Apoer2* insufficient pups have altered developmental trajectories**

in calling amount. (A) Schematic depicts the canonical Reelin-signaling pathway.

Signal is transduced via Reelin binding to receptors *Vldlr* and *Apoer2* to initiate phosphorylation of *Dab1* via Src-family kinases.

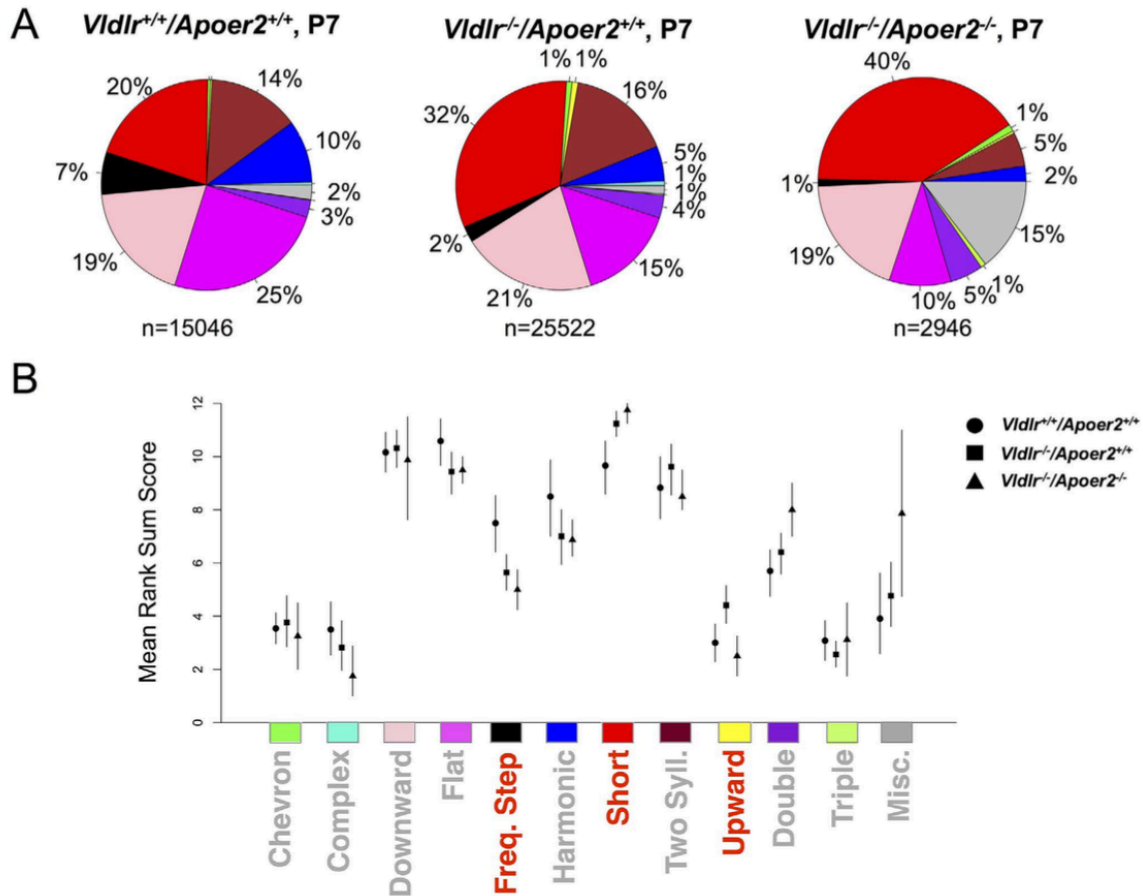
(B) Quantification of P7 call counts from wild-type pups (*Vldlr*^{+/+}/*Apoer2*^{+/+}, N=12), *Vldlr* single receptor mutants (*Vldlr*^{-/-}/*Apoer2*^{+/+}; N=18) and double receptor mutants (*Vldlr*^{-/-}/*Apoer2*^{-/-}; N=4). Trends suggest that the double receptor mutants call less than the other genotypes.

(C) Quantification of P14 call counts for pups of all three genotypes reveal no significant differences.

(D) Developmental trajectories between P7 and P14 differ by genotype. Call amounts of

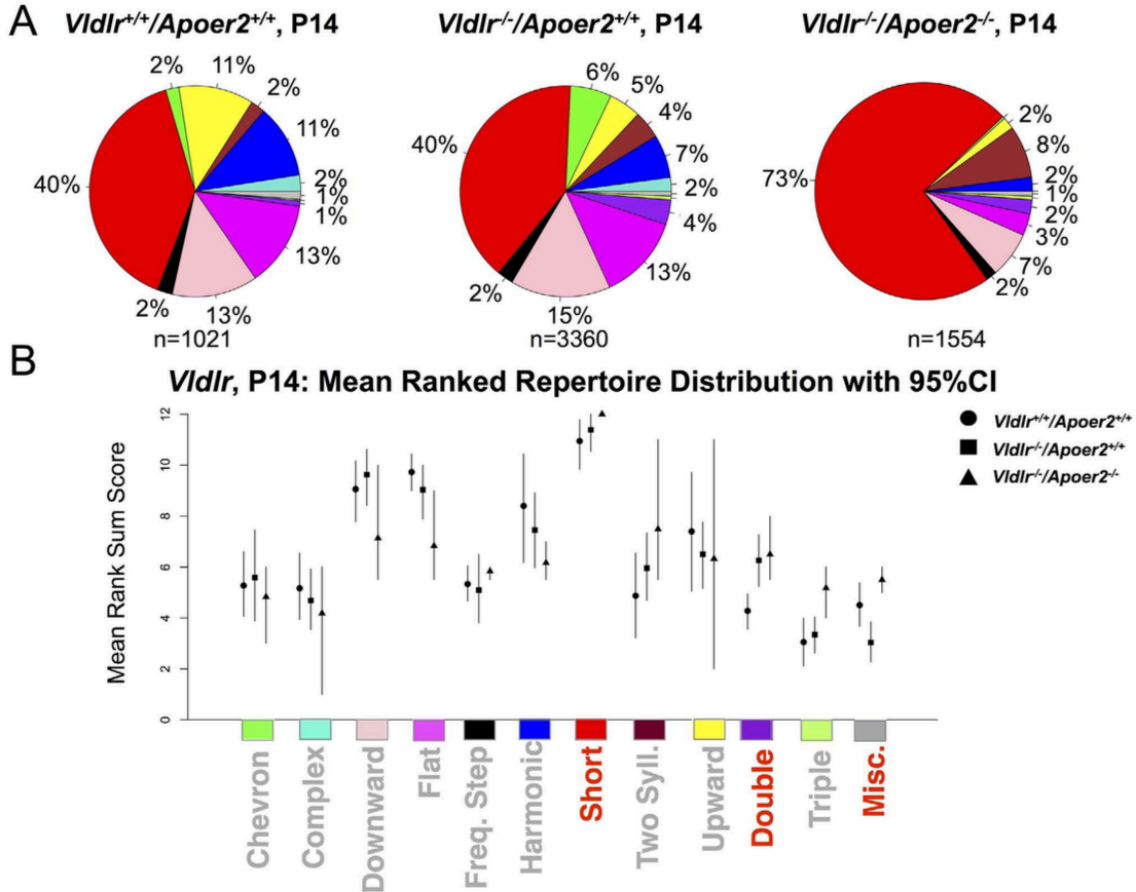
Vldlr^{+/+}/*Apoer2*^{+/+} pups ($p=0.0001$) and *Vldlr*^{-/-}/*Apoer2*^{+/+} pups decline (** $p<0.0001$) but those of *Vldlr*^{-/-}/*Apoer2*^{-/-} pups do not ($p=0.486$, NS).

Figure 5



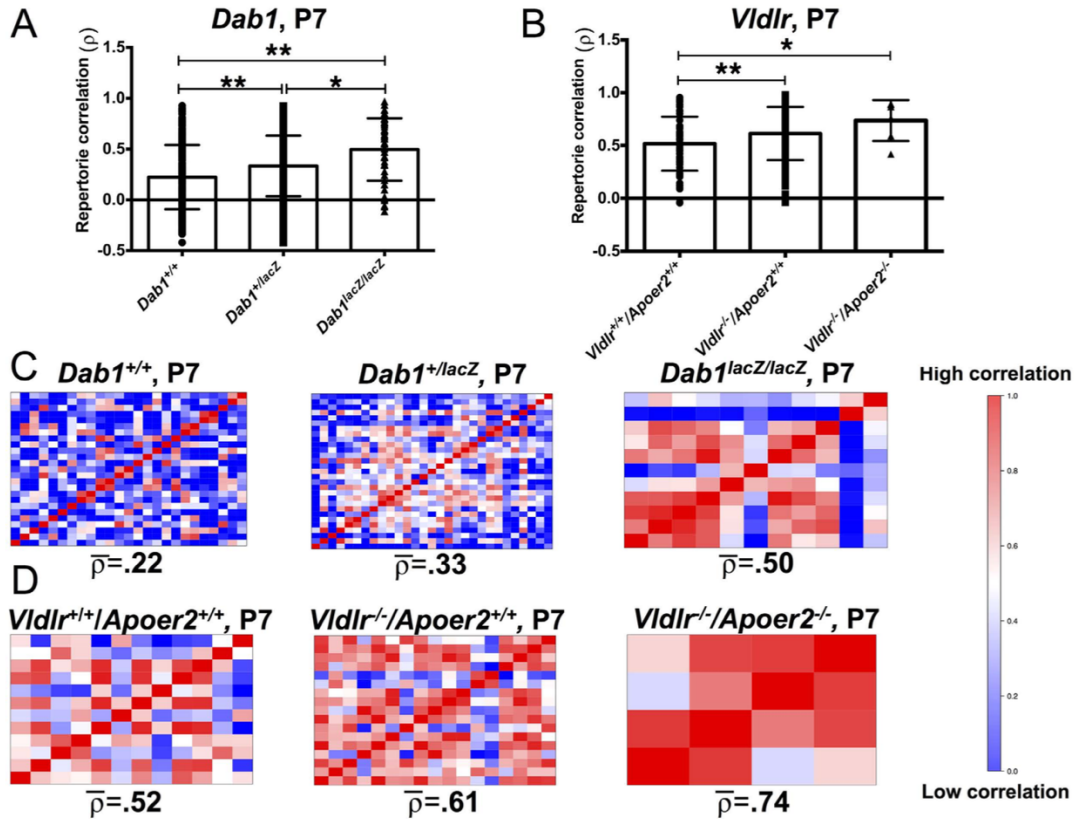
***P7* call repertoire is influenced by *Vldlr/Apoer2* genotype.** Repertoires were determined and are depicted as in Fig. 2. Mice of *Vldlr*^{+/+}/*Apoer2*^{+/+} (N=15,046 calls from 12 pups), *Vldlr*^{-/-}/*Apoer2*^{+/+} (N=25,522 calls from 18 pups), and *Vldlr*^{-/-}/*Apoer2*^{-/-} genotypes (N=2,946 from 4 pups) exhibit increasingly restricted repertoires, respectively. (B) Quantification of calling repertoire differences between genotypes. Each shape corresponds to a genotype: Circle signifies *Vldlr*^{+/+}/*Apoer2*^{+/+}; square *Vldlr*^{-/-}/*Apoer2*^{+/+}, triangle *Vldlr*^{-/-}/*Apoer2*^{-/-}. Significant differences (highlighted in red) were found for the following call types: frequency steps, short and upward.

Figure 6



P14 call repertoire is influenced by *Vldlr/Apoer2* genotype. (A) Pie charts depict call repertoires of *Vldlr*^{+/+}/*Apoer2*^{+/+} (N=1021 calls from 9 pups), *Vldlr*^{-/-}/*Apoer2*^{+/+} (N=3360 from 13 pups) and *Vldlr*^{-/-}/*Apoer2*^{-/-} mice (n=1554 calls from 3 pups). (B) Repertoire analysis shows significant differences in the short, double and miscellaneous categories as revealed by non-overlapping confidence intervals.

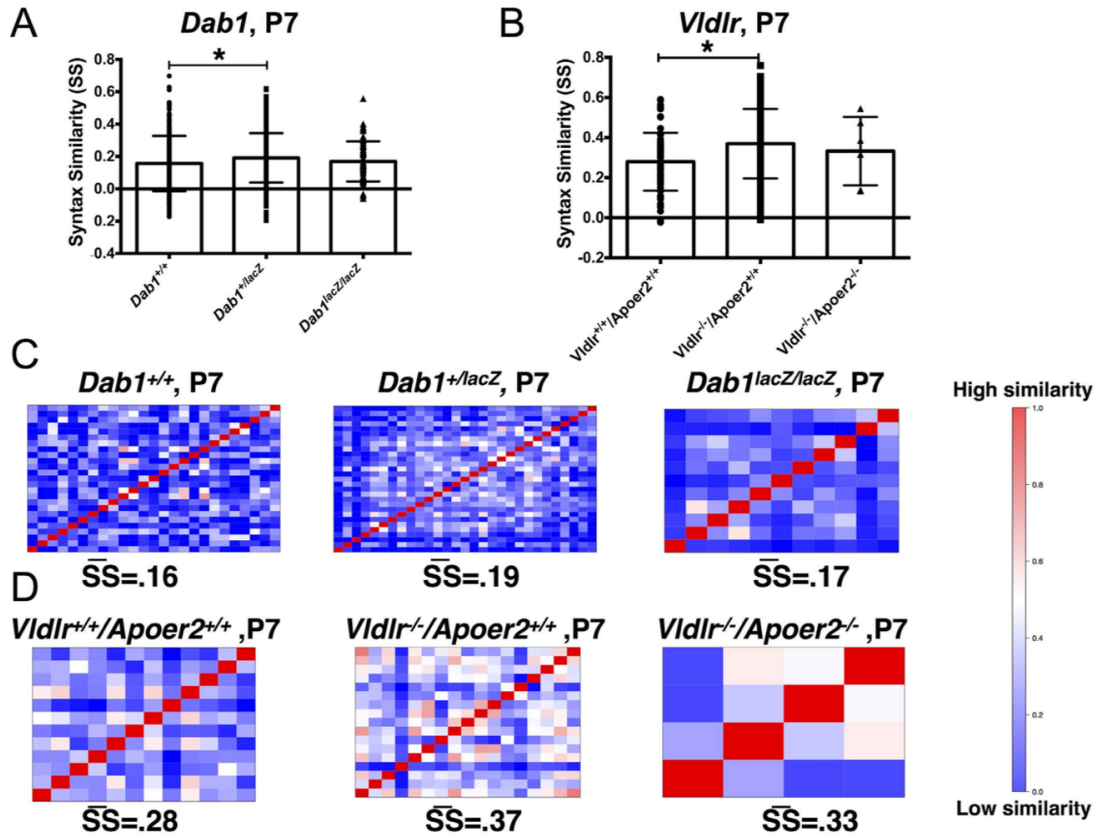
Figure 7



***Dab1* and *Vldlr/Apoer2* pups exhibit a gene-dose dependent increase in repertoire correlation at P7.** (A) Repertoire correlation scores across all animals of each genotype. *Dab1*^{+/*lacZ*} pups have higher scores, reflecting a more restricted repertoire than *Dab1*^{+/+} pups (**, $p < 0.0001$). *Dab1*^{*lacZ*/*lacZ*} have higher scores than either *Dab1*^{+/*lacZ*} (*, $p = 0.0005$) or *Dab1*^{+/+} pups (**, $p < 0.0001$). *Vldlr*^{-/-}/*Apoer2*^{+/+} have higher scores than *Vldlr*^{+/+}/*Apoer2*^{+/+} (**, $p = 0.0131$), and *Vldlr*^{-/-}/*Apoer2*^{-/-} pups exhibit a higher repertoire correlation than *Vldlr*^{+/+}/*Apoer2*^{+/+} pups (*, $p = 0.038$). This pattern of increasing repertoire correlation in gene reduced or deficient pups is parallel across both lines (*Dab1*, *Vldlr/Apoer2*). (B) Repertoire correlation matrices for *Dab1* and *Vldlr/Apoer2* mice.

Average repertoire correlation score is shown below each matrix (ρ). Red indicates high correlation, and blue indicates low correlation on a scale of 0-1.

Figure 8



***Dab1*^{+/*lacZ*} and *Vldlr*^{-/-}/*Apoer2*^{+/+} pups have high syntax similarity scores.** (A) Syntax similarity scores across all animals of each genotype. *Dab1*^{+/*lacZ*} pups have higher scores than *Dab1*^{+/+} pups (*, p=0.005). There is no detectable difference between *Dab1*^{*lacZ*/*lacZ*} and *Dab1*^{+/+} pups. *Vldlr*^{-/-}/*Apoer2*^{+/+} pups have higher scores than *Vldlr*^{+/+}/*Apoer2*^{+/+} (**, p=0.0002). *Vldlr*^{-/-}/*Apoer2*^{-/-} mice do not differ from *Vldlr*^{+/+}/*Apoer2*^{+/+}. (B) Syntax similarity matrices for *Dab1* and *Vldlr/Apoer2* mice. Average repertoire correlation score is shown below each matrix (SS). Red indicates high correlation, and blue indicates low correlation on a scale of 0-1.

References

- Abadesco, A.D. et al., 2014. Novel Disabled-1-expressing neurons identified in adult brain and spinal cord. *The European journal of neuroscience*, 39(4), pp.579–592.
- Akbarian, S. & Huang, H.-S., 2006. Molecular and cellular mechanisms of altered GAD1/GAD67 expression in schizophrenia and related disorders. *Brain research reviews*, 52(2), pp.293–304.
- Ammassari-Teule, M. et al., 2009. Reelin haploinsufficiency reduces the density of PV+ neurons in circumscribed regions of the striatum and selectively alters striatal-based behaviors. *Psychopharmacology*, 204(3), pp.511–521.
- Ashley-Koch, A.E. et al., 2007. Investigation of potential gene-gene interactions between APOE and RELN contributing to autism risk. *Psychiatric genetics*, 17(4), pp.221–226.
- Biamonte, F. et al., 2014. Associations among exposure to methylmercury, reduced Reelin expression, and gender in the cerebellum of developing mice. *Neurotoxicology*, 45, pp.67–80.
- Biamonte, F. et al., 2009. Interactions between neuroactive steroids and reelin haploinsufficiency in Purkinje cell survival. *Neurobiology of disease*, 36(1), pp.103–115.
- Bock, H.H. & Herz, J., 2003. Reelin activates SRC family tyrosine kinases in neurons. *Current biology : CB*, 13(1), pp.18–26.
- Bolhuis, J.J., Okanoya, K. & Scharff, C., 2010. Twitter evolution: converging mechanisms in birdsong and human speech. *Nature reviews. Neuroscience*, 11(11), pp.747–759.
- Bowers, J.M. et al., 2013. Foxp2 mediates sex differences in ultrasonic vocalization by rat pups and directs order of maternal retrieval. *The Journal of neuroscience : the official journal of the Society for Neuroscience*, 33(8), pp.3276–3283.
- Burkett, Z.D. et al., 2015. VoICE: A semi-automated pipeline for standardizing vocal analysis across models. *Scientific reports*, 5, p.10237.
- Caviness, V.S. & Rakic, P., 1978. Mechanisms of cortical development: a view from mutations in mice. *Annual review of neuroscience*, 1(1), pp.297–326.
- Chabout, J. et al., 2015. Male mice song syntax depends on social contexts and influences female preferences. *Frontiers in behavioral neuroscience*, 9, p.76.
- Chadman, K.K. et al., 2008. Minimal aberrant behavioral phenotypes of neuroligin-3 R451C knockin mice. *Autism research : official journal of the International Society*

- for *Autism Research*, 1(3), pp.147–158.
- Condro, M.C. & White, S.A., 2014. Recent Advances in the Genetics of Vocal Learning. *Comparative cognition & behavior reviews*, 9, pp.75–98.
- Courchesne, E. et al., 1988. Hypoplasia of cerebellar vermal lobules VI and VII in autism. *The New England journal of medicine*, 318(21), pp.1349–1354.
- Crawley, J.N., 2004. Designing mouse behavioral tasks relevant to autistic-like behaviors. *Mental retardation and developmental disabilities research reviews*, 10(4), pp.248–258.
- D'Arcangelo, G. et al., 1995. A protein related to extracellular matrix proteins deleted in the mouse mutant reeler. *Nature*, 374(6524), pp.719–723.
- D'Arcangelo, G. et al., 1999. Reelin is a ligand for lipoprotein receptors. *Neuron*, 24(2), pp.471–479.
- Day, N.F. & Fraley, E.R., 2013. Insights from a nonvocal learner on social communication. *The Journal of neuroscience : the official journal of the Society for Neuroscience*, 33(31), pp.12553–12554.
- Developmental Disabilities Monitoring Network Surveillance Year 2010 Principal Investigators Centers for Disease Control and Prevention (CDC), 2014. Prevalence of autism spectrum disorder among children aged 8 years - autism and developmental disabilities monitoring network, 11 sites, United States, 2010. *Morbidity and mortality weekly report. Surveillance summaries (Washington, D.C. : 2002)*, 63(2), pp.1–21.
- Di Martino, A. et al., 2011. Aberrant striatal functional connectivity in children with autism. *Biological psychiatry*, 69(9), pp.847–856.
- Dutta, S. et al., 2007. Reelin gene polymorphisms in the Indian population: a possible paternal 5'UTR-CGG-repeat-allele effect on autism. *American journal of medical genetics. Part B, Neuropsychiatric genetics : the official publication of the International Society of Psychiatric Genetics*, 144B(1), pp.106–112.
- Enard, W. et al., 2009. A humanized version of Foxp2 affects cortico-basal ganglia circuits in mice. *Cell*, 137(5), pp.961–971.
- Ey, E., Leblond, C.S. & Bourgeron, T., 2011. Behavioral profiles of mouse models for autism spectrum disorders. J. Crawley, E. DiCicco-Bloom, & A. J. Bailey, eds. *Autism research : official journal of the International Society for Autism Research*, 4(1), pp.5–16.
- Falconer, D.S., 1951. Two new mutants, 'trembler' and "reeler," with neurological actions in the house mouse (*Mus musculus* L.). *Journal of genetics*, 50(2), pp.192–201.

- Fatemi, S.H. et al., 2005. Reelin signaling is impaired in autism. *Biological psychiatry*, 57(7), pp.777–787.
- Folsom, T.D. & Fatemi, S.H., 2013. The involvement of Reelin in neurodevelopmental disorders. *Neuropharmacology*, 68, pp.122–135.
- Frykman, P.K. et al., 1995. Normal plasma lipoproteins and fertility in gene-targeted mice homozygous for a disruption in the gene encoding very low density lipoprotein receptor. *Proceedings of the National Academy of Sciences of the United States of America*, 92(18), pp.8453–8457.
- Goffinet, A.M. et al., 1984. Architectonic and hodological organization of the cerebellum in reeler mutant mice. *Brain research*, 318(2), pp.263–276.
- Hahn, M.E. & Lavooy, M.J., 2005. A review of the methods of studies on infant ultrasound production and maternal retrieval in small rodents. *Behavior genetics*, 35(1), pp.31–52.
- Hammerschmidt, K. et al., 2015. Mice lacking the cerebral cortex develop normal song: insights into the foundations of vocal learning. *Scientific reports*, 5, p.8808.
- Herz, J. & Chen, Y., 2006. Reelin, lipoprotein receptors and synaptic plasticity. *Nature reviews. Neuroscience*, 7(11), pp.850–859.
- Hiesberger, T. et al., 1999. Direct binding of Reelin to VLDL receptor and ApoE receptor 2 induces tyrosine phosphorylation of disabled-1 and modulates tau phosphorylation. *Neuron*, 24(2), pp.481–489.
- Hilliard, A.T. et al., 2012. Molecular microcircuitry underlies functional specification in a basal ganglia circuit dedicated to vocal learning. *Neuron*, 73(3), pp.537–552.
- Holt, R. et al., 2010. Linkage and candidate gene studies of autism spectrum disorders in European populations. *European journal of human genetics : EJHG*, 18(9), pp.1013–1019.
- Howell, B.W. et al., 1997. Neuronal position in the developing brain is regulated by mouse disabled-1. *Nature*, 389(6652), pp.733–737.
- Kelemenova, S. et al., 2010. Polymorphisms of candidate genes in Slovak autistic patients. *Psychiatric genetics*, 20(4), pp.137–139.
- Kemper, T.L. & Bauman, M.L., 1993. The contribution of neuropathologic studies to the understanding of autism. *Neurologic clinics*, 11(1), pp.175–187.
- Laviola, G. et al., 2006. Paradoxical effects of prenatal acetylcholinesterase blockade on neuro-behavioral development and drug-induced stereotypies in reeler mutant mice. *Psychopharmacology*, 187(3), pp.331–344.

- Li, H. et al., 2008. The association analysis of RELN and GRM8 genes with autistic spectrum disorder in Chinese Han population. *American journal of medical genetics. Part B, Neuropsychiatric genetics : the official publication of the International Society of Psychiatric Genetics*, 147B(2), pp.194–200.
- Li, J. et al., 2013. Association study between genes in Reelin signaling pathway and autism identifies DAB1 as a susceptibility gene in a Chinese Han population. *Progress in neuro-psychopharmacology & biological psychiatry*, 44, pp.226–232.
- Liu, W.S. et al., 2001. Down-regulation of dendritic spine and glutamic acid decarboxylase 67 expressions in the reelin haploinsufficient heterozygous reeler mouse. *Proceedings of the National Academy of Sciences of the United States of America*, 98(6), pp.3477–3482.
- Marrone, M.C. et al., 2006. Altered cortico-striatal synaptic plasticity and related behavioural impairments in reeler mice. *The European journal of neuroscience*, 24(7), pp.2061–2070.
- Mullen, B.R. et al., 2013. Decreased reelin expression and organophosphate pesticide exposure alters mouse behaviour and brain morphology. *ASN neuro*, 5(1), p.e00106.
- Nakatani, J. et al., 2009. Abnormal behavior in a chromosome-engineered mouse model for human 15q11-13 duplication seen in autism. *Cell*, 137(7), pp.1235–1246.
- Niu, S. et al., 2004. Reelin promotes hippocampal dendrite development through the VLDLR/ApoER2-Dab1 pathway. *Neuron*, 41(1), pp.71–84.
- Niu, S., Yabut, O. & D'Arcangelo, G., 2008. The Reelin signaling pathway promotes dendritic spine development in hippocampal neurons. *The Journal of neuroscience : the official journal of the Society for Neuroscience*, 28(41), pp.10339–10348.
- Noirot, E., 1966. Ultra-sounds in young rodents. I. Changes with age in albino mice. *Animal behaviour*, 14(4), pp.459–462.
- Ognibene, E., Adriani, W., Granstrem, O., et al., 2007. Impulsivity-anxiety-related behavior and profiles of morphine-induced analgesia in heterozygous reeler mice. *Brain research*, 1131(1), pp.173–180.
- Ognibene, E., Adriani, W., Macrì, S., et al., 2007. Neurobehavioural disorders in the infant reeler mouse model: interaction of genetic vulnerability and consequences of maternal separation. *Behavioural brain research*, 177(1), pp.142–149.
- Ozonoff, S. et al., 2010. A prospective study of the emergence of early behavioral signs of autism. *Journal of the American Academy of Child and Adolescent Psychiatry*, 49(3), pp.256–66.e1–2.
- Paul, R. et al., 2011. Out of the mouths of babes: vocal production in infant siblings of

- children with ASD. *Journal of child psychology and psychiatry, and allied disciplines*, 52(5), pp.588–598.
- Peñagarikano, O. et al., 2011. Absence of CNTNAP2 leads to epilepsy, neuronal migration abnormalities, and core autism-related deficits. *Cell*, 147(1), pp.235–246.
- Persico, A.M. et al., 2001. Reelin gene alleles and haplotypes as a factor predisposing to autistic disorder. *Molecular psychiatry*, 6(2), pp.150–159.
- Persico, A.M., Levitt, P. & Pimenta, A.F., 2006. Polymorphic GGC repeat differentially regulates human reelin gene expression levels. *Journal of neural transmission (Vienna, Austria : 1996)*, 113(10), pp.1373–1382.
- Pramatarova, A., Chen, K. & Howell, B.W., 2008. A genetic interaction between the APP and Dab1 genes influences brain development. *Molecular and cellular neurosciences*, 37(1), pp.178–186.
- Rice, D.S. & Curran, T., 2001. Role of the reelin signaling pathway in central nervous system development. *Annual review of neuroscience*, 24(1), pp.1005–1039.
- Romano, E. et al., 2013. Characterization of neonatal vocal and motor repertoire of reelin mutant mice. R. Zhou, ed. *PloS one*, 8(5), p.e64407.
- Scattoni, M.L., Gandhi, S.U., et al., 2008. Unusual repertoire of vocalizations in the BTBR T+tf/J mouse model of autism. W. E. Crusio, ed. *PloS one*, 3(8), p.e3067.
- Scattoni, M.L., McFarlane, H.G., et al., 2008. Reduced ultrasonic vocalizations in vasopressin 1b knockout mice. *Behavioural brain research*, 187(2), pp.371–378.
- Scearce-Levie, K. et al., 2008. Abnormal social behaviors in mice lacking Fgf17. *Genes, brain, and behavior*, 7(3), pp.344–354.
- Sears, L.L. et al., 1999. An MRI study of the basal ganglia in autism. *Progress in neuro-psychopharmacology & biological psychiatry*, 23(4), pp.613–624.
- Serajee, F.J., Zhong, H. & Mahbubul Huq, A.H.M., 2006. Association of Reelin gene polymorphisms with autism. *Genomics*, 87(1), pp.75–83.
- Sheinkopf, S.J. et al., 2012. Atypical cry acoustics in 6-month-old infants at risk for autism spectrum disorder. *Autism research : official journal of the International Society for Autism Research*, 5(5), pp.331–339.
- Shu, W. et al., 2005. Altered ultrasonic vocalization in mice with a disruption in the Foxp2 gene. *Proceedings of the National Academy of Sciences of the United States of America*, 102(27), pp.9643–9648.
- Silverman, J.L. et al., 2010. Behavioural phenotyping assays for mouse models of autism. *Nature reviews. Neuroscience*, 11(7), pp.490–502.

- Skaar, D.A. et al., 2005. Analysis of the RELN gene as a genetic risk factor for autism. *Molecular psychiatry*, 10(6), pp.563–571.
- Takahashi, T. et al., 2015. Structure and function of neonatal social communication in a genetic mouse model of autism. *Molecular psychiatry*.
- Tissir, F. & Goffinet, A.M., 2003. Reelin and brain development. *Nature reviews. Neuroscience*, 4(6), pp.496–505.
- Trommsdorff, M. et al., 1999. Reeler/Disabled-like disruption of neuronal migration in knockout mice lacking the VLDL receptor and ApoE receptor 2. *Cell*, 97(6), pp.689–701.
- Vernes, S.C. et al., 2007. High-throughput analysis of promoter occupancy reveals direct neural targets of FOXP2, a gene mutated in speech and language disorders. *American journal of human genetics*, 81(6), pp.1232–1250.
- Vorstman, J.A.S. et al., 2006. The 22q11.2 deletion in children: high rate of autistic disorders and early onset of psychotic symptoms. *Journal of the American Academy of Child and Adolescent Psychiatry*, 45(9), pp.1104–1113.
- Weeber, E.J. et al., 2002. Reelin and ApoE receptors cooperate to enhance hippocampal synaptic plasticity and learning. *The Journal of biological chemistry*, 277(42), pp.39944–39952.
- Winslow, J.T. et al., 2000. Infant vocalization, adult aggression, and fear behavior of an oxytocin null mutant mouse. *Hormones and behavior*, 37(2), pp.145–155.
- Young, D.M. et al., 2010. Altered ultrasonic vocalizations in a tuberous sclerosis mouse model of autism. *Proceedings of the National Academy of Sciences of the United States of America*, 107(24), pp.11074–11079.
- Zhubi, A. et al., 2014. Increased binding of MeCP2 to the GAD1 and RELN promoters may be mediated by an enrichment of 5-hmC in autism spectrum disorder (ASD) cerebellum. *Translational psychiatry*, 4(1), p.e349.

Chapter 4: Reelin signaling in the basal ganglia: Comparative neuroanatomy and implications for vocal behavior

Fraley, ER; Gu Y; DeLu A; Phelps PE; White SA

Abstract

Our previous work established that Reelin signaling is regulated by singing in adult male zebra finch song nucleus Area X. Here, we confirm that singing-driven regulation is also found in juvenile male (~65d) zebra finch Area X, is not observed in ventral striato-pallidum (VSP, non-song dedicated region), and is not observed in an analogous Area X region in non-vocal learning females. Injections of recombinant Reelin to Area X in juvenile finches enhances learning and song similarity to tutor at 5 days post injection, mirroring previous findings in mice where Reelin injections enhanced learning and memory. To understand the cell population that Reelin injections targeted in zebra finch, we investigated the identity of Dab1-expressing cells in Area X using immunohistochemical techniques. We identified two types of pallidal cells and cholinergic cells as being Dab1-positive. We also identified Reelin-expressing cell types in Area X: medium spiny neurons, interneurons; and compared to the basal ganglia of mice. We uncovered a striato-pallidal connection in the basal ganglia whereby Reelin is secreted by cell type/s in the striatum that target Dab-1 expressing pallidal cells. Both direct (GPI) and indirect (GPe) motor pathways appear to be involved, suggesting a broad effect of Reelin on vocal motor learning, and possibly motor learning generally.

Introduction

Reelin is a large secreted extracellular glycoprotein responsible for coordinating early neuronal migration and brain organization, particularly of laminated structures in the brain (D'Arcangelo et al. 1995; Rice & Curran 2001). Reelin has additional roles in the adult brain, including regulation of synaptic plasticity and dendritic spine density (Beffert et al. 2005; Qiu & Weeber 2007; Qiu et al. 2006; Rogers & Weeber 2008; Niu et al. 2004; Niu et al. 2008). Reelin mainly signals through two high-affinity receptors: Apolipoprotein E receptor 2 (Apoer2) and very-low-density lipoprotein receptor (Vldlr; D'Arcangelo et al. 1999; Trommsdorff et al. 1999). Binding to one or both receptors initiates downstream signaling through phosphorylation of Disabled-1 (Dab1) at critical tyrosine residues (Howell et al. 1997; Hiesberger et al. 1999). Impaired or reduced Reelin signaling has been associated with human pathologies including schizophrenia, bipolar disorder and autism spectrum disorders (ASD; Herz & Chen 2006; Lammert & Howell 2016; Persico et al. 2001). Intriguingly, supplementation of Reelin has been associated with enhanced hippocampal-based learning and memory in wild type mice (Rogers et al. 2011) and ameliorates learning and behavioral deficits observed in Reelin heterozygous mice (*Reln*^{+/-}; Rogers et al. 2013) and mice modeling Angelman syndrome (*Ube3a*^{+/-}; Hethorn et al. 2015). These effects on behavior appear to be mediated by increasing synaptic spine density in the hippocampus. Outside of the hippocampus, little is known about the role of Reelin signaling in learning.

The zebra finch is an important animal model for studying vocal learning, a process that shares many parallels to language learning in humans (Doupe & Kuhl

1999). Zebra finch males sing to court females; singing ability in males is based on exposure to an adult male tutor during two critical developmental periods (sensory acquisition period: ~d25-d65, sensorimotor learning ~d35-d90, crystallization ~d90; Y. Funabiki & K. Funabiki 2009). Lack of a tutor results in poor song quality (Marler 1997). The song control system provides a privileged network of interconnected brain regions with which we can study the neural basis of vocal learning (Nottebohm et al. 1976). One such song nucleus located in the basal ganglia, Area X, is part of the anterior forebrain pathway critical for song learning (Scharff & Nottebohm 1991). We originally observed that levels of Reelin signaling (Reelin, *Vldlr* mRNA and Vldlr protein levels; phosphorylated Dab1 levels) were regulated by singing in Area X of adult males, much like the speech and language-related transcription factor FoxP2 (Teramitsu et al. 2010; Hilliard et al. 2012; Lai et al. 2001). Additionally, we found that *Vldlr* had a co-expression pattern that was tightly interconnected to that of FoxP2 (Hilliard et al. 2012). It was later established that, as in humans (Vernes et al. 2007), *Vldlr* is a transcriptional target of FoxP2 in the zebra finch and is regulated by singing in juvenile male finches (Adam et al. 2016).

Based on our analysis of gene networks, and the tight coupling of *Vldlr* levels to singing behavior in juvenile finches, we hypothesized that Reelin signaling in Area X could subserve FoxP2 function and be important for sensorimotor learning. To test this, we first measured protein levels of Reelin and phosphorylated-Dab1 in juvenile singing and non-singing finches, to confirm that singing activates Reelin signaling in male juvenile finches. We then manipulated levels of Reelin signaling exogenously by

injecting Reelin protein directly into Area X of juvenile finches undergoing sensorimotor learning (at ~50 days post-hatch; 50d) and measured the effect on song learning.

Study of the function of Reelin signaling in the basal ganglia is somewhat limited. Mice are not vocal learners (Day & Fraley 2013) but do exhibit other forms of motor learning that require basal ganglia function. Mice lacking Reelin expression, *reeler* (*Reln*^{-/-}) have hyperexcitable cortico-striatal synapses (Marrone et al. 2006) similar to mice with altered FoxP2 (Enard et al. 2009; Groszer et al. 2008). Unlike other brain regions, the basal ganglia of *Reln*^{-/-} mice exhibit only mild migrational deficits (Nishikawa et al. 2003). *Reln*^{-/-} mice also have a significant reduction in the number of parvalbumin expressing interneurons in striatum when compared to wild-type mice (Ammassari-Teule et al. 2009). *Dab1* is expressed in a GABA-ergic cell type in the striatum of adult mice, and Reelin is co-expressed with calbindin (Sharaf et al. 2015). Reportedly, *Apoer2* is not expressed in the adult striatum and *Vldlr* is expressed only in the oligodendrocytes (Sharaf et al. 2015). Therefore, no cell in the adult murine striatum contains both receptor (*Vldlr*) and downstream signaling molecule (*Dab1*). This leaves open the possibility that, in the adult murine basal ganglia, Reelin signals to cells that are outside of the striatum.

We hypothesized that the mouse pallidum could be a target. The Allen Brain Atlas reported that *Reelin* mRNA is expressed in both the striatum and to a lesser degree in the pallidum of mice. Further, *Vldlr* and *Dab1* mRNAs are also expressed in both the striatum and pallidum while *Apoer2* is neither expressed in the striatum nor pallidum. This expression pattern suggests that Reelin signaling occurs widely across both structures and primarily utilizes *Vldlr* as the receptor. Here, we further investigate

the specific cellular identify of Reelin and Dab1 expressing cells in the basal ganglia of adult mouse.

Because Area X is an unusual striato-pallidal hybrid structure (Carrillo & Doupe 2004; Reiner et al. 2004; Goldberg et al. 2010; Goldberg & Fee 2010) with a specialized function, it is possible that Reelin signaling in zebra finches could occur in this region differently than in the mouse. Previous findings in the male canary, another songbird, indicate that *Reelin*, *Apoer2*, *Vldlr* and *Dab1* are all expressed in male Area X (Balthazart et al. 2008). *Apoer2* expression in Area X is a surprising finding that contrasts with recent work in the murine basal ganglia (Sharaf et al. 2015). Area X is also unique in that it has high levels of neurogenesis even into adulthood (Nottebohm 2004).

In the present study, we investigate specific cell types expressing Reelin and Dab1 in male zebra finch Area X in order to understand the role Reelin signaling plays in song learning. We also compare to these findings to those of the mouse basal ganglia.

Through this comparative approach we aim to refine how Reelin signaling works in the basal ganglia across both animal models. Differences between the two could reflect the molecular mechanisms underpinning vocal learning.

Methods

Behavior. Animal use was in accordance with NIH guidelines for experiments involving vertebrate animals and approved by the University of California at Los Angeles Chancellor's Institutional Animal Care and Use Committee. Behaviorally regulated birds were collected 3 hours after lights on in the morning, as described (Miller et al. 2008). A set of 6 birds (~65d) were allowed to sing in isolation chambers without a female (UD), and a set of 6 birds (~65d) were kept from singing by the presence of an investigator (NS). Numbers of motifs or calls were quantified by hand using spectrograms generated in Sound Analysis Pro (Figure 1c; Tchernichovski et al. 2000).

Song Analysis. Finches were individually recorded in sound attenuation chambers using Shure SM57 microphones. Songs were, digitized with a PreSonus Firepod, and processed using SAP recorder (44.1 kHz sampling rate, 24 bit depth)(Tchernichovski et al. 2000). Songs were then analyzed using Similarity Index scores to compare pupil to tutor as described (Mandelblat-Cerf & Fee 2014). Similarity index scores were compared between treatment groups (RL versus HEK, Figure 2 c – f) using one-tailed, paired T-tests. Paired T-tests were assessed because the same animals were measured at two different time points. One-tailed statistics were used because prior studies in the hippocampus suggested that Reelin supplementation should improve learning (Rogers & Weeber 2008; Rogers et al. 2011). To normalize the similarity index scores, an effect size was calculated ($(post - pre) / (pre + post)$). Effect sizes were then analyzed at each time point using unpaired, one-tailed T-tests.

Western blot tissue preparation. Birds were overdosed via isoflurane inhalation and

rapidly decapitated. Brains were dissected and flash frozen in liquid nitrogen, then stored at -80°C until use. Brains were micro-dissected for Area X or VSP in males, or a region of similar depth and orientation in females “Area X”. Microdissections were punched using 20 gauge Leuer (BD) adaptors to a depth of 1 mm as described (Miller et al. 2008). Sections of the remaining brain tissue were thionin-stained to assess the accuracy of the tissues punches. Only accurate punches were used in further analyses. Protein punches were stored in RIPA lysis buffer with protease inhibitors at -80°C until use. Protein punches were homogenized, mixed with loading buffer, and then boiled in preparation for Western blotting.

Western blotting and quantification. Western blots were run as described (Hilliard et al. 2012). Antibodies used for western blotting are shown in Table 2. Quantification of immunosignals was conducted using Image J (NIH) and Prism (Graphpad). All protein levels were normalized using signals for Gapdh. Normalized values were then compared between groups using unpaired, one-tailed T-tests (UD v NS, Figure 1b). Normalized protein levels were plotted per number of vocalizations for each animal (Figure 1d, e). Linear regression analysis was run on the data set, and R^2 values reported.

Cell cultures. Human embryonic kidney cells (HEK293) stably transfected with a vector that expresses Reelin (*pCrl*; D’Arcangelo et al. 1995) were cultured as described (Qiu & Weeber 2007). Cells were grown for ~2 weeks until 90% confluent in Dulbecco’s Modified Eagle Medium (DMEM; Sigma-Aldrich) enriched with Fetal Bovine Serum (FBS; Peak Serum). 72 hours before collection, cells were washed 3 times with warmed phosphate saline buffer (PBS) and enriched media was replaced with DMEM alone. The

day of collection, media was aspirated into a centrifugal filter unit (Amicon Ultra- 15, Ultracel 100k) within a 50 mL collection tube. Samples were centrifuged for 10 minutes at 600 x g (Beckman Coulter, Rotor GH3-8). 15mL of PBS was then added and the sample was spun again for 10 minutes at 600 x g. We achieved a concentration of ~8.5 μ M, and recombinant Reelin extract identity was confirmed using Western blotting (Figure 2b, inset). Full length and cleavage products were observed at ~ 350 and 150kD.

Bilateral Reelin injections to Area X. Pairs of male siblings were acoustically recorded in sound attenuation chambers from ~d45 until the morning before surgery (~d50). Birds were allowed to sing 3 hours in the morning for pre-surgery song analysis. Birds were fasted for 30 minutes prior to surgery then anesthetized using isoflurane gas, and placed into the stereotactic apparatus (Herb Adams engineering). For all injections, the bird's head angle was 45 degrees, and Area X was targeted using the following coordinates: 5.15mm rostral, 1.6mm lateral, 3.2mm deep. Injection volumes totaled 250nL on each side (Area X) and were delivered in a series of 5x 50nL injections with 30 seconds between injections. Scalp incisions were sealed with dental cement (A-M Systems), and birds were given Meloxicam post-surgery (Boehringer Ingelheim). Birds were returned to sound attenuation chambers and recorded until ~d80.

Unilateral Reelin injections to Area X. One set of birds (N=2) was injected with RL on the right side and control media (HEK) on the left in the same manner as the bilaterally injected birds. Song analysis was not conducted on these animals. Birds were sacrificed

and brains extracted and micro-punched for Area X at 3 and 5 days post injection as described above (Western blot tissue preparation).

Immunohistochemistry tissue preparation. All birds used for immunohistochemical analyses were zebra finch males (~65d-120d). Birds were overdosed with isoflurane gas, and then perfused with warmed saline solution followed by 4% paraformaldehyde in phosphate buffered saline (PBS). Brains were dissected and cryoprotected in 30% sucrose solution for a minimum of 3 days. Brains were then mounted using Optimal Cutting Temperature Compound (OCT, Tissue-Tek) and rapidly frozen on dry ice. Brains were cryosectioned at ~-20°C (Leica, CM1900). 40 µm sections were collected on glass slides (Fisherbrand Colorfrost Plus) and used for analyses.

Mice used in this study were all male wild-type mice (~2 months). Mice were perfused using 4% paraformaldehyde in PBS, post-fixed for 3 hours in 4% paraformaldehyde, and then cryoprotected in 30% sucrose solution for 2 days. Tissue was then blocked in OCT and stored in -80°C until cryosectioning at ~-20°C (Leica). 40 µm sections were collected and mounted on glass slides (Fisherbrand Colorfrost Plus) and used for analyses.

Immunohistochemistry. Sections on slides were outlined with PAP Pen (Ted Pella Inc.) and allowed to dry for 20 minutes. We used conventional techniques as follows: Slides were washed with PBS with 0.3% Triton 10 minutes, then placed in blocking for 1 hour, 5% Normal Donkey serum (NDS); followed by overnight incubation of primary antibody in 3% NDS (See Table 2 for antibody list and concentrations). The next day, slides were washed in PBS-Tween followed by incubation in 1:500 concentration of

secondary antibody for 2 hours (Alexafluor Donkey anti-goat 488, Alexafluor donkey anti-goat 548, Alexafluor donkey anti-rabbit 555, Alexafluor donkey anti-rabbit 488). Slides were washed again with PBS-Tween and mounted (ProLong Gold w/ DAPI, Molecular Probes).

For Tyramide signal amplification we followed protocol reported by Yvone et al. 2017: Slides were washed with Tris-buffered saline with 0.3% Triton (TNT). Blocking steps included: 1) 30 minute incubation in 1% H₂O₂ and 0.1% sodium azide 2) TNB 0.1M Tris-HCl, 0.15M NaCl, 0.5% Blocking reagent (PerkinElmer FP10203) Serial avidin and biotin incubations (Vector Laboratories). Overnight incubation in primary diluted in TNB. (Primary antibody concentrations used in Table 2). The next day, slides were washed with TNT, and secondary bridge antibody was used at 1:800 in TNB for 1 hour (Jackson Laboratories, biotinylated donkey anti-mouse, biotinylated donkey anti-rabbit, biotinylated donkey anti-rat). Slides were washed in TNT and then incubated in streptavidin-HRP at 1:800 in TNB for 1 hour (Vector Labs). Slides were washed and then reacted with TSA-kits for Fluorescein, Cy3, or Cy5 (Perkin Elmer). Slides were washed in TNT and mounted (ProLong Gold with DAPI, Molecular Probes) prior to visualization.

Immunofluorescent visualization. Slides were visualized using a confocal microscope (Zeiss, LSM 800) and software (Zen Digital Imaging Software). Z-stacks were created with ~1 μ M slices, and used to determine co-localization.

Results

Behavioral regulation of Reelin-signaling is specific to males and to song nucleus

Area X in juvenile zebra finches. We previously determined that in Area X of adult male zebra finches, levels of Reelin expression and Dab1 phosphorylation were higher in the undirected singing (UD) birds compared to non-singing (NS) birds (Hilliard et al. 2012). Here, we compared the level of Reelin protein and Dab1 phosphorylation in juvenile (~65d) male Area X of UD and NS birds (Figure 1a). To determine if the effect is specific to Area X, we also analyzed a region of the ventral striato-pallidum (VSP) that subserves non-vocal motor function. Additionally, we asked if Reelin protein and Dab1 phosphorylation are regulated by the unlearned vocalizations of juvenile female zebra finches within a region analogous to Area X in males (“Area X”). Western blot quantification indicated that Reelin (~150kD) and phosphorylated Dab1 (~61kD) levels were higher in the UD condition compared to NS only in Area X of juvenile males (Figure 1b; one tailed t-test: Reelin $p=0.05$, $N=8$; Dab1 $p=0.01$, $N=8$), similar to what we had observed in adult males²⁵. We also observed a positive correlation between Reelin levels in Area X and the number of motifs sung by juvenile males (Figure 1c, d; $R^2=0.91$). In contrast, there was no correlation between Reelin levels in the VSP and the number of motifs sung by for males (Figure 1d, middle panel). Nor was there a correlation between Reelin levels in female “Area X” and calling (Figure 1d, right panel). Likewise, the correlation between Dab1 phosphorylation in Area X or VSP and the number motifs sung by males was only significant in Area X (Figure 1e, dotted line; $R^2=0.90$). There was no correlation between Dab1 phosphorylation in “Area X” of

females and calling amount (Figure 1e). These results indicate that behavioral regulation of the Reelin-signaling pathway occurs in male juvenile finches and, within the basal ganglia, is specific to Area X.

Reelin supplementation acutely enhances song learning. Pairs of zebra finch male siblings were individually placed into sound attenuation chambers at ~45d and acoustically recorded (Figure 2a). At this age, male finches are engaged in the sensorimotor phase of song learning and practicing their songs (UD) in the chambers. Recombinant Reelin (RL) was isolated from cell media as previously described (Weeber et al. 2002; Qiu & Weeber 2007; Rogers et al. 2011). At 50d, half of the sibling pairs received injections of RL into Area X bilaterally. The other half received injections of mock cell media without Reelin (HEK) as the control. The purified RL used for injection contained the full length (~440kD) isoform and two cleavage products (~330kD, ~150kD; Figure 2b, inset). Finches were recorded until 60d, and songs were analyzed using similarity index software as previously described (Mandelblat-Cerf & Fee 2014) (Figure 2c - e).

In order to test that exogenous RL stimulated endogenous Reelin-signaling within Area X, a separate subset of 50d birds were injected on the right side with RL and the left side with control media (HEK). Levels of phosphorylated Dab1, the intracellular signaling molecule of the canonical Reelin-signaling pathway, were measured on each side at 3 and 5 days post injection (Figure 2b). We observed increased levels of phosphorylated Dab1 in Area X of the RL injected hemisphere compared to the HEK

injected hemisphere. These observations suggest that exogenous RL injected into zebra finch Area X activates Reelin-signaling.

Previous reports of exogenous Reelin injected into mouse cerebrospinal fluid revealed behavioral effects in the hippocampus at 5 days post injection (Rogers et al. 2011). We therefore assessed song learning at that time point (see Methods). At 5 days post injection, RL injected pupils had songs that were more similar to those of their tutors than were HEK injected siblings (RL: One tailed, paired T-test, $p=0.01$, $N=6$; HEK: One tailed, paired T-test, $p=0.32$, $N=6$; Figure 2c, d). Differences between the two groups were less pronounced at 10 days post injection (RL: One tailed, paired T-test, $p=0.07$, $N=6$; HEK: One tailed, paired T-test, $p=0.17$, $N=6$; Figure 2d). Importantly, we did not observe differences in similarity index scores between the RL and HEK groups before surgery (two-tailed, unpaired t-test $p=0.96$, Figure 2e).

We then looked at effect sizes in order to normalize the data, and more effectively compare pre- and post- surgery similarity index scores across groups. Effect sizes were significantly different at 5 days post injection, when RL birds had a strong positive increase in similarity index scores whereas HEK birds had an effect size ~zero (Figure 2f, Two-tailed unpaired T-test, $p=0.01$). At 10 days post injection, no significant difference between effect sizes was observed (Figure 2f, two-tailed unpaired t-test, $p=0.37$). Thus, bilateral Reelin injections to Area X enhanced song learning acutely (5 days post injection) in juvenile male zebra finches.

Reelin and Dab1 expression and distribution in the basal ganglia of mouse and zebra finch. To better understand the mechanisms underlying the singing-driven

regulation of Reelin signaling and its enhancement on learning in the zebra finch, we conducted a series of immunohistochemical studies. Simultaneous parallel experiments in the basal ganglia of each species enabled us to determine similarities and differences and thereby highlight neural mechanisms specific to vocal-learning birds. Reelin immunostaining in the mouse revealed prominent expression in the caudate putamen (CPu; Figure 3b, c). Reelin-positive cells were quite numerous and widely distributed throughout the region. In the zebra finch basal ganglia, Reelin-expressing cells were located throughout VSP and Area X, with a more dense concentration of cells within Area X (Figure 3d, e). This expression was similar to what has been previously described for both *Reelin* mRNA and Reelin protein in Area X of canary (Balthazart & Ball 2014).

Dab1 serves as a marker for cells that can respond to Reelin signal through the canonical pathway. In mouse, Dab1 expression is particularly robust in the globus pallidus (GP; Figure 3f, g). Based on mRNA expression profiling of the CPu, we expected to see Dab1-positive cells in that region, however, Dab1 expression in mouse CPu was quite low and cells were difficult to identify. In the zebra finch, Dab1 positive cells are scattered throughout Area X and VSP (Figure 3 h, i). Two groups of Dab1 positive cells are observed in Area X, one is intensely stained for Dab1 and contains cells with large (~13 μm) somata; the other group contains smaller, lightly staining cells (~7 μm). These Dab1 immunostaining patterns replicate previous immunohistochemical findings in canary and zebra finch male Area X (Balthazart & Ball 2014; Adam et al. 2016).

Reelin and Darpp-32 co-expression patterns in mouse and zebra finch basal

ganglia. Reelin expression in the mouse appeared in the mouse CPu which mostly contains medium spiny neurons (MSNs). We hypothesized that Reelin is expressed in MSNs across both species. Protein phosphatase 1 regulatory inhibitor subunit 1B (Darpp-32) is a marker for certain MSNs (Table 1). We immunostained for Reelin and Darpp-32 in mouse CPu (Figure 4a – f) and zebra finch Area X (Figure 4g – l). Anti-Reelin and Darpp-32 antibodies co-stained many cells in mouse CPu (Figure 4a - c, arrows). These cells exhibited the morphology and size of MSNs, and many Reelin positive cells expressed Darpp-32 (Figure 4c – f). Unexpectedly, in zebra finch Area X, Reelin and Darpp-32-positive cells were rarely co-stained (Figure 4g – l). Low levels of Reelin colocalized with Darpp32 (Figure 4j – l, double arrows), but intensely staining Reelin cells did not co-express Darpp-32. This leaves open the possibility that cell types other than MSNs are a source of Reelin in zebra finch Area X.

Reelin and FoxP2 co-expression patterns in mouse and zebra finch basal ganglia.

FoxP2 is another marker for MSNs (Table 1). We next asked if Reelin and FoxP2 were colocalized in MSNs in each species. In the mouse CPu, co-staining of Reelin and FoxP2 was evident (Figure 5a – f). FoxP2-positive cells were co-stained for Reelin (Figure 5a – c, arrows). At high resolution, the Reelin and FoxP2 co-staining cells were strikingly similar in appearance to the Reelin and Darpp-32 co-staining cells (Figure 5d – f, double arrows). In zebra finch Area X, Reelin and FoxP2 co-staining was rarely observed (Figure 5g – l). In summary, in zebra finch Area X, we observed a population

of brightly staining Reelin-positive cells that did not express FoxP2, further suggesting a non-MSN source of Reelin in Area X.

Reelin is expressed in two populations of interneurons in zebra finch Area X.

Zebra finch Area X is composed of multiple cell types. The structure contains a hybrid of striatal and pallidal cells, and includes multiple phenotypes of interneurons (Reiner et al. 2004; Carrillo & Doupe 2004; Goldberg & Fee 2010; Goldberg et al. 2010) (Table 1). GABAergic interneuron cell populations of the striatum can be divided using different cell markers including: Parvalbumin, somatostatin/nNOS/neuropeptide Y, calretinin, and choline acetyltransferase (ChAT). We hypothesized that one or more interneuron populations would express Reelin because in other brain regions of the mouse, such as cortex, adult GABAergic interneurons are a source of Reelin (Ramos-Moreno et al. 2006). Immunostaining for the interneuron marker calretinin and Reelin (Figure 6a – f, arrows) revealed that some, but not all Reelin-expressing cells co-stained for calretinin (~1 in 20).

Somatostatin-positive interneurons are strikingly sexually dimorphic in their distribution throughout the song control system of zebra finches (Bottjer et al. 1997). Compared with females, males have higher concentrations of somatostatin-positive interneurons within the song control nuclei, including Area X, as well as in auditory regions essential for song learning (Bottjer et al. 1997). As described above, because we observed a sex difference in Reelin-signaling behavioral regulation, we hypothesized that if Reelin was expressed in somatostatin interneurons, this could provide a cellular basis underlying that sex difference. Indeed, immunostaining

experiments for somatostatin revealed cells co-stained for Reelin (Figure 6g – l, arrows). Therefore, in addition to some MSNs, two interneuron populations that express calretinin or somatostatin also express Reelin within zebra finch Area X.

Dab1 and Nkx2.1 co-localize in zebra finch Area X but not in mouse globus

pallidus. In the mouse, we observed a high level of Dab1 in the pallidum (Figure 3 e, f). We suspected therefore, that in the zebra finch Area X, Dab1 would also be expressed in a pallidal cell-type. Because Area X is a hybrid structure composed of striatum and pallidum, which, in mammals, are anatomically distinct; we had to rely on markers for distinct pallidal cell types. Nkx2.1 is a homeobox transcription factor that marks cells originating from the medial ganglionic eminence (MGE; Puelles et al. 2000). After migration, these cells develop into striatal interneurons and pallidal cells (Marin et al. 2000). In mice, loss of Nkx2.1 expression results in a re-specification of pallidum to striatum and a decrease in ChAT-positive cells and other interneurons in the basal ganglia and other structures (Sussel et al. 1999). In the zebra finch, immunostaining for Nkx2.1 was used to identify a cell population similar to that of the indirect pallidal pathway (GPe; Carrillo & Doupe 2004).

Immunostaining for Nkx2.1 and Dab1 in Area X revealed numerous cells that exhibited co-staining (Figure 7g – i, arrows). Nkx2.1 and Dab1 co-stained in somewhat large cells (~13 um, Figure 7j – l, double arrows). In contrast, antibodies against Nkx2.1 and Dab1 did not co-stain cells in the mouse globus pallidus (GP, Figure 7a – c). Higher magnification imaging showed that Nkx2.1 cells were present in mouse GP, but none expressed Dab1 (Figure 7d – f, double arrows). In mouse (Marin et al. 2000), chicken

(Abellán & Medina 2009), and zebra finch (Garcia-Calero & Scharff 2013), Nkx2.1 is postnatally downregulated in certain subsets of cells. Thus, raising the possibility that some cells of MGE origin no longer express Nkx2.1 in adulthood.

Dab1 is expressed in cholinergic cells in zebra finch Area X but not in mouse.

Nkx2.1 expression alone does not conclusively identify the pallidal cell type within Area X (Table 1)(Carrillo & Doupe 2004). Nkx2.1 expression is also observed in the cell bodies of mature cholinergic interneurons. To determine the cellular phenotype of Dab1 positive cells, we immunostained Area X for ChAT and Dab1. As expected, we observed cells that were co-labeled for ChAT and Dab1 in Area X (Figure 8g – i, arrows). These cells were large (~13um) and nearly all ChAT cells stained for Dab1 (Figure 8j – l). In contrast, in the mouse few cells stained for ChAT in the GP (Figure 8a – c), and ChAT-positive cells were never found co-stained with Dab1 in the GP or CPu (Figure 8 d – f, double arrows). To summarize, a contrast is observed between zebra finch and mouse basal ganglia, whereby ChAT and Dab1 co-stained cells in Area X but not in the mouse GP or CPu.

Both cholinergic interneurons and indirect pallidal-like neurons express Dab1 in zebra finch Area X. Dab1 and ChAT co-expression in Area X raised the possibility that the only Nkx2.1 cell population that expresses Dab1 are the cholinergic interneurons. To distinguish these sub-populations, we then triple labeled cells within Area X for ChAT, Dab1, and Nkx2.1 expression. We found cells that expressed Nkx2.1, Dab1, and ChAT (Figure 9 a – d, arrows). We also found that some Nkx2.1 cells co-stained with

Dab1 but not ChAT (Figure 9 a – d, arrowheads). Higher magnification showed that these latter cells were aspiny, and slightly smaller than the cholinergic interneurons (Figure 9 e – h, double arrows). These results indicate that Dab1 is expressed in a Nkx2.1 population that is not a cholinergic interneuron species, and is likely the indirect pallidal (GPe) cells within Area X. This parallels what is observed in mouse, where Dab1 is expressed in the lateral GP (GPe) indicating Reelin-signaling could affect the indirect motor pathway.

Dab1 and Lant6 co-localize in pallidal cells of both mouse and zebra finch Area X.

Lant6 is a marker of projecting pallidal cells across species (Reiner et al. 2004; Reiner 1987; Brauth et al. 1986; Reiner & Carraway 1985). Here, we asked if direct pallidal neurons (GPi) express Dab1. In the medial GP of mice, we found some cells that co-expressed Dab1 and Lant6 (Figure 10a – c, arrows). However, not all GPi neurons expressed Dab1 (Figure 10a – c, arrowheads). Confocal images of the medial GP revealed that the cells expressing Lant6 and Dab1 are large (~15um; Figure 10d – f, double arrows). In the zebra finch, cells in Area X also co-stained for Lant6 and Dab1 (Figure 10g – i, arrows). High resolution imaging revealed that the cells type were large (~13um; Figure 10 j – l, double arrows). In summary, we uncovered Dab1 expression in direct projecting pallidal cells across both mouse and zebra finch species. This suggests that Reelin-signaling could also affect the direct motor pathway.

Discussion

This study confirmed that similar to adult zebra finches, Reelin signaling is regulated by singing in Area X of juvenile zebra finches. Behavioral regulation was found to be specific to song nucleus Area X and was only observed in males. Thus, Reelin-signaling in Area X is behaviorally regulated throughout the life of the male zebra finch and is probably important to both song learning and maintenance. To further probe the role Reelin-signaling plays in vocal learning, we artificially elevated levels of Reelin-signaling by injecting Reelin directly into Area X of juvenile male finches undergoing sensorimotor song learning. We found that Reelin injection to Area X acutely enhanced song learning (5 days post injection). This parallels the enhancement of hippocampal-based learning observed in Reelin injected mice (Rogers et al. 2011; Rogers et al. 2013; Hethorn et al. 2015). We believe that this is the first example of a Reelin-mediated enhancement of learning in the basal ganglia and in zebra finch. Our data suggest that in Area X, the Reelin-signaling pathway contributes to song learning.

It is likely that, similar to the murine hippocampus, Reelin supplementation is acting to enhance dendritic spine density and plasticity within Area X (Rogers & Weeber 2008; Rogers et al. 2011; Hethorn et al. 2015; Rogers et al. 2013). One locus of enhancement could be the cortico-striatal synapse because: 1) Dab1 is observed in some MSNs, 2) NMDAR maturation is regulated by Reelin, and 3) *reeler* mice have abnormal cortico-striatal plasticity (Groc et al. 2007; Marrone et al. 2006; Adam et al. 2016). This does not rule out the involvement of other classes of neurons. We observed strong Dab1 expression in pallidal cells of Area X. Therefore, enhancement of dendritic

spine density could also occur at the striato-pallidal synapse. This would effectively mediate the output of Area X. Because cholinergic interneurons also expressed Dab1, Reelin signaling could also impact Area X through the regulating microcircuit excitability intrinsic to Area X. It is possible that Reelin is simultaneously affecting all three Dab1 expressing cell types in Area X, and thus creating a robust effect across the nucleus.

We observed that when juvenile male finches sing, Reelin signaling increases in Area X, replicating what we had previously observed in adults (Hilliard et al. 2012). At the same time, *Vldlr* expression decreases when birds sing (Hilliard et al. 2012; Adam et al. 2016). This result is somewhat surprising given that activation of the Reelin pathway involves Reelin binding to its receptors, one of which is *Vldlr*. However, this result is consistent given that *Vldlr* transcription is activated by FoxP2. When birds sing UD song, Area X FoxP2 levels go down (Teramitsu & White 2006; Hilliard et al. 2012; Adam et al. 2016), thus *Vldlr* transcription is no longer enhanced.

This scenario is plausible in those medium spiny neurons that co-express FoxP2, *Vldlr* and Dab1. However, we also observed Dab1 in other cell types (pallidal, cholinergic and expressing interneurons) that do not express FoxP2. *Vldlr* expression in these cells could therefore evade behavioral regulation and remain high during singing. Additionally, unlike the murine basal ganglia, the other Reelin receptor, *Apoer2*, is expressed in mature Area X (Balthazart & Ball 2014). Reelin could thus signal through *Apoer2* in addition to *Vldlr* in zebra finch Area X.

In Area X, there is a high degree of neuronal turnover that continues into adulthood (Alvarez-Buylla & Kirn 1997). Reelin has well established roles in regulating neuronal migration during development, and continues to be expressed in regions of

high neurogenesis in the adult dentate gyrus (Herz & Chen 2006). Reelin signaling could thus play a role in guiding and incorporating newly born neurons to Area X. Reelin supplementation in Area X could elicit an increase in neurogenesis. We observed some cells that co-expressed doublecortin, a marker of adult neurogenesis, and Dab1 near the ventricle. Moreover, cells in the region co-expressed Apoer2 and high levels of FoxP2, a marker of cells destined to become medium spiny neurons in Area X (Thompson et al. 2013; Rochefort et al. 2007). This evidence suggests that cells migrating cells to Area X are maybe influenced by Reelin signaling, but further investigation into the relationship between Reelin in Area X and neurogenesis/neural recruitment is needed. Increasing song stereotypy correlates with a decline in neurogenesis (Pytte et al. 2007). Conversely, increasing levels of neurogenesis may facilitate exploration of vocal motor space (Woolley & Kao 2015), which could underlie the enhancement of song learning observed here.

Neuroanatomical studies into the identity of Reelin signaling cells of Area X were guided by our previous findings in the mouse. We originally observed robust Dab1 signal in both the lateral (GPe, indirect motor pathway) and medial (GPi, direct motor pathway) segments of the murine globus pallidus. Here, we confirmed that pallidal cells in Area X also express Dab1. This provides a striking parallel across species, and suggests a common mechanism whereby Reelin secreted by striatal cells could target Dab1-positive cells in the pallidum. We also observed striking differences between zebra finch Area X and mouse basal ganglia. In the zebra finch, Dab1 is also expressed in the cholinergic interneurons. Cholinergic Dab1-positive neurons however, were not observed in any region of the mouse basal ganglia. Our studies suggest that projecting

pallidal cells (Lant6-positive) express Dab1, representing an important cell type for Reelin signaling in the region. Future studies could examine the globus pallidus of *Dab1*^{-/-} mice, for it is likely there are organizational, structural, or plasticity changes in the region.

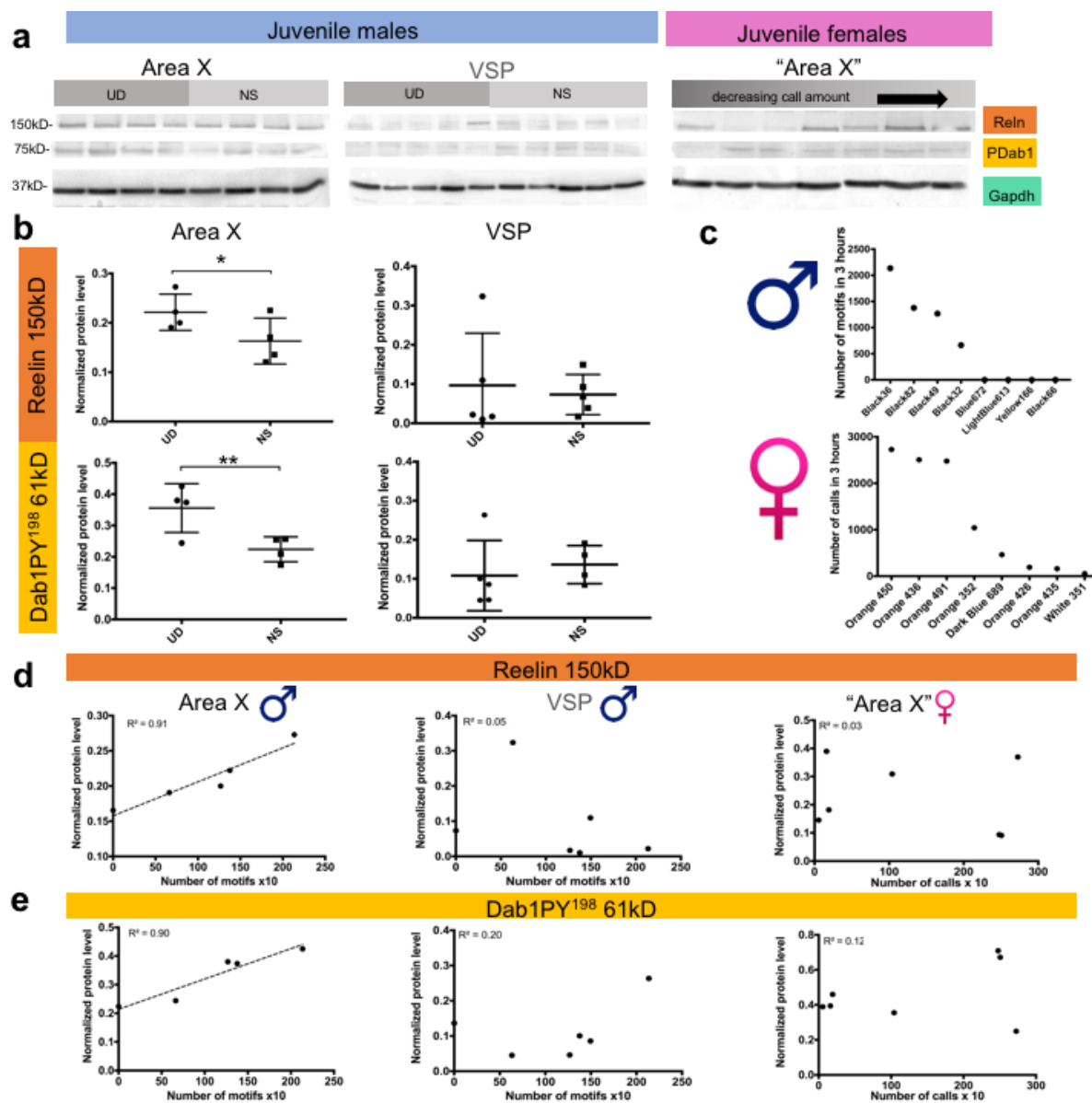
Another contrast between the zebra finch Area X and mouse basal ganglia is the source of Reelin. In the mouse caudate-putamen, medium spiny neurons appeared to be the primary source of Reelin. In the zebra finch, Reelin expression was observed in a minority of medium spiny neurons, but was also found in calretinin expressing and somatostatin expressing interneurons. Somatostatin interneurons are sexually dimorphic in the zebra finch, being densely populated in the song control system of male finches compared to brain areas at the same level in females (Bottjer et al. 1997). We did not observe behavioral regulation of Reelin signaling in female zebra finch "Area X." This could be due to the lack of one of the Reelin sources in the brain region. We therefore suggest that the sex difference in behavioral regulation of Reelin that we observed between male and female zebra finches could be partly due to the sparser somatostatin interneuron population in female finches.

Differences observed between the mouse and zebra finch basal ganglia likely reflect the unusual organization of Area X. Area X is a hybrid of striatal and pallidal cells in one structure (Carrillo & Doupe 2004; Reiner et al. 2004; Goldberg & Fee 2010; Person et al. 2008; Farries et al. 2005). Based on evolutionary evidence, the separation of striatum and pallidum happened long ago; separate structures are observed in the early vertebrates including lobe-finned fishes (e.g. lungfish), ray finned fishes (e.g. teleost zebrafish), and cartilaginous fishes (e.g. lesser-spotted dogfish) (Medina et al.

2014). Therefore, Area X containing both striatum and pallidum is not a holdover from a more ancient basal ganglia organization, but rather a result of a more recent hybridization of the two brain regions. This hybridization, or morphing of a group of cells into a separate structure, likely occurred to optimize the region's specialized function for song learning. Pallidal cells in the direct motor pathway (GPi) of Area X that project to DLM exhibit enkephalin staining (Carrillo & Doupe 2004). This immunohistochemical profile is typical of medium spiny neurons projecting out of the rodent caudate putamen to GPi. Pallidal neurons that project out of Area X in particular have dual striatal and pallidal characteristics. Differences in expression patterns of Reelin signaling components may also reflect specialization in Area X that subserves vocal learning in finches, but is absent in the non-vocal learning mouse (Mahrt et al. 2013; Kikusui et al. 2011; Hammerschmidt et al. 2015).

Humans are vocal learners. The role that Reelin-signaling plays in the human basal ganglia is not well-described, yet, based on mRNA expression there are some parallels to the rodent and avian basal ganglia. In the humans, *Reelin* is primarily expressed in the body of the caudate (Lein et al. 2007; Pfenning et al. 2014). *Vldlr* is expressed in both the putamen as well as in the external and internal portions of globus pallidus (GPe and GPi; Lein et al. 2007). *Apoer2* does not exhibit expression in any region of the human basal ganglia (Allen Brain Atlas). *Dab1* is expressed in the pallidum of the direct motor pathway (GPi). Future studies focusing on cell types expressing Reelin-signaling components in the human basal ganglia will give insight into the whether the function of Reelin- signaling in the brain region is more like that of non-vocal learning mammals or vocal learning birds.

Figure 1



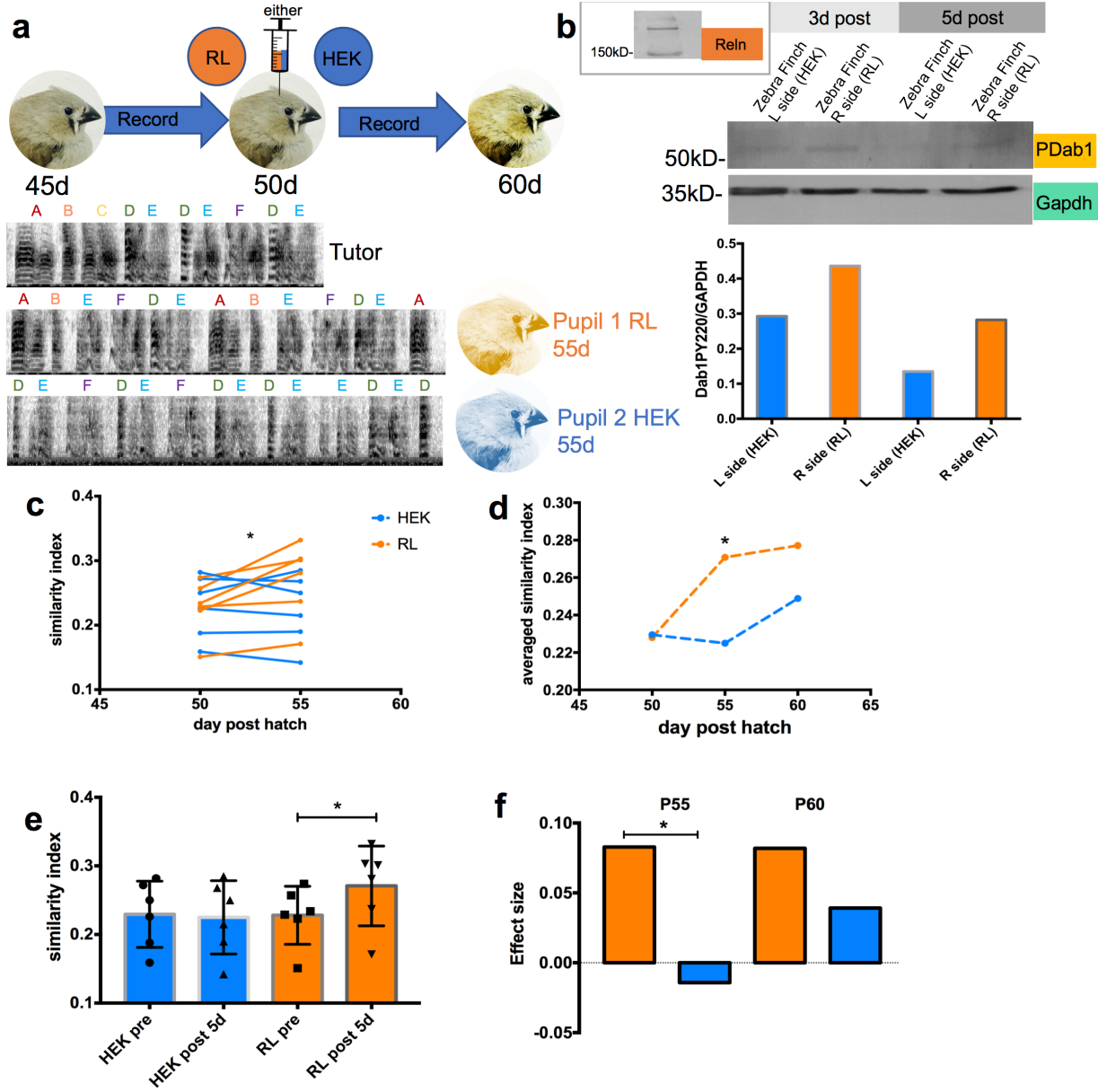
Behavioral regulation of Reelin-signaling is specific to males and to song nucleus

Area X in juvenile zebra finches.

(a) Western blots depict protein levels of Reelin, phosphorylated Dab1 (Y220), and the control Gapdh in singing (UD) and non-singing (NS) 65d finches. Male Area X, male ventro-striatal pallidum (VSP), and a basal ganglia region at the level of male Area X ("Area X") in females are compared. (b) Quantification of the blots shown in (a). In Area X, Reelin and Dab1PY220 levels were higher in the

UD birds compared with NS birds (* $p=0.05$, ** $p=0.01$; $N=8$). No difference was observed in the VSP. (c) Number of vocalizations made by male (song motifs) and female (calls) finches shown in (a). (d) Levels of Reelin protein in Area X or VSP are plotted as a function of the amount of singing in males or calling in “Area X” of females. A significant correlation is observed only in male Area X (dotted line; $R^2=0.91$). (e) Levels of phosphorylated Dab1 in Area X or VSP are plotted as a function of singing in males or calling in “Area X” of females. A positive correlation is observed only in male Area X (dotted line; $R^2=0.90$).

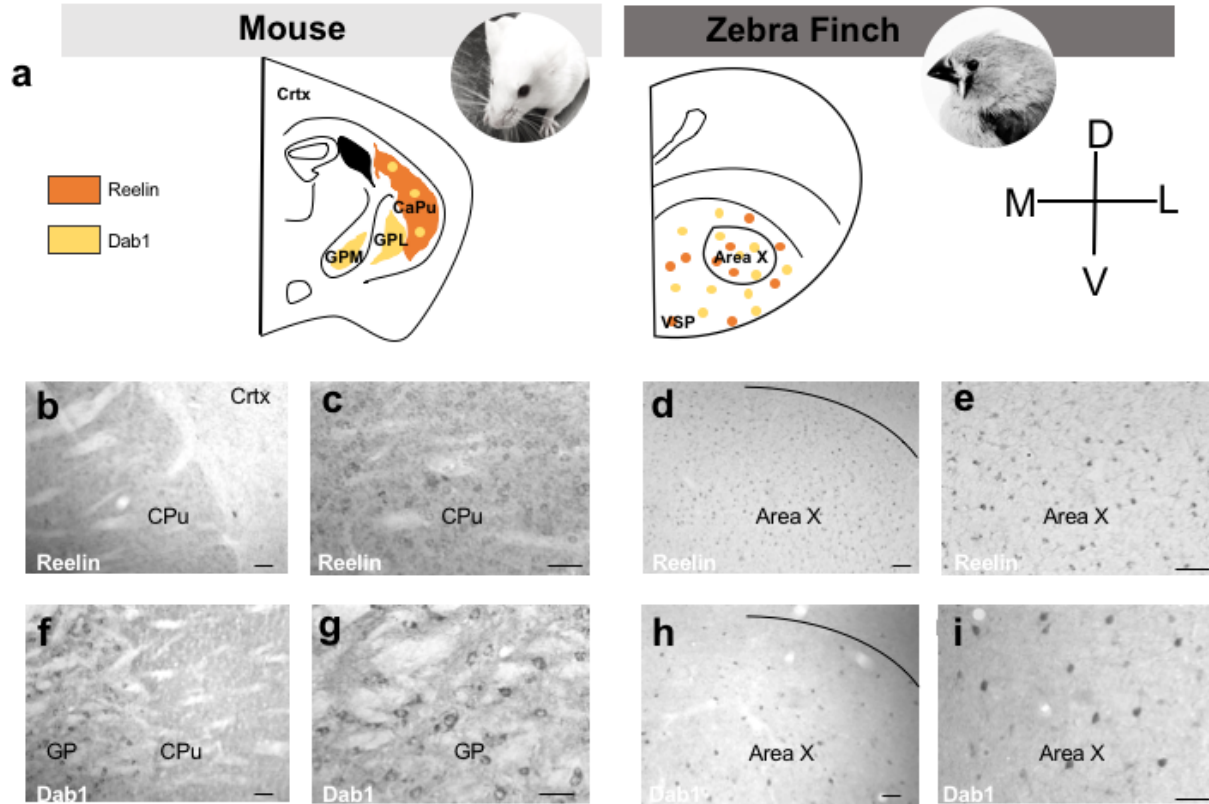
Figure 2



Reelin supplementation acutely enhances song learning. (a) Top, the experimental paradigm is shown: Male zebra finches were placed in sound attenuation chambers at 45d and their vocalizations recorded. At 50d, sibling males received injections of either HEK media (HEK) or Reelin conditioned media (RL) into Area X bilaterally. Birds were then recorded until 60d. Bottom, exemplar spectrograms of a tutor and his two pupils.

Syllables are indicated by colored letters. Pupil 1 was injected with RL whereas pupil 2 received HEK. (b) Inset: Western blot shows Reelin purification product from HEK cells transfected with Reelin expressing pCrl plasmid. Full length (~440kD) Reelin and 2 cleavage products are observed. To assess whether Reelin injections activated the canonical signaling pathway, a subset of 50d birds received an injection of HEK in one hemisphere (L side) and Reelin on the other (R side). Area X was punched bilaterally ~4 days later. Western blots show levels of Dab1 phosphorylation at tyrosine 220 on each side. Below) Graph indicates greater levels on the side of the Reelin-injected hemispheres. (c) To assess song learning pre- versus post- surgery, a similarity index was calculated for each pupil. Five days post-surgery, the songs of RL-injected pupils were more similar to their tutors than were those of HEK-injected pupils ($p=0.01$; $N=6$ per group). (d) Average similarity index scores from (c) with the addition of 60d songs. (e) Similarity index pre- and post-surgery for HEK and RL injected birds. No significant difference was observed between groups prior to surgery ($p=0.88$, $N=12$). Similarity index scores of HEK injected pupils did not improve 5 days post-surgery ($p=0.32$, $N=6$) whereas those for RL- injected pupils did ($p=0.01$, $N=6$). (f) Effect size at 5 (55d) and 10 days (60d) post-surgery. At the earlier time point, there is a strong positive effect in the RL-injected birds (orange bars) that is not apparent in HEK injected pupils (blue bars). At 10 days post-surgery, both groups exhibit positive effect sizes.

Figure 3



Reelin and Dab1 expression and distribution in the basal ganglia of mouse and zebra finch. (a) Schematic summarizing immunohistochemical results for Reelin (orange) and Dab1 (yellow) expression as observed in the experiments below. Coordinates: D=dorsal, V=ventral, L=lateral, M=medial. (b) Reelin immunostaining in the mouse caudate putamen (CPu). (c) Enlargement of mouse CPU. (d) Reelin immunostaining in the zebra finch basal ganglia, including Area X. Line indicates the striatopallidal border. (e) Enlargement of zebra finch Area X. (f) Dab1 immunostaining in the mouse CPU and globus pallidus (GP) shows particularly robust expression in the GP. (g) Enlargement of mouse GP. (h) Dab1 immunostaining in the basal ganglia of zebra finch including Area X. (i) Enlargement of Area X. Scale bars=50µm.

Table 1

Cell type	Markers	Projects to	Average Perikaryal size	Firing Pattern
striatal medium spiny neuron (MSN)	GAD, FoxP2, Darpp-32, Substance P	pallidal within X(Gpi)	~7 μ m, 5-10 μ m	(SN) Medium spiny neuron firing
striatal medium spiny neuron (MSN)	GAD, FoxP2, Darpp-32, Enkephalin	pallidal within X(Gpe)	~7 μ m, 5-10 μ m	(SN) Medium spiny neuron firing
Pallidal (Gpe) like	GAD, Nkx2.1 /TTF1	STN	~13 μ m	(AF) Aspiny fast firing
Pallidal (Gpi) like	GAD, LANT6, Enkephalin	DLM	~13 μ m	(AF) Aspiny fast firing
striatal interneuron	GAD, Parv, LANT6	striatal MSNs	~9 μ m	(FS) Fast spiking
striatal interneuron	GAD, Parvalbumin	striatal MSNs	~7.5 μ m	(FS) Fast spiking
striatal interneuron	GAD, Somatostatin, nNOS, NPY	striatal MSNs	~7 μ m	(LTS) low threshold to spiking
cholinergic interneuron	ChAT, Nkx2.1	striatal MSNs	~13 μ m	(LA)Late activating
striatal interneuron	GAD, Calretinin, Calbindin	striatal MSNs	~9 μ m	(LTS) Low threshold to spiking
migrating neurons	Hu, Doublecortin, FoxP2 (high), PSA-NCAM	NA	~5 μ m	NA

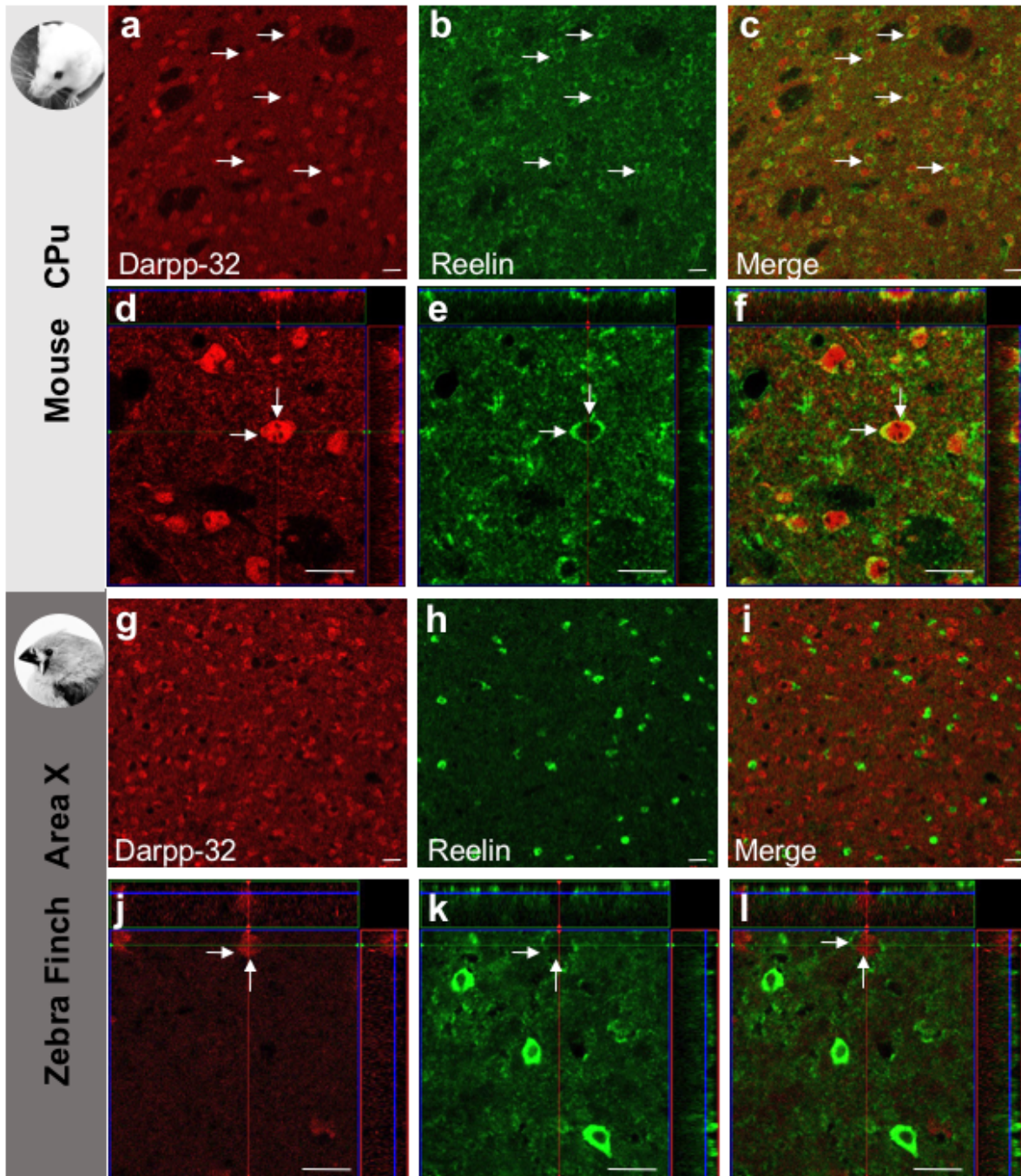
Cell types in Area X of the zebra finch. Table depicts cell markers for different cell types.

Table 2

Marker	Source	Host	Conditions	used in
LANT6	R. Carraway	Rabbit	1 to 250 w/TSA	ZF & M
Nkx2.1	Neomarkers (8G7G3/1)	Mouse	1 to 500 w/TSA	ZF & M
ChAT	Chemicon (AB144P)	Goat	1 to 100	ZF & M
FoxP2	Abcam (ab1307)	Goat	1 to 500	ZF & M
Darpp-32	Cell Signaling (#2302)	Rabbit	1 to 500	ZF & M
Calretinin	Swant (7699/4)	Rabbit	1 to 1,000	ZF
Somatostatin	Milipore clone YC7	Rat	1 to 500 w/TSA	ZF
Doublecortin	Santa Cruz (c-18) (sc-8066)	Goat	1 to 100	ZF
Dab1 (B3)	Brian Howell	Rabbit	1:10k (ZF) 1:5k(M) w/TSA	ZF & M
Reelin 142	Milipore (MAB5366)	Mouse	1:250 w/TSA	ZF & M
Apoer2	J. Herz	Rabbit	1 to 500	ZF & M
Dab1PY220	Santa Cruz (133292)	Rabbit	1 to 250	ZF (WB only)
Dab1 PY198	Thermo-Fisher (44906G)	Rabbit	1 to 250	ZF (WB only)

Antibodies and conditions for the results of this paper. Table depicts conditions and antibodies used in immunostaining (see Methods).

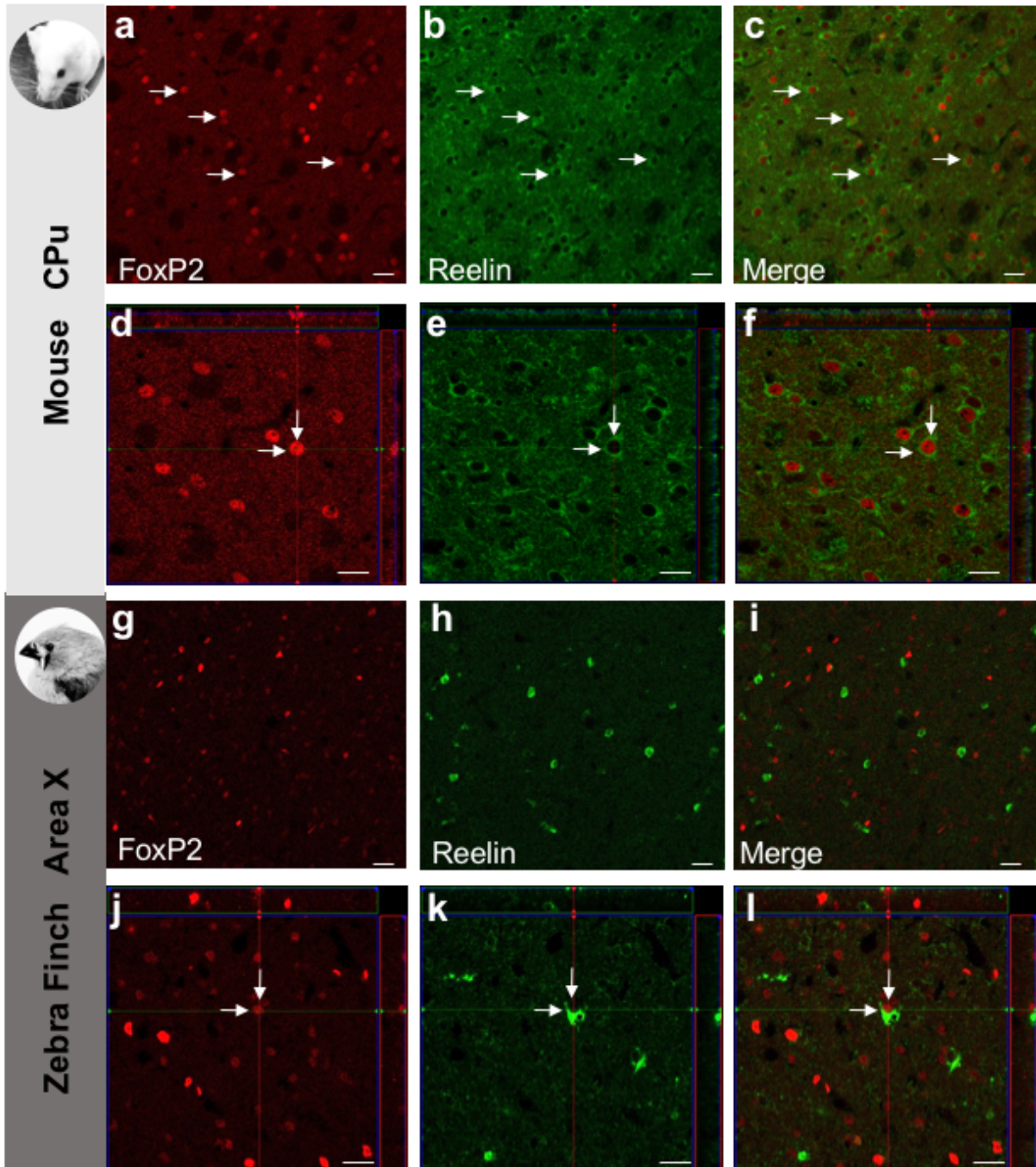
Figure 4



Reelin and Darpp-32 co-expression patterns in mouse and zebra finch basal ganglia. In mouse CPU, Darpp-32 (red; a) and Reelin, (green; b) co-localize (merge; c) indicating that some medium spiny neurons are a source of Reelin. Arrows indicate co-

expression. (d – f) Darpp32, Reelin, and merged images at higher magnification. In zebra finch Area X, Darpp-32 (red; g) and Reelin (green; h) rarely co-localize (i).(j - l) Higher magnification images indicate that some Darpp-32-expressing cells exhibit a low level of immunostaining for Reelin. Intense Reelin expression, however, appears mainly in cells that do not express Darpp-32. Scale bars=20µm.

Figure 5

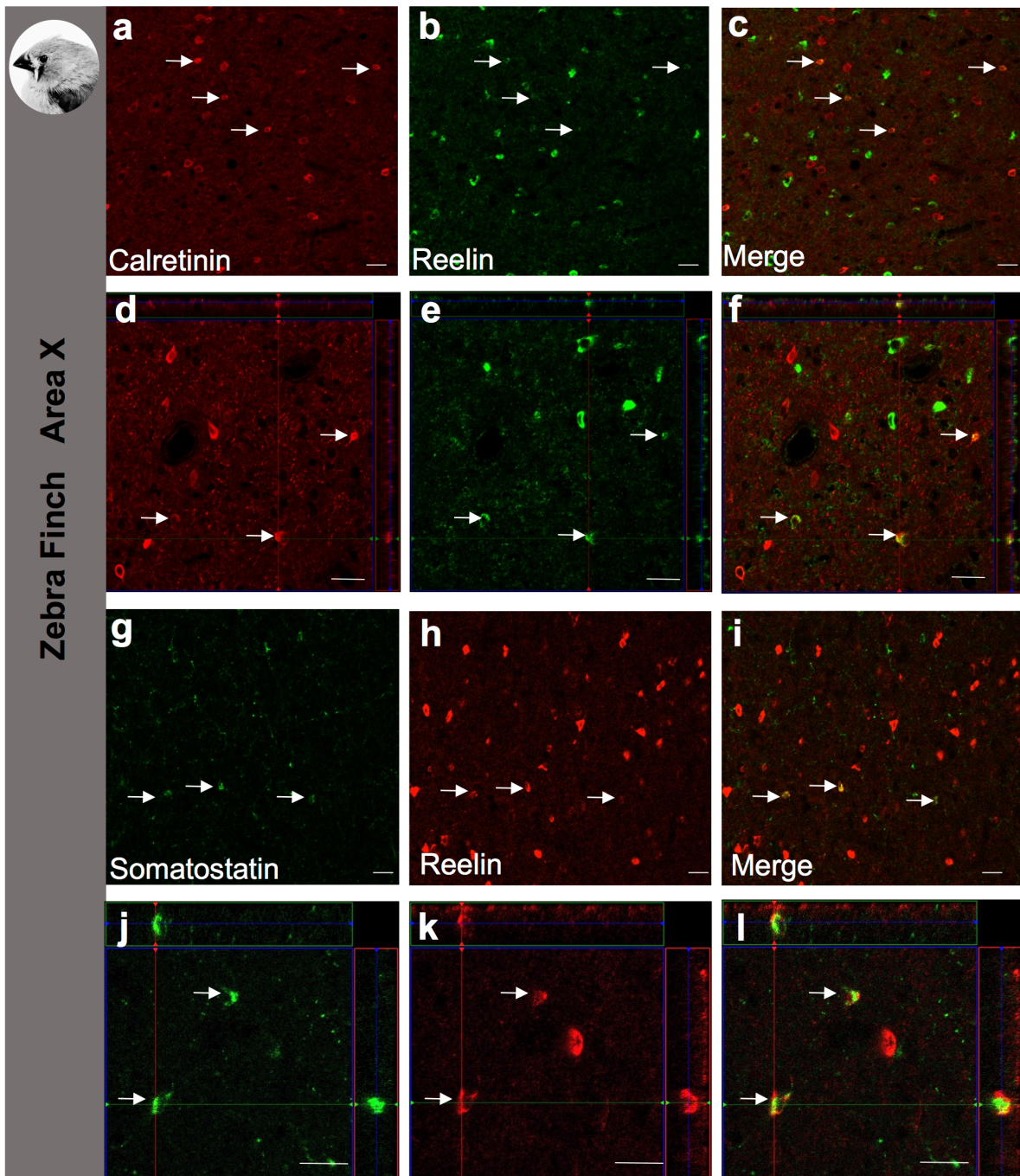


Reelin and FoxP2 co-expression patterns in mouse and zebra finch basal ganglia.

In mouse CPU, FoxP2 (red; a) and Reelin (green; b) co-localize (merge; c) indicating that some medium spiny neurons are a source of Reelin. Arrows indicate co-expression.

(d - f) FoxP2, Reelin, and merged images at higher magnification. In zebra finch Area X, FoxP2 (red; g) and Reelin (green; h) rarely co-localize (merge; i). (j - l) Higher magnification images reveal that rarely, some FoxP2-expressing cells exhibit immunostaining for Reelin. Scale bars=20 μ m.

Figure 6



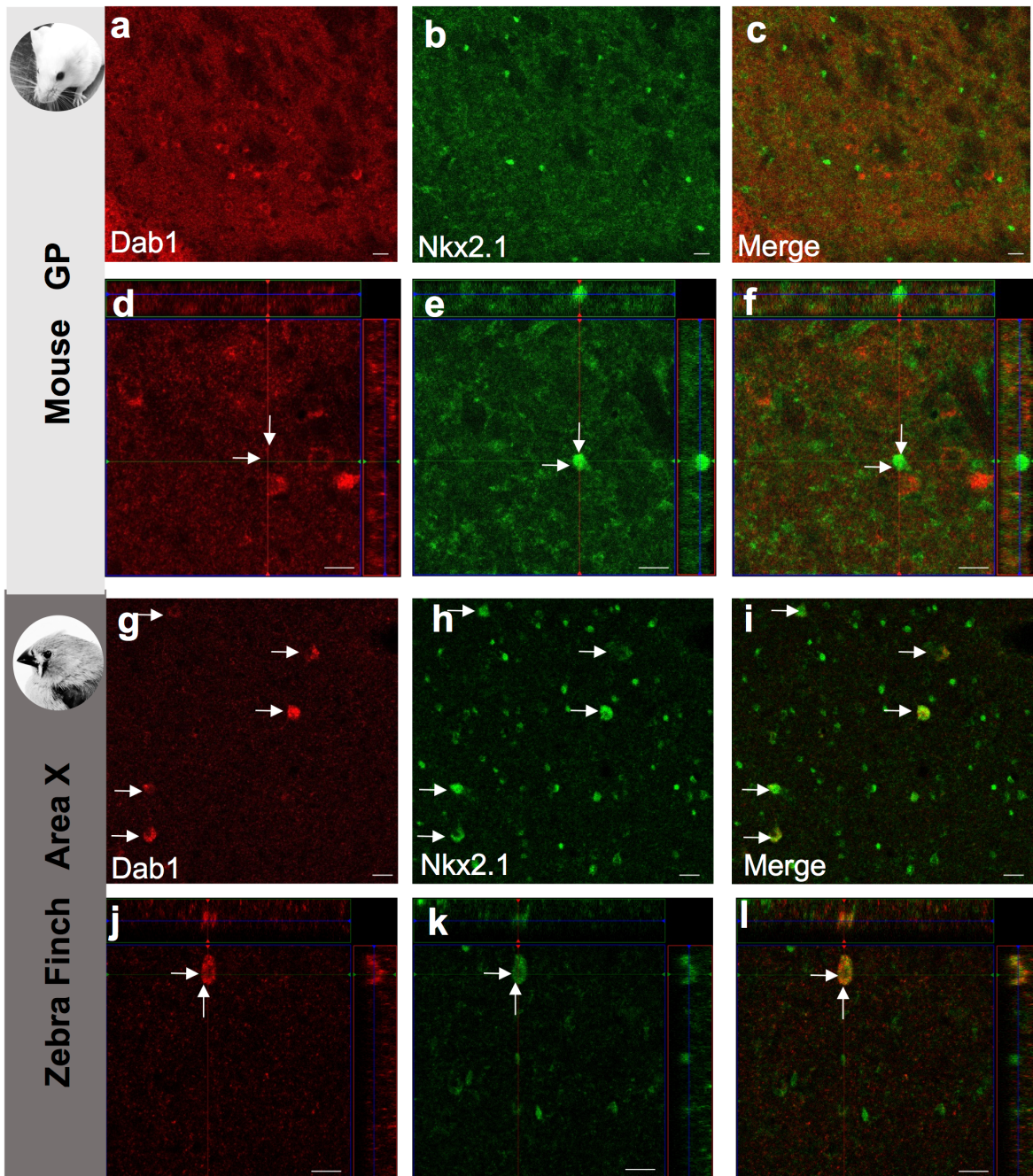
Reelin is expressed in two populations of interneurons in zebra finch Area X.

Calretinin, a marker for a subset of Area X interneurons (red; a) and Reelin (green; b)

co-localize (merge; c). Arrows indicate co-expression. (d - f) Calretinin, Reelin, and

merged images at higher magnification. (g) Somatostatin, a marker for another interneuron population that is sexually dimorphic in its distribution (green; g), and Reelin (red; h) co-localize (merge; i). Arrows indicate co-expressing cells. (j - l) Higher magnification images reveal that some but not all Reelin expressing cells are somatostatin positive. Scale bars=20 μ m.

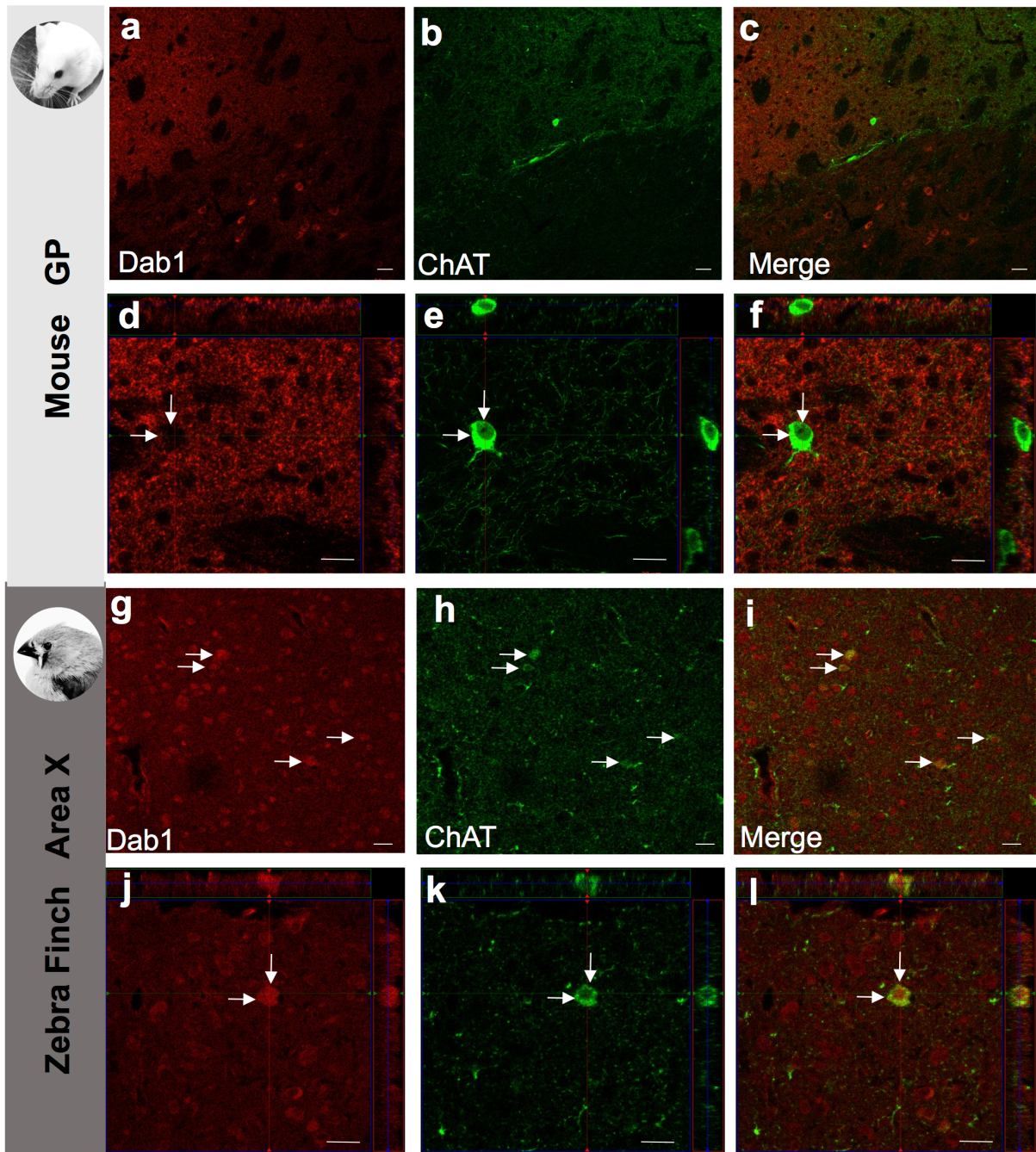
Figure 7



Dab1 and Nkx2.1 co-localize in zebra finch Area X but not in mouse globus pallidus. Dab1 expression in the mouse globus pallidus, GP (red; a) and Nkx2.1 (green; b) fail to co-localize (merge; c). (d - f) Dab1, Nkx2.1 and merged images at

higher magnification. In zebra finch Area X, Dab1 (red; g) and Nkx2.1 (green; h) co-localize (merge; i). Arrows indicate co-localization. Many Nkx2.1 cells do not co-localize with Dab1. (j - l) Higher magnification images show cells with large cell bodies contain both Dab1 and Nkx2.1 (~13 μ m). Scale bars=20 μ m.

Figure 8

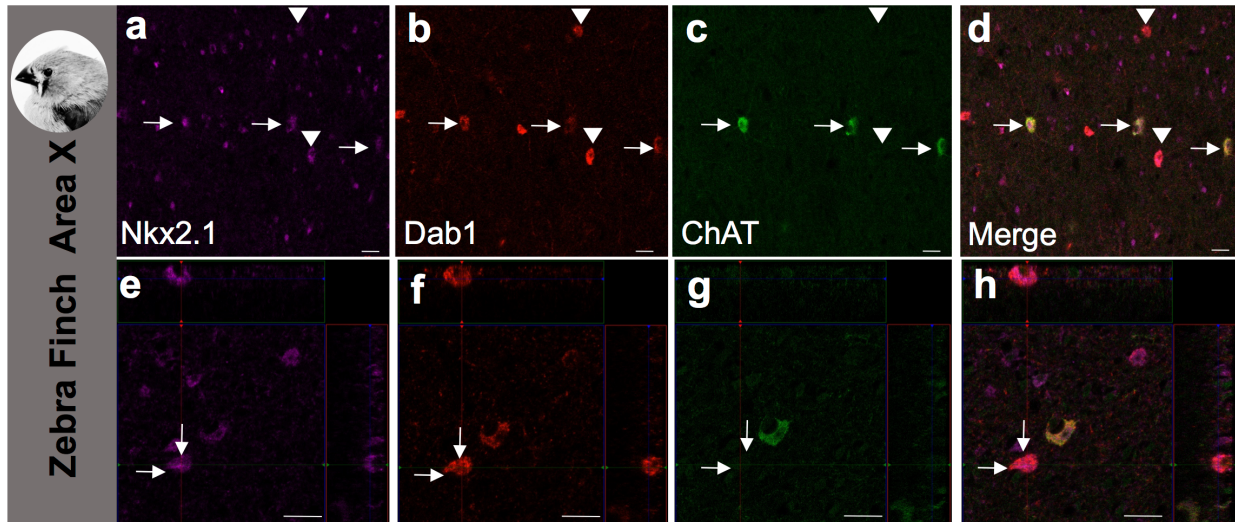


Dab1 is expressed in cholinergic cells in zebra finch Area X but not in mouse.

Dab1 expression is robust in the globus pallidus, (red; a), but ChAT expression (green; b) is absent from this region; and no co-expression is observed (merge, c). (d - f) Higher

magnification images of Dab1 and ChAT confirm lack of co-expression. In contrast, in the zebra finch Area X, Dab1 (red; g) and ChAT (green; h) co-localize in some cells (merge, i). Arrows indicate co-staining in cells. (j - l) Higher magnification images show co-localization of Dab1 and ChAT in large cells (~13 μ m). Scale bars=20 μ m.

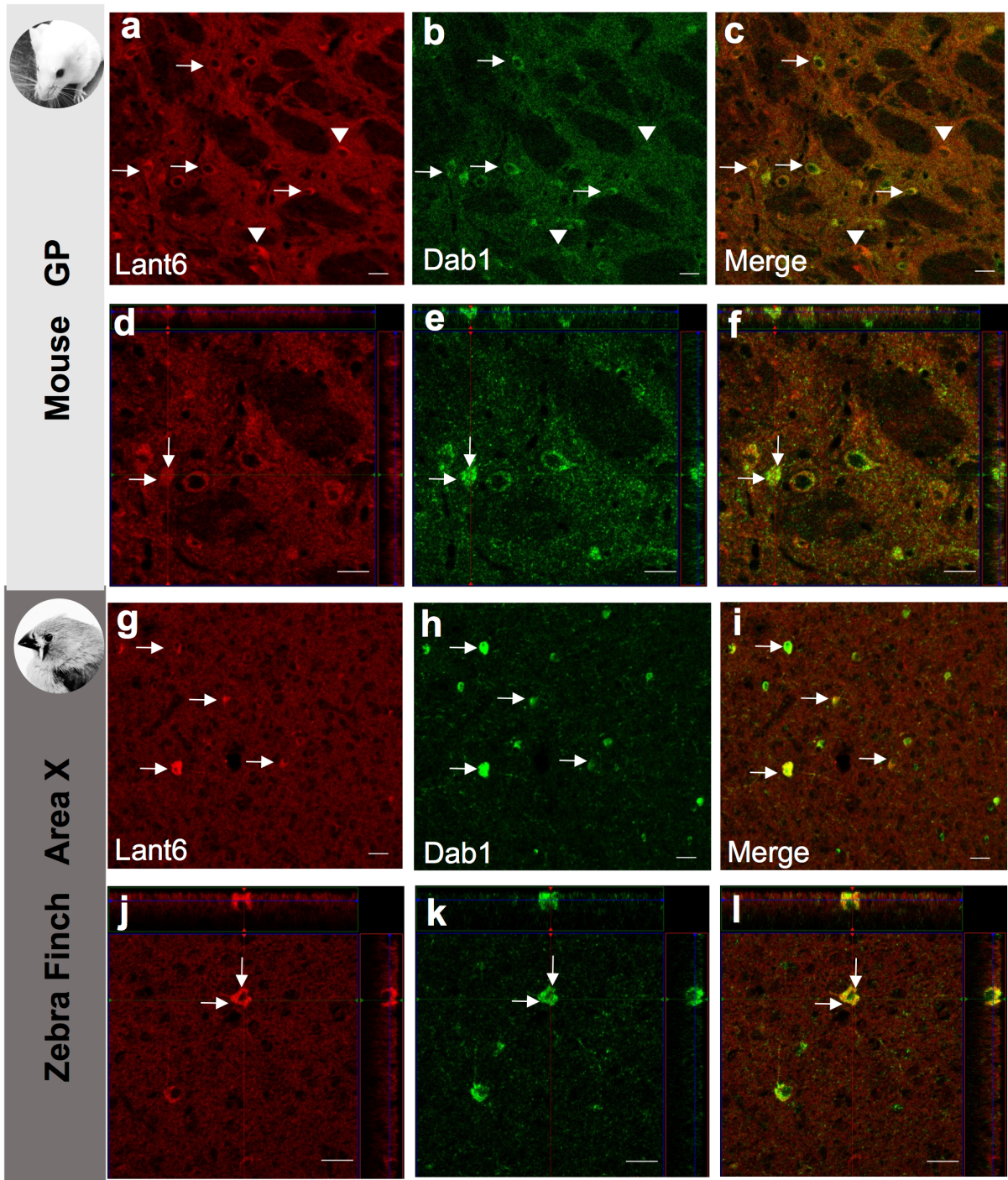
Figure 9



Both cholinergic and indirect pallidal-like neurons express Dab1 in zebra finch

Area X. Nkx2.1 (purple; a) Dab1 (red; b) and ChAT (green; c) co-localize in a subset of cells (merge, d). All cholinergic cells express Dab1 and Nkx2.1, (arrows) and some Nkx2.1 cells express Dab1 but not ChAT (arrowheads). (e - h) Higher magnification images of Nkx2.1 Dab1 and ChAT. Scale bars=20 μ m.

Figure 10

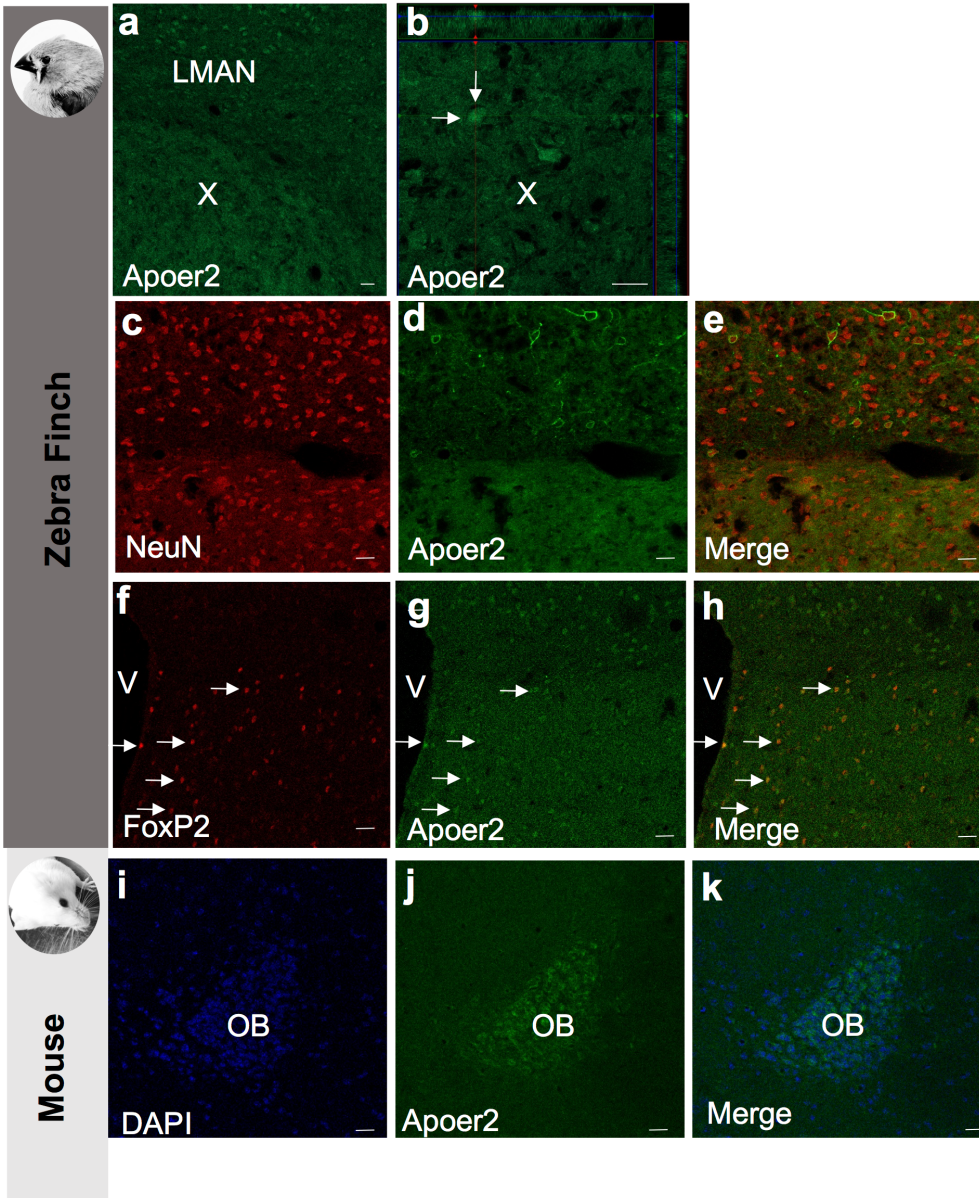


Dab1 and Lant6 co-localize in pallidal cells of both mouse zebra finch Area X.

Lant6 (red; a) and Dab1 (green; b) co-localize in the medial globus pallidus of mouse

(merge, c). Co-localization is marked with arrows. Arrowheads indicate Dab1 cells that are not Lant6 positive. (d - f) High magnification images of Lant6 and Dab1. In zebra finch Area X, Lant6 (red, g) and Dab1 (green, h) co-localize in some cells (merge, i). Arrows indicate cells with co-localization. Lant6 is a marker for neurons that project from Area X to downstream thalamic nucleus DLM. (j - l) Higher resolution images of Lant6 and Dab1. Scale bars=20 μ m.

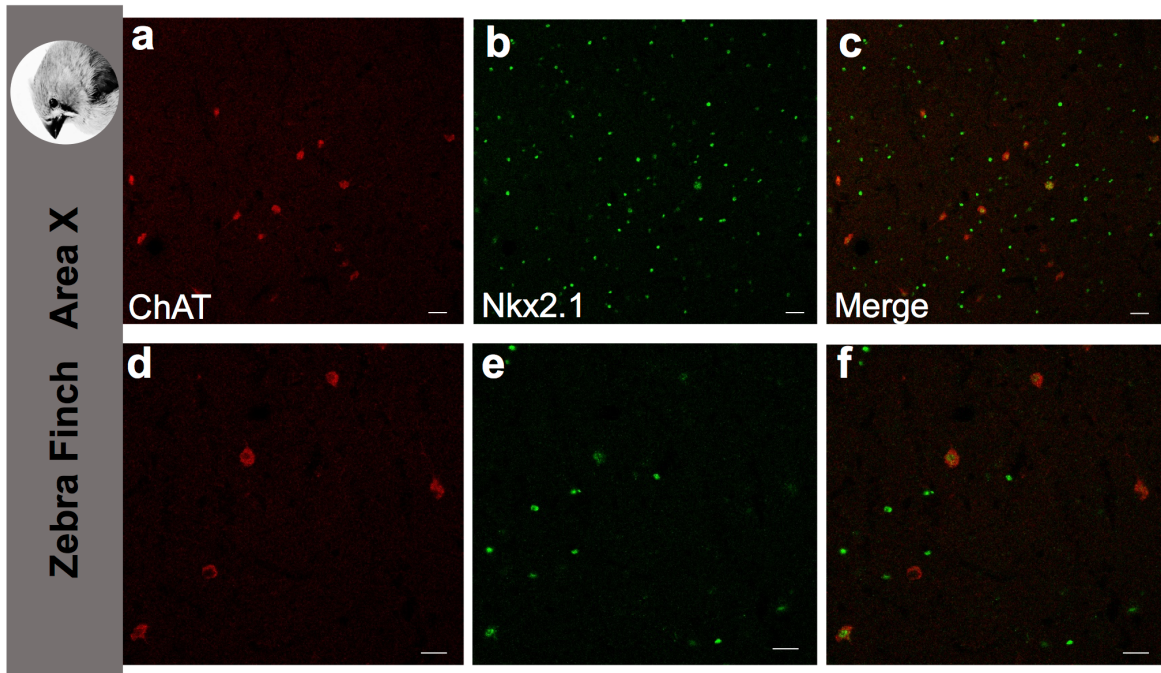
Supplemental Figure 1



Apoer2 immunostaining across species. (a – h) Immunostaining for Apoer2 in zebra finch. (a) LMAN and Area X stain positively for Apoer2 (green). (c – d) The nido-striatal-pallial border where Apoer2 is more pronounced in the cortex, including many processes. These cells co-stain for neuronal marker NeuN (red). (f – h) Co-staining of FoxP2 (red) and Apoer2 (green) reveals cells at the ventricle that have both. (i – k)

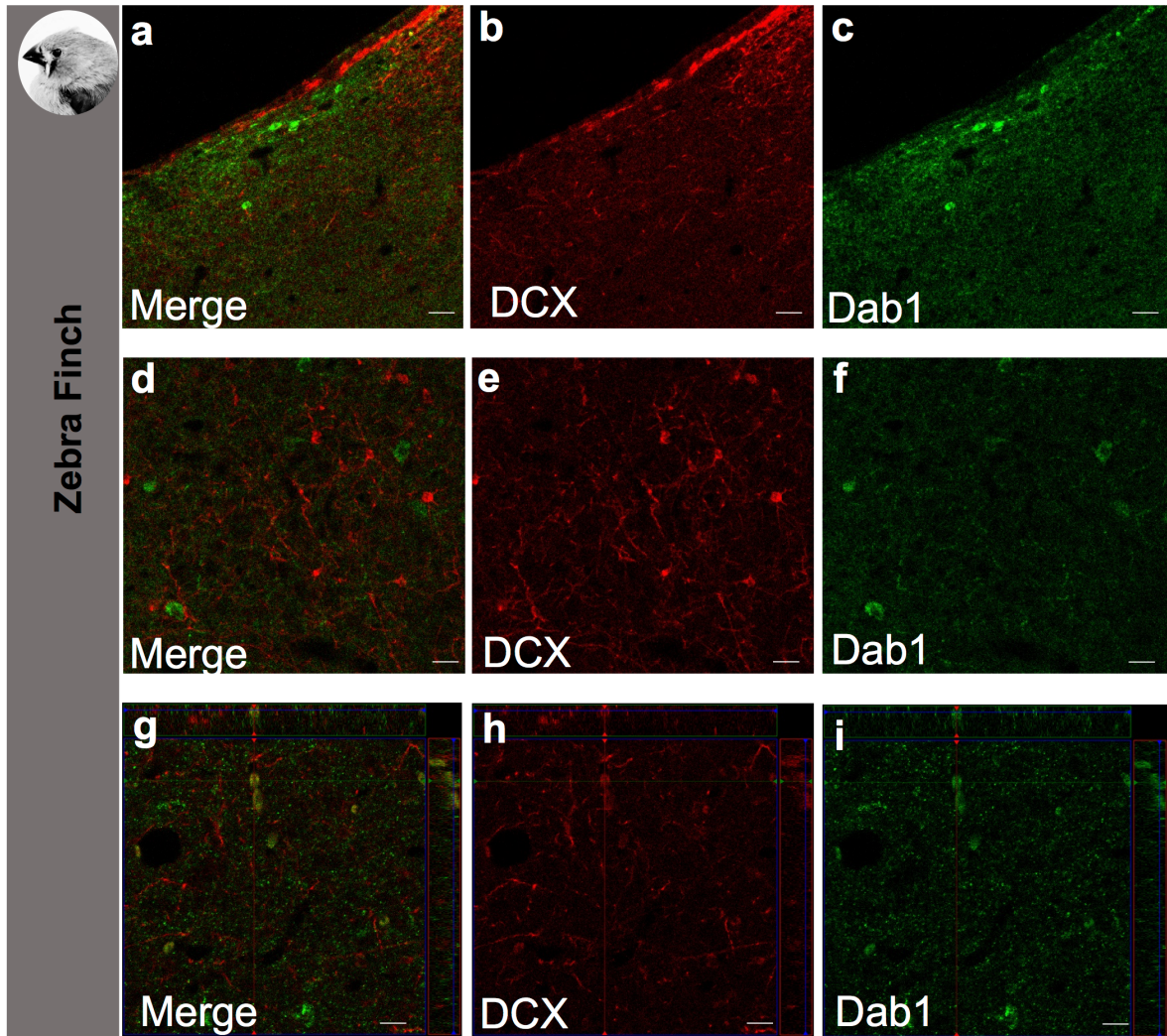
Staining in mouse shows staining thereby acting as a positive control in the olfactory bulb (OB). All scale bars are 20um.

Supplemental Figure 2



Some but not all Nkx2.1 cells are cholinergic in Area X. Immunostaining in Area X of zebra finch for ChAT (red) and Nkx2.1 (green). Scale bars are 20um

Supplemental Figure 3



Doublecortin and Dab1 co-stain cells in zebra finch. (a – c) Staining at the ventricle in zebra finch for Dab1 (green) and doublecortin (DCX, red). (d – i) in Area X. Scale bars are 20um.

References

- Abellán, A. & Medina, L., 2009. Subdivisions and derivatives of the chicken subpallium based on expression of LIM and other regulatory genes and markers of neuron subpopulations during development. *The Journal of comparative neurology*, 515(4), pp.465–501.
- Adam, I. et al., 2016. FoxP2 directly regulates the reelin receptor VLDLR developmentally and by singing. *Molecular and cellular neurosciences*.
- Alvarez-Buylla, A. & Kirn, J.R., 1997. Birth, migration, incorporation, and death of vocal control neurons in adult songbirds. *Journal of neurobiology*, 33(5), pp.585–601.
- Ammassari-Teule, M. et al., 2009. Reelin haploinsufficiency reduces the density of PV+ neurons in circumscribed regions of the striatum and selectively alters striatal-based behaviors. *Psychopharmacology*, 204(3), pp.511–521.
- Balthazart, J. & Ball, G.F., 2014. Doublecortin is a highly valuable endogenous marker of adult neurogenesis in canaries. Commentary on Vellema M et al. (2014): Evaluating the predictive value of doublecortin as a marker for adult neurogenesis in canaries (*Serinus canaria*). *J Comparative Neurol* 522:1299-1315. *Brain, behavior and evolution*, 84(1), pp.1–4.
- Balthazart, J. et al., 2008. Expression of reelin, its receptors and its intracellular signaling protein, Disabled1 in the canary brain: relationships with the song control system. *Neuroscience*, 153(4), pp.944–962.
- Beffert, U. et al., 2005. Modulation of synaptic plasticity and memory by Reelin involves differential splicing of the lipoprotein receptor Apoer2. *Neuron*, 47(4), pp.567–579.
- Bottjer, S.W., Roselinsky, H. & Tran, N.B., 1997. Sex differences in neuropeptide staining of song-control nuclei in zebra finch brains. *Brain, behavior and evolution*, 50(5), pp.284–303.
- Brauth, S.E. et al., 1986. Neurotensin binding sites in the forebrain and midbrain of the pigeon. *The Journal of comparative neurology*, 253(3), pp.358–373.
- Carrillo, G.D. & Doupe, A.J., 2004. Is the songbird Area X striatal, pallidal, or both? An anatomical study. *The Journal of comparative neurology*, 473(3), pp.415–437.
- D'Arcangelo, G. et al., 1995. A protein related to extracellular matrix proteins deleted in the mouse mutant reeler. *Nature*, 374(6524), pp.719–723.
- D'Arcangelo, G. et al., 1999. Reelin is a ligand for lipoprotein receptors. *Neuron*, 24(2), pp.471–479.
- Day, N.F. & Fraley, E.R., 2013. Insights from a nonvocal learner on social

- communication. *The Journal of neuroscience : the official journal of the Society for Neuroscience*, 33(31), pp.12553–12554.
- Doupe, A.J. & Kuhl, P.K., 1999. Birdsong and human speech: common themes and mechanisms. *Annual review of neuroscience*, 22(1), pp.567–631.
- Enard, W. et al., 2009. A humanized version of Foxp2 affects cortico-basal ganglia circuits in mice. *Cell*, 137(5), pp.961–971.
- Farries, M.A., Ding, L. & Perkel, D.J., 2005. Evidence for "direct" and "indirect" pathways through the song system basal ganglia. *The Journal of comparative neurology*, 484(1), pp.93–104.
- Funabiki, Y. & Funabiki, K., 2009. Factors limiting song acquisition in adult zebra finches. *Developmental neurobiology*, 69(11), pp.752–759.
- Garcia-Calero, E. & Scharff, C., 2013. Calbindin expression in developing striatum of zebra finches and its relation to the formation of area X. *The Journal of comparative neurology*, 521(2), pp.326–341.
- Goldberg, J.H. & Fee, M.S., 2010. Singing-related neural activity distinguishes four classes of putative striatal neurons in the songbird basal ganglia. *Journal of neurophysiology*, 103(4), pp.2002–2014.
- Goldberg, J.H. et al., 2010. Singing-related neural activity distinguishes two putative pallidal cell types in the songbird basal ganglia: comparison to the primate internal and external pallidal segments. *The Journal of neuroscience : the official journal of the Society for Neuroscience*, 30(20), pp.7088–7098.
- Groc, L. et al., 2007. NMDA receptor surface trafficking and synaptic subunit composition are developmentally regulated by the extracellular matrix protein Reelin. *The Journal of neuroscience : the official journal of the Society for Neuroscience*, 27(38), pp.10165–10175.
- Groszer, M. et al., 2008. Impaired synaptic plasticity and motor learning in mice with a point mutation implicated in human speech deficits. *Current biology : CB*, 18(5), pp.354–362.
- Hammerschmidt, K. et al., 2015. Mice lacking the cerebral cortex develop normal song: insights into the foundations of vocal learning. *Scientific reports*, 5, p.8808.
- Herz, J. & Chen, Y., 2006. Reelin, lipoprotein receptors and synaptic plasticity. *Nature reviews. Neuroscience*, 7(11), pp.850–859.
- Hethorn, W.R. et al., 2015. Reelin supplementation recovers synaptic plasticity and cognitive deficits in a mouse model for Angelman syndrome. *The European journal of neuroscience*, 41(10), pp.1372–1380.

- Hiesberger, T. et al., 1999. Direct binding of Reelin to VLDL receptor and ApoE receptor 2 induces tyrosine phosphorylation of disabled-1 and modulates tau phosphorylation. *Neuron*, 24(2), pp.481–489.
- Hilliard, A.T. et al., 2012. Molecular microcircuitry underlies functional specification in a basal ganglia circuit dedicated to vocal learning. *Neuron*, 73(3), pp.537–552.
- Howell, B.W. et al., 1997. Neuronal position in the developing brain is regulated by mouse disabled-1. *Nature*, 389(6652), pp.733–737.
- Kikusui, T. et al., 2011. Cross fostering experiments suggest that mice songs are innate. B. Brembs, ed. *PloS one*, 6(3), p.e17721.
- Lai, C.S. et al., 2001. A forkhead-domain gene is mutated in a severe speech and language disorder. *Nature*, 413(6855), pp.519–523.
- Lammert, D.B. & Howell, B.W., 2016. RELN Mutations in Autism Spectrum Disorder. *Frontiers in cellular neuroscience*, 10, p.84.
- Lein, E.S. et al., 2007. Genome-wide atlas of gene expression in the adult mouse brain. *Nature*, 445(7124), pp.168–176.
- Mahrt, E.J. et al., 2013. Engineered deafness reveals that mouse courtship vocalizations do not require auditory experience. *The Journal of neuroscience : the official journal of the Society for Neuroscience*, 33(13), pp.5573–5583.
- Mandelblat-Cerf, Y. & Fee, M.S., 2014. An automated procedure for evaluating song imitation. J. J. Bolhuis, ed. *PloS one*, 9(5), p.e96484.
- Marin, O., Anderson, S.A. & Rubenstein, J.L., 2000. Origin and molecular specification of striatal interneurons. *The Journal of neuroscience : the official journal of the Society for Neuroscience*, 20(16), pp.6063–6076.
- Marler, P., 1997. Three models of song learning: evidence from behavior. *Journal of neurobiology*, 33(5), pp.501–516.
- Marrone, M.C. et al., 2006. Altered cortico-striatal synaptic plasticity and related behavioural impairments in reeler mice. *The European journal of neuroscience*, 24(7), pp.2061–2070.
- Medina, L. et al., 2014. Evolutionary and developmental contributions for understanding the organization of the basal ganglia. *Brain, behavior and evolution*, 83(2), pp.112–125.
- Miller, J.E. et al., 2008. Birdsong decreases protein levels of FoxP2, a molecule required for human speech. *Journal of neurophysiology*, 100(4), pp.2015–2025.
- Nishikawa, S. et al., 2003. Lack of Reelin causes malpositioning of nigral dopaminergic

- neurons: evidence from comparison of normal and *Reln(rl)* mutant mice. *The Journal of comparative neurology*, 461(2), pp.166–173.
- Niu, S. et al., 2004. Reelin promotes hippocampal dendrite development through the VLDLR/ApoER2-Dab1 pathway. *Neuron*, 41(1), pp.71–84.
- Niu, S., Yabut, O. & D'Arcangelo, G., 2008. The Reelin signaling pathway promotes dendritic spine development in hippocampal neurons. *The Journal of neuroscience : the official journal of the Society for Neuroscience*, 28(41), pp.10339–10348.
- Nottebohm, F., 2004. The road we travelled: discovery, choreography, and significance of brain replaceable neurons. *Annals of the New York Academy of Sciences*, 1016(1), pp.628–658.
- Nottebohm, F., Stokes, T.M. & Leonard, C.M., 1976. Central control of song in the canary, *Serinus canarius*. *The Journal of comparative neurology*, 165(4), pp.457–486.
- Persico, A.M. et al., 2001. Reelin gene alleles and haplotypes as a factor predisposing to autistic disorder. *Molecular psychiatry*, 6(2), pp.150–159.
- Person, A.L. et al., 2008. Organization of the songbird basal ganglia, including area X. *The Journal of comparative neurology*, 508(5), pp.840–866.
- Pfenning, A.R. et al., 2014. Convergent transcriptional specializations in the brains of humans and song-learning birds. *Science (New York, N.Y.)*, 346(6215), pp.1256846–1256846.
- Puelles, L. et al., 2000. Pallial and subpallial derivatives in the embryonic chick and mouse telencephalon, traced by the expression of the genes *Dlx-2*, *Emx-1*, *Nkx-2.1*, *Pax-6*, and *Tbr-1*. *The Journal of comparative neurology*, 424(3), pp.409–438.
- Pytte, C.L. et al., 2007. Increasing stereotypy in adult zebra finch song correlates with a declining rate of adult neurogenesis. *Developmental neurobiology*, 67(13), pp.1699–1720.
- Qiu, S. & Weeber, E.J., 2007. Reelin signaling facilitates maturation of CA1 glutamatergic synapses. *Journal of neurophysiology*, 97(3), pp.2312–2321.
- Qiu, S. et al., 2006. Differential reelin-induced enhancement of NMDA and AMPA receptor activity in the adult hippocampus. *The Journal of neuroscience : the official journal of the Society for Neuroscience*, 26(50), pp.12943–12955.
- Ramos-Moreno, T. et al., 2006. Extracellular matrix molecules and synaptic plasticity: immunomapping of intracellular and secreted Reelin in the adult rat brain. *The European journal of neuroscience*, 23(2), pp.401–422.
- Reiner, A., 1987. A LANT6-like substance that is distinct from neuromedin N is present

- in pallidal and striatal neurons in monkeys. *Brain research*, 422(1), pp.186–191.
- Reiner, A. & Carraway, R.E., 1985. Phylogenetic conservatism in the presence of a neurotensin-related hexapeptide in neurons of globus pallidus. *Brain research*, 341(2), pp.365–371.
- Reiner, A. et al., 2004. An immunohistochemical and pathway tracing study of the striatopallidal organization of area X in the male zebra finch. *The Journal of comparative neurology*, 469(2), pp.239–261.
- Rice, D.S. & Curran, T., 2001. Role of the reelin signaling pathway in central nervous system development. *Annual review of neuroscience*, 24(1), pp.1005–1039.
- Rochefort, C. et al., 2007. Recruitment of FoxP2-expressing neurons to area X varies during song development. *Developmental neurobiology*, 67(6), pp.809–817.
- Rogers, J.T. & Weeber, E.J., 2008. Reelin and apoE actions on signal transduction, synaptic function and memory formation. *Neuron glia biology*, 4(3), pp.259–270.
- Rogers, J.T. et al., 2011. Reelin supplementation enhances cognitive ability, synaptic plasticity, and dendritic spine density. *Learning & memory (Cold Spring Harbor, N.Y.)*, 18(9), pp.558–564.
- Rogers, J.T. et al., 2013. Reelin supplementation recovers sensorimotor gating, synaptic plasticity and associative learning deficits in the heterozygous reeler mouse. *Journal of psychopharmacology (Oxford, England)*, 27(4), pp.386–395.
- Scharff, C. & Nottebohm, F., 1991. A comparative study of the behavioral deficits following lesions of various parts of the zebra finch song system: implications for vocal learning. *The Journal of neuroscience : the official journal of the Society for Neuroscience*, 11(9), pp.2896–2913.
- Sharaf, A. et al., 2015. Localization of reelin signaling pathway components in murine midbrain and striatum. *Cell and tissue research*, 359(2), pp.393–407.
- Sussel, L. et al., 1999. Loss of Nkx2.1 homeobox gene function results in a ventral to dorsal molecular respecification within the basal telencephalon: evidence for a transformation of the pallidum into the striatum. *Development (Cambridge, England)*, 126(15), pp.3359–3370.
- Tchernichovski, O. et al., 2000. A procedure for an automated measurement of song similarity. *Animal behaviour*, 59(6), pp.1167–1176.
- Teramitsu, I. & White, S.A., 2006. FoxP2 regulation during undirected singing in adult songbirds. *The Journal of neuroscience : the official journal of the Society for Neuroscience*, 26(28), pp.7390–7394.
- Teramitsu, I. et al., 2010. Striatal FoxP2 is actively regulated during songbird

- sensorimotor learning. H. Tanimoto, ed. PloS one, 5(1), p.e8548.
- Thompson, C.K. et al., 2013. Young and intense: FoxP2 immunoreactivity in Area X varies with age, song stereotypy, and singing in male zebra finches. *Frontiers in neural circuits*, 7, p.24.
- Trommsdorff, M. et al., 1999. Reeler/Disabled-like disruption of neuronal migration in knockout mice lacking the VLDL receptor and ApoE receptor 2. *Cell*, 97(6), pp.689–701.
- Vernes, S.C. et al., 2007. High-throughput analysis of promoter occupancy reveals direct neural targets of FOXP2, a gene mutated in speech and language disorders. *American journal of human genetics*, 81(6), pp.1232–1250.
- Weeber, E.J. et al., 2002. Reelin and ApoE receptors cooperate to enhance hippocampal synaptic plasticity and learning. *The Journal of biological chemistry*, 277(42), pp.39944–39952.
- Woolley, S.C. & Kao, M.H., 2015. Variability in action: Contributions of a songbird cortical-basal ganglia circuit to vocal motor learning and control. *Neuroscience*, 296, pp.39–47.
- Yvone G et al. 2017. Disabled-1 dorsal horn spinal cord neurons co-express LMx1b and function in nociceptive circuits. *European Journal of Neuroscience*, 45 (5) pp. 733-747.

Chapter 5: Conclusion

Novel role for Reelin signaling in vocal behavior

My work presented here implicates Reelin signaling in vocal behavior across multiple species. Components of the Reelin signaling pathway were originally identified as regulated by singing behavior in the adult male zebra finch (Hilliard et al. 2012). These findings prompted my investigation into the role this pathway plays in the song development of in the juvenile zebra finch (Chapter 4) and the development of unlearned neonatal vocalizations (USVs) in genetically altered mice (Chapter 3; Fraley et al. 2016). In zebra finches, my experimental augmentation of Reelin signaling in Area X in juveniles undergoing sensorimotor learning, and our observation of natural regulation of the pathway during singing in both juveniles and adults, strongly suggests that Reelin signaling influences vocal learning. This effect was specific to the vocal learning male and to Area X. Behavioral regulation of the pathway, like that of FoxP2 (Teramitsu & White 2006; Miller et al. 2008), occurs throughout the lifespan of the male zebra finch, indicating that, in addition to song learning, there could also be a role for Reelin signaling in adult song maintenance.

Through the study mice with low or no expression of *Dab1*, *Vldlr* and *Apoer2*, this work showed that the Reelin-signaling pathway is important to unlearned murine neonatal vocalizations. Other molecules essential for vocal learning have produced abnormal communicative phenotypes when insufficient or completely lacking in mice, including *Cntnap2* (Peñagarikano et al. 2011) and *Foxp2* (Shu et al. 2005). Previous reports indicated that Reelin insufficiency or complete knock-out led to abnormal neonatal pup vocalizations (Laviola et al. 2006; Ognibene et al 2007; Romano et al.

2013) . My work replicated those findings, and confirmed that the effect was mediated by the canonical Reelin-signaling pathway (*Dab1*, *Vldlr/Apoer2*).

By observing phenotypes across the spectrum of vocal learners, we can infer the importance this pathway plays in vocal communication. Future studies could examine if Reelin signaling is behaviorally regulated in the basal ganglia of mice, particularly in the anterior striatum which is most like Area X based on genetic profiling of zebra finches and humans (Pfenning et al. 2014). If behavioral regulation is specific to songbirds, it is likely that it is a phenomenon specific to vocal learners. Investigations into other vocal learning species' ability to vocally regulate components of the Reelin-signaling pathway in the basal ganglia would also be of interest (e.g. Bengalese finches, bats).

Behavioral regulation in Area X

Vldlr is a FoxP2 target in human (Vernes et al. 2007) and FoxP2 enhances *Vldlr* expression in zebra finch brain (Adam et al. 2016). When a male zebra finch sings undirected song, *FoxP2* levels fall in Area X, so one would expect *Vldlr* levels to also decline in the same cells (Hilliard et al. 2012). Paradoxically, we observed that Reelin protein level and *Dab1* phosphorylation *increase* in Area X when males sing (Chapter 4, Appendix A). Area X is a hybrid structure containing both striatal and pallidal cell types as well as many classes of interneurons (Person et al. 2008; Carrillo & Doupe 2004; Reiner et al. 2004; Farries & Perkel 2002; Goldberg & Fee 2010). This adds to the complexity of cellular constituents in the song nucleus. To reconcile the above paradox, it is possible that *Vldlr* and *FoxP2* are co-expressed only in certain cell populations. During singing, *Vldlr* levels would not be expected to decline in cells that do not co-

express FoxP2. Reelin signal would be free to be picked up by cells continually expressing Vldlr. My work presented here identified 2 classes of cells (pallidal, cholinergic) that express Dab1 but not FoxP2. This provides evidence that Reelin signal targets multiple cell populations in addition to the medium spiny neurons as previously reported (Adam et al. 2016). Reelin's action could therefore be directed to target the striato-pallidal synapse and cholinergic interneurons during undirected singing.

Reelin-signaling cell types: differences, implications, future directions

Immunohistochemical findings in zebra finch are visually summarized for Area X and mouse basal ganglia (Figures 1 and 2, respectively). My work identified Dab1 expressing pallidal cells across both the zebra finch and mouse. Reelin-secreting cells were also identified in the striatum of both species. This led me to hypothesize that Reelin signaling in the basal ganglia could occur in a striato-pallidal manner. Dab1-positive cells were present in both the mouse GPL and GPM, indicating both the indirect and direct pallidal cells are sensitive to Reelin. In the zebra finch, cells with characteristics similar to the GPe (Nkx2.1+/ChAT-) and GPi (Lant6+) were also both Dab1-positive. Similarities shared between mouse and zebra finch could represent a general mechanism of Reelin signaling in the basal ganglia.

Interestingly, there were also some contrasts between the mouse and zebra finch. In zebra finch Area X, cholinergic interneurons were Dab1 positive. This was not observed in the mouse, and the appearance of cholinergic interneurons but is often seen in avian pallidum (Reiner et al. 2004). I hypothesize that cholinergic interneurons

in the zebra finch Area X could be acting to regulate synaptic activity of the nucleus, and use Reelin signaling to do this could be a unique feature of Area X.

Another difference between murine basal ganglia and zebra finch Area X was the source of Reelin. Murine Reelin secreting cells were identified as the medium spiny neurons in the striatum (FoxP2+, Darpp-32+). In the zebra finch on the other hand, few of these cells stained for Reelin. Instead, in Area X, GABAergic interneurons expressed Reelin including both somatostatin and calretinin interneuron populations. In future experiments, it will be of interest to determine whether or not parvalbumin interneurons also express Reelin.

Apoer2 expression in the basal ganglia is an unusual feature observed in birds (Balthazart et al. 2008), as it is not found in the murine basal ganglia (Lein et al. 2007). We used a novel anti-*Apoer2* antibody (courtesy of Joachim Herz) to identify *Apoer2*-positive cells in Area X and near the lateral ventricle. I found that FoxP2 co-stained with *Apoer2*, suggesting that migrating or resident medium spiny neurons could be *Apoer2*-positive (Rocheffort et al. 2007)(Chapter 4, Supplemental figure). Some cells also co-stained for doublecortin, a marker of new neurons, and *Apoer2*. A majority of doublecortin-labeled cells however, did not express *Apoer2*. It has been suggested that doublecortin may not be the most accurate marker for neurogenesis in the song system (Vellema et al. 2014), so future studies could co-stain for PSA-NCAM and *Apoer2* and investigate both the lateral ventricle and Area X. Further establishment of medium spiny neurons as expressing *Apoer2* will be important, so co-staining for Darpp-32 and TH with *Apoer2* in zebra finch Area X are also recommended for future experiments.

Notably, I found it challenging to immunostain for Vldlr. Many Vldlr antibodies produced non-specific signal when tested in mouse *Vldlr*^{-/-} and *Apoer2*^{-/-}/*Vldlr*^{-/-} sections. This includes a published antibody used in immunostaining of zebra finch Area X (Adam et al. 2016). Adapting a different anti-Vldlr antibody produced no signal in zebra finch brain (Sharaf et al. 2015). Future work is needed to identify and verify a reliable Vldlr antibody for use in zebra finch. Verification using negative control mouse tissue is imperative, as many low density lipoprotein receptors are highly homologous (Herz & Chen 2006).

Once identified, using a reliable antibody to identify Vldlr-positive cell types in Area X of zebra finch is essential to confirm that this canonical Reelin receptor couples to the Dab1 intracellular signaling molecule reported upon here. To further overcome this shortfall, our lab is currently using FISH-seq to investigate Area X cell identities based on mRNA expression on a large scale (Coskun & Cai 2016). This ongoing study includes all Reelin signaling components discussed here (*Reelin*, *Apoer2*, *Vldlr*, and *Dab1*) and many additional markers for basal ganglia cell phenotypes. This work will allow us to reliably identify cellular phenotypes, without reliance on antibody specificity, including those essential to Reelin-signaling in Area X.

Overall, there are many similarities in the Reelin signaling patterns between the mouse and the zebra finch. The striato-pallidal mechanism is likely to appear in other taxa, and is worth investigating to understand basal ganglia function more broadly. Differences between zebra finch and mouse may reflect the unusual nature of Area X: a striato-pallidal hybrid structure unique to avian species; or these differences may reflect the difference between vocal learners and non-vocal learners. Further study of the basal

ganglia of other vocal learning species with respect to Reelin-signaling can illuminate these questions.

Reelin signaling and autism models

The full phenotype representing autism spectrum disorders (ASD) is challenging to model in laboratory animals. While mice are genetically tractable, they are not vocal learners (Kikusui et al. 2011; Mahrt et al. 2013). While songbirds are vocal learners, creating transgenic lines is difficult, and they are more evolutionarily distant from humans. Songbirds can provide a model for learned vocal deficits observed with autism-risk genes such as *Cntnap2* (Adam et al. 2017; Condro & White 2014). Thus, to that combine the best attributes of each model species may better capture the vocal phenotype associated with Reelin signaling.

The *reeler* heterozygous mutant is a mouse model that is often used in ASD research (Biamonte et al. 2014; Laviola et al. 2009; Ognibene et al. 2007; Tueting et al. 1999). The vocal behavior of *Dab1*^{+/-} mice closely follows that of *reeler* heterozygotes, namely reduction in calling frequency and complexity (Chapter 3). The *Dab1*^{+/-} mice, like the *Reln*^{+/-}, may represent an autism-susceptible mouse model. Additional studies using striatal-specific promoters for Reelin expression could knock-out *Reln* specifically in that structure, disrupting Reelin signaling in the basal ganglia. This could confirm that vocal deficits observed in *reeler*, *Dab1*, and *Vldlr/Apoer2* mice were due to a reduction of Reelin signaling the basal ganglia.

Reelin supplementation can enhance vocal learning

Juvenile finches, when injected with exogenous recombinant Reelin, showed improved song learning compared to control brothers (Chapter 4). This was a novel finding, and was observed across 6 sibling pairs. The effect was acute, peaked at 5 days post-injection, which mirrors previous work in mouse hippocampus (Rogers et al. 2013; Rogers et al. 2011). At 10 days post injection, the effect was less pronounced, as learning in the control animals was no longer differed from that in the Reelin-treated birds. In the future, brain cannulations could be used to deliver Reelin protein over the long-term to discover whether the learning curves would be elevated throughout song development.

The mechanism whereby Reelin acts in Area X and enhances song learning is still not clear. I hypothesize that Reelin enhances learning by 1) increasing neurogenesis and neuronal recruitment to Area X, 2) increasing synaptic plasticity at the cortico-striatal synapse, 3) maturing NMDAR subunit makeup in medium spiny neurons, and 4) enhancing plasticity at the striato-pallidal synapse. To follow up on these findings, electrophysiological experiments looking at cortico-striatal or striato-pallidal excitability in the presence or absence of exogenous Reelin would be useful. Lastly, using Western blotting, one could look at NMDAR-alpha/NMDAR-beta subunit protein ratios between Reelin injected birds and control birds (~5d post injection) since Reelin signaling can shift the ratio of NMDAR (Groc et al. 2007; Qiu et al. 2006).

LMAN potential mechanisms

I uncovered was that the song nucleus upstream of Area X, LMAN, robustly stained in immunohistochemical experiments for Apoer2 (Chapter 4, Supplemental

figure). If, as previous studies have shown, Reelin can move trans-axonally (Nishikawa et al. 2003), then another potential locus of Reelin action could be LMAN. LMAN has a known role in the anterior forebrain pathway of injecting variability to the vocal output (Kao & Brainard 2006; Scharff & Nottebohm 1991). It could be that Reelin injections to Area X influence LMAN and vocal variability. An increase in vocal variability, or exploration of vocal motor space could lead to the enhanced song performance we observed. Further study into this intriguing observation should include: 1) establishing Dab1 phosphorylation levels in LMAN when Reelin is injected into Area X; and 2) determining if vocal variability increases immediately after Reelin injection (2-3d post-surgery).

Motor learning enhancement

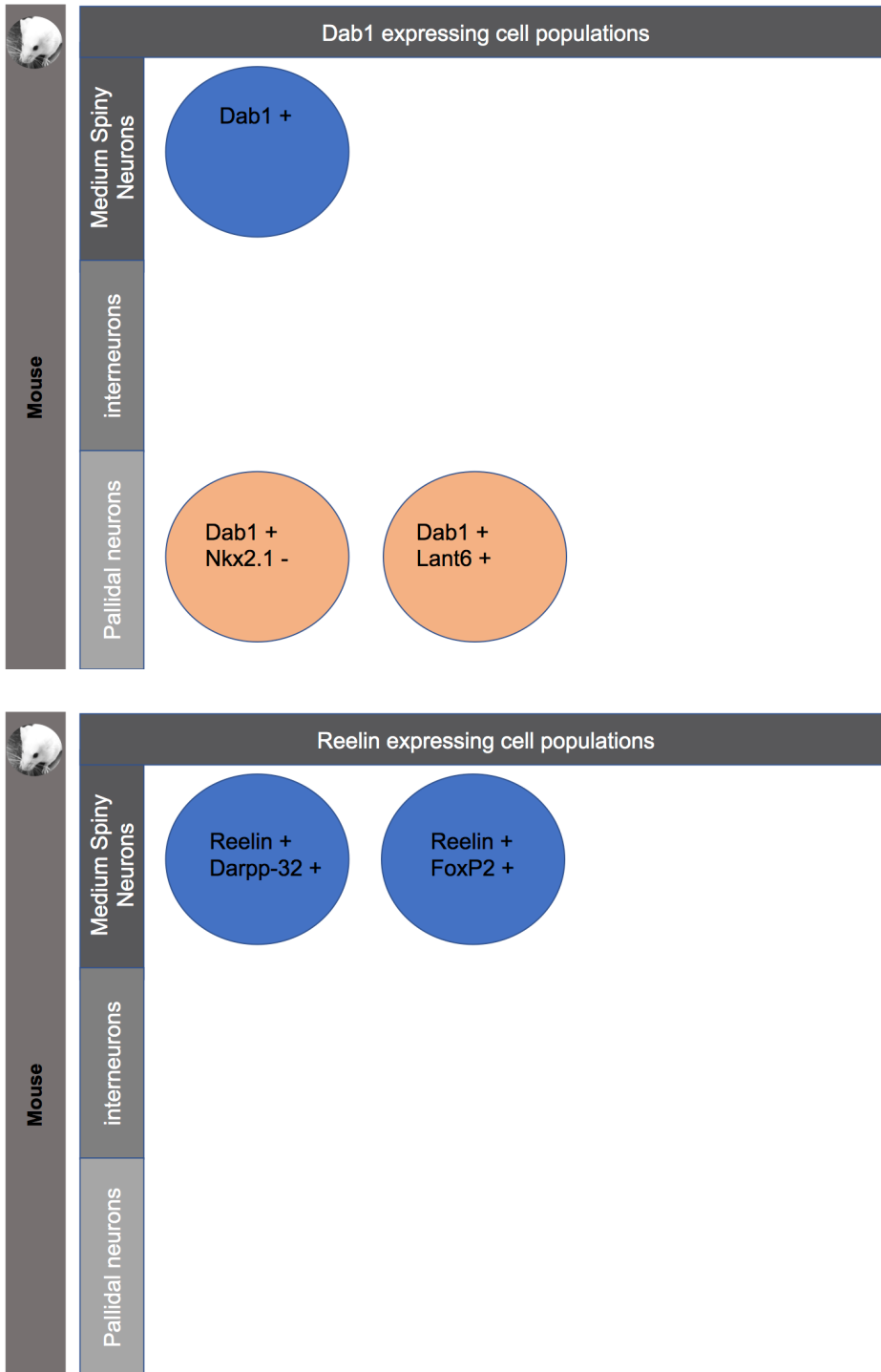
Since I observed a Reelin-mediated effect on vocal motor learning, it is possible that Reelin injections to the basal ganglia could affect other types of motor learning. It would be interesting to inject mice with recombinant Reelin in the striatum and measure if motor learning (i.e. accelerating roto-rod, tilted running wheel) is enhanced. If this is found, then mechanisms of Reelin-signaling could underlie motor learning more generally.

Figure 1



Cell types expressing Reelin and Dab1 in the zebra finch Area X. Graphical summary of immunohistochemistry findings of cell types to date. Novel findings presented here are marked with a star.

Figure 2



Cell types expressing Reelin and Dab1 in the mouse basal ganglia. Graphical summary of immunohistochemistry results in mouse.

References

- Adam, I. et al., 2017. CNTNAP2 is a direct FoxP2 target in vitro and in vivo in zebra finches: complex regulation by age and activity. *Genes, brain, and behavior*.
- Adam, I. et al., 2016. FoxP2 directly regulates the reelin receptor VLDLR developmentally and by singing. *Molecular and cellular neurosciences*.
- Balthazart, J. et al., 2008. Expression of reelin, its receptors and its intracellular signaling protein, Disabled1 in the canary brain: relationships with the song control system. *Neuroscience*, 153(4), pp.944–962.
- Biamonte, F. et al., 2014. Associations among exposure to methylmercury, reduced Reelin expression, and gender in the cerebellum of developing mice. *Neurotoxicology*, 45, pp.67–80.
- Carrillo, G.D. & Doupe, A.J., 2004. Is the songbird Area X striatal, pallidal, or both? An anatomical study. *The Journal of comparative neurology*, 473(3), pp.415–437.
- Condro, M.C. & White, S.A., 2014. Distribution of language-related Cntnap2 protein in neural circuits critical for vocal learning. *The Journal of comparative neurology*, 522(1), pp.169–185.
- Coskun, A.F. & Cai, L., 2016. Dense transcript profiling in single cells by image correlation decoding. *Nature methods*, 13(8), pp.657–660.
- Farries, M.A. & Perkel, D.J., 2002. A telencephalic nucleus essential for song learning contains neurons with physiological characteristics of both striatum and globus pallidus. *The Journal of neuroscience : the official journal of the Society for Neuroscience*, 22(9), pp.3776–3787.
- Goldberg, J.H. & Fee, M.S., 2010. Singing-related neural activity distinguishes four classes of putative striatal neurons in the songbird basal ganglia. *Journal of neurophysiology*, 103(4), pp.2002–2014.
- Groc, L. et al., 2007. NMDA receptor surface trafficking and synaptic subunit composition are developmentally regulated by the extracellular matrix protein Reelin. *The Journal of neuroscience : the official journal of the Society for Neuroscience*, 27(38), pp.10165–10175.
- Herz, J. & Chen, Y., 2006. Reelin, lipoprotein receptors and synaptic plasticity. *Nature reviews. Neuroscience*, 7(11), pp.850–859.
- Hilliard, A.T. et al., 2012. Molecular microcircuitry underlies functional specification in a basal ganglia circuit dedicated to vocal learning. *Neuron*, 73(3), pp.537–552.

- Kao, M.H. & Brainard, M.S., 2006. Lesions of an avian basal ganglia circuit prevent context-dependent changes to song variability. *Journal of neurophysiology*, 96(3), pp.1441–1455.
- Kikusui, T. et al., 2011. Cross fostering experiments suggest that mice songs are innate. B. Brembs, ed. *PloS one*, 6(3), p.e17721.
- Laviola, G. et al., 2009. Gene-environment interaction during early development in the heterozygous reeler mouse: clues for modelling of major neurobehavioral syndromes. *Neuroscience and biobehavioral reviews*, 33(4), pp.560–572.
- Lein, E.S. et al., 2007. Genome-wide atlas of gene expression in the adult mouse brain. *Nature*, 445(7124), pp.168–176.
- Li, R. & Sakaguchi, H., 1997. Cholinergic innervation of the song control nuclei by the ventral paleostriatum in the zebra finch: a double-labeling study with retrograde fluorescent tracers and choline acetyltransferase immunohistochemistry. *Brain research*, 763(2), pp.239–246.
- Mahrt, E.J. et al., 2013. Engineered deafness reveals that mouse courtship vocalizations do not require auditory experience. *The Journal of neuroscience : the official journal of the Society for Neuroscience*, 33(13), pp.5573–5583.
- Miller, J.E. et al., 2008. Birdsong decreases protein levels of FoxP2, a molecule required for human speech. *Journal of neurophysiology*, 100(4), pp.2015–2025.
- Nishikawa, S. et al., 2003. Lack of Reelin causes malpositioning of nigral dopaminergic neurons: evidence from comparison of normal and *Reln*(*rl*) mutant mice. *The Journal of comparative neurology*, 461(2), pp.166–173.
- Ognibene, E. et al., 2007. Impulsivity-anxiety-related behavior and profiles of morphine-induced analgesia in heterozygous reeler mice. *Brain research*, 1131(1), pp.173–180.
- Peñagarikano, O. et al., 2011. Absence of CNTNAP2 leads to epilepsy, neuronal migration abnormalities, and core autism-related deficits. *Cell*, 147(1), pp.235–246.
- Person, A.L. et al., 2008. Organization of the songbird basal ganglia, including area X. *The Journal of comparative neurology*, 508(5), pp.840–866.
- Pfenning, A.R. et al., 2014. Convergent transcriptional specializations in the brains of humans and song-learning birds. *Science (New York, N.Y.)*, 346(6215), pp.1256846–1256846.
- Qiu, S. et al., 2006. Differential reelin-induced enhancement of NMDA and AMPA receptor activity in the adult hippocampus. *The Journal of neuroscience : the official journal of the Society for Neuroscience*, 26(50), pp.12943–12955.

- Reiner, A. et al., 2004. An immunohistochemical and pathway tracing study of the striatopallidal organization of area X in the male zebra finch. *The Journal of comparative neurology*, 469(2), pp.239–261.
- Rochefort, C. et al., 2007. Recruitment of FoxP2-expressing neurons to area X varies during song development. *Developmental neurobiology*, 67(6), pp.809–817.
- Rogers, J.T. et al., 2011. Reelin supplementation enhances cognitive ability, synaptic plasticity, and dendritic spine density. *Learning & memory (Cold Spring Harbor, N.Y.)*, 18(9), pp.558–564.
- Rogers, J.T. et al., 2013. Reelin supplementation recovers sensorimotor gating, synaptic plasticity and associative learning deficits in the heterozygous reeler mouse. *Journal of psychopharmacology (Oxford, England)*, 27(4), pp.386–395.
- Scharff, C. & Nottebohm, F., 1991. A comparative study of the behavioral deficits following lesions of various parts of the zebra finch song system: implications for vocal learning. *The Journal of neuroscience : the official journal of the Society for Neuroscience*, 11(9), pp.2896–2913.
- Sharaf, A. et al., 2015. Localization of reelin signaling pathway components in murine midbrain and striatum. *Cell and tissue research*, 359(2), pp.393–407.
- Shu, W. et al., 2005. Altered ultrasonic vocalization in mice with a disruption in the *Foxp2* gene. *Proceedings of the National Academy of Sciences of the United States of America*, 102(27), pp.9643–9648.
- Teramitsu, I. & White, S.A., 2006. FoxP2 regulation during undirected singing in adult songbirds. *The Journal of neuroscience : the official journal of the Society for Neuroscience*, 26(28), pp.7390–7394.
- Tueting, P. et al., 1999. The phenotypic characteristics of heterozygous reeler mouse. *Neuroreport*, 10(6), pp.1329–1334.
- Vellema, M. et al., 2014. Evaluating the predictive value of doublecortin as a marker for adult neurogenesis in canaries (*Serinus canaria*). *The Journal of comparative neurology*, 522(6), pp.1299–1315.
- Vernes, S.C. et al., 2007. High-throughput analysis of promoter occupancy reveals direct neural targets of FOXP2, a gene mutated in speech and language disorders. *American journal of human genetics*, 81(6), pp.1232–1250.

**Appendix: Molecular microcircuitry underlies functional specification in a
basal ganglia circuit dedicated to vocal learning**

Austin T. Hilliard, Julie E. Miller, Elizabeth Fraley, Steve Horvath & Stephanie A. White

Statement of Contribution

The experiments described in this publication involved uncovering singing regulated gene networks in basal ganglia song nucleus Area X of adult male zebra finches. This study employed zebra finch microarray analysis. To confirm that singing related RNA changes correlated to protein levels, and therefore had functional biological significance, it was critical to correlate protein levels to behavioral state. I conducted the biological validation experiments and provided all data in figure 8. I found significant behavioral regulation at the protein level confirming what was suggested by the microarray data for multiple proteins: Reelin, Dab1, Ypel5. These were all genes suggested by the weighted gene co-expression network analysis to be critical within their gene network. Ypel5 protein level also significantly correlated to the amount of song. Additionally, using immunohistochemical analyses I visualized Ypel5 and Dab1 in area X of adult male zebra finches. Ypel5 protein levels did not appear as intense in singing “UD” birds, reflecting the downregulation quantified by western blot. I visualized for the first time Dab1 positive cells in Area X.

Abstract

Similarities between speech and birdsong make songbirds advantageous for investigating the neurogenetics of learned vocal communication; a complex phenotype likely supported by ensembles of interacting genes in cortico-basal ganglia pathways of both species. To date, only *FoxP2* has been identified as critical to both speech and birdsong. We performed weighted gene co-expression network analysis on microarray data from singing zebra finches to discover gene ensembles regulated during vocal behavior. We found ~2,000 singing-regulated genes comprising 3 co-expression groups unique to area X, the basal ganglia subregion dedicated to learned vocalizations. These contained known targets of human FOXP2 and potential avian targets. We validated novel biological pathways for vocalization. Higher order gene co-expression patterns, rather than expression levels, molecularly distinguish area X from the ventral striato-pallidum during singing. The previously unknown structure of singing-driven networks enables prioritization of molecular interactors that likely bear on human motor disorders, especially those affecting speech.

Introduction

Speech and birdsong are examples of the rare ability to learn new vocalizations. Both depend on hearing and are supported by analogous neural pathways through the cortex and basal ganglia (Lieberman, 2006). In humans, such pathways support an array of behaviors, but songbirds like the zebra finch possess well-defined sub-circuitry specialized for song learning and production, enabling the design of experiments to uncover vocal-motor specific function (Figure 1A; Jarvis, 2004). The transcription factor *FoxP2*, critical for birdsong and the only molecule directly linked to speech and language dysfunction (White, 2010), is expressed similarly in these pathways in both species (Teramitsu et al., 2004). The discovery of *FOXP2*'s link to vocal-motor dysfunction was a constructive step towards understanding the genetic basis of speech, but learned vocalization is a complex phenotype and likely depends on interactions between many genes. Methodological limitations preclude the study of gene expression in behaving humans, so the neuromolecular underpinnings of speech remain poorly understood. Zebra finches, however, are well-suited as a model system for neurogenetic investigations of learned vocal-motor behaviors including speech; bolstered by the sequencing and assembly of their genome (Warren et al., 2010).

To elucidate gene ensembles underlying learned vocalizations, we used weighted gene co-expression network analysis (WGCNA; Zhang and Horvath, 2005) to identify and investigate groups of genes co-regulated during singing. This biologically-inspired method (Supplemental Experimental Procedures) has previously yielded results that could not have been obtained using traditional microarray analyses (Oldham et al., 2008), with gene co-expression groups typically corresponding to functional

pathways. Past uses have uncovered novel genes important for human evolution and brain development, and highlighted genes with clinical significance for pathologies such as cancer (Zhao et al., 2010).

Our experimental design was based upon prior studies showing that *FoxP2* levels within the song-specialized basal ganglia subregion, striato-pallidal area X, decrease after 2 hours of undirected singing (Miller et al., 2008; Teramitsu and White, 2006; Teramitsu et al., 2010), a form of vocal practice (Jarvis and Nottebohm, 1997; Jarvis et al., 1998), with the magnitude of downregulation correlated to how much the birds sang (Teramitsu et al., 2010). In addition, we observed increased vocal variability after 2 hours of undirected singing (Miller et al., 2010), and another group found abnormally variable acoustic structure in the adult song of birds that underwent knockdown of area X *FoxP2* during song development (Haesler et al., 2007). Together, these findings imply that low *FoxP2* levels in area X are coincident with increased vocal variability, and that genes normally repressed by *FoxP2* become activated with increasing amounts of singing.

Using this behavioral paradigm, we performed WGCNA on microarray data arising from 2 anatomically adjacent, yet functionally distinct, regions of the songbird basal ganglia: song-dedicated area X and the ventral striato-pallidum (VSP; Figure 1B), an area important for non-vocal motor function (e.g. posture) that is also active during singing (Feenders et al., 2008). We then quantitatively related network structure to singing measurements (Table S1), representing the first application of WGCNA to a procedurally learned behavior. We hypothesized, and subsequently confirmed, that area X and the VSP would have distinct network structures and that *FoxP2*, along with its

transcriptional targets, would be members of singing-regulated co-expression groups unique to area X. These results are substantiated by the identification and functional annotation of previously known singing genes in our network, and biological validation of molecular pathways not previously linked to vocal motor behavior.

Experimental Procedures

Behavior

Animal use was in accordance with NIH guidelines for experiments involving vertebrate animals and approved by the University of California at Los Angeles Chancellor's Institutional Animal Care & Use Committee. For the microarrays, experiments were conducted in the morning from the time of light onset to death, 2 hours later, according to Miller et al. (2008). During this time, 18 adult male birds sang undirected song of varying amounts. An additional 9 males were designated 'non-singers' (Table S1). If any potential non-singing bird sang >10 motifs, it was excluded from the study. Males performing to a female were not included because *FOXP2* mRNA levels in such directed singers are similar to non-singers and are not correlated to the amount of song (Teramitsu and White, 2006). For biological validation, 18 non-singers and 19 undirected singers were collected 3 hours following lights-on or from their 1st song motif, respectively. Songs were recorded using Shure SM57 microphones, digitized with a PreSonus Firepod (44.1 kHz sampling rate, 24 bit depth), and acquired using Sound Analysis Pro 2.091 (SAP2, Tchernichovski et al., 2000). Acoustic features of song were computed for each bird using the Feature Batch module in SAP2, and the mean values of each feature were obtained to provide 1 representative number for each bird. Motifs were counted independently by 2 experimenters via visual inspection of spectrograms in Audacity (version 1.3; <http://audacity.sourceforge.net/>).

Antibodies and Assays

Tissue was processed for immunoblotting or immunohistochemistry following

conventional methodologies using primary antibodies to detect the following proteins: Reelin, Vldlr, phosphorylated Dab 1, Dab1, Ypel5, RanBPM, Trpv1, NeuN and Gapdh. See Supplemental Experimental Procedures for details.

Microarrays

Agilent zebra finch oligoarrays (ver. 1) containing 42,921 60-mer cDNA probes were constructed through a collaboration between the Jarvis Laboratory of Duke University, Duke Bioinformatics, and The Genomics group of RIKEN, under the direction of Drs. Erich Jarvis and Jason Howard (<http://songbirdtranscriptome.net>; Duke University). These arrays represent cDNA libraries obtained from Michigan State University (Dr. Juli Wade), Rockefeller University (Dr. Fernando Nottebohm), the Keck Center of the University of Illinois (Dr. David Clayton) and Duke (Wada et al., 2006; Li et al., 2007; Replogle et al., 2008). Area X and VSP tissue samples were extracted from all birds (n=27). Each RNA sample was hybridized to a single array, totaling 54 arrays, 2 per bird. Each slide, containing 4 arrays, had 4 samples hybridized: bilateral area X and VSP samples from 2 different birds. Birds were selected per slide such that low or non-singers were paired with high singers to minimize possible inter-slide bias or batch effects (Table S1). During data pre-processing, 1 area X sample and 2 VSP samples, all from non-singing birds, were removed as outliers. See Supplemental Experimental Procedures for details on tissue collection, RNA isolation, array hybridization and pre-processing.

Nomenclature: Probes vs Genes

“Probe” refers to a single probe on the array. GS measurements were computed for each probe. In many cases, multiple probes for a single “gene”, e.g. *FOXP2*, were present on the array (Figure S5, Table S2). There were 20,104 probes in the network, 16,448 of which were annotated with a gene symbol at the time of analysis (February 2011, see <http://songbirdtranscriptome.net> for up-to-date annotations). Since many genes were represented by >1 probe, only 8,015 annotations were unique. Of these 8,015 unique genes, there were 2,496 unique annotations in the 5 singing-related modules. When we report GS.motifs.X for a gene, that value is the average GS.motifs.X score of all probes for that gene unless otherwise noted. The area X co-expression network was constructed using probes, thus when we report the number of genes in a module we are referring to the number of unique gene annotations found for probes in that module. Due to sources of natural and experimental variability, different probes to the same gene were sometimes assigned to different, though usually similar, modules during network construction, e.g. probes made to different regions of the same gene may bind to alternatively-spliced transcript variants with varying levels of efficiency.

Network Construction

Many methods exist for analyzing gene expression microarray data. We chose WGCNA because of its biological relevance, and other advantages (Supplemental Experimental Procedures). All WGCNA computations were done in the free statistical software R (<http://www.r-project.org/>) using functions in the WGCNA library (Langfelder and Horvath, 2008), available via R's package installer. After pre-processing the raw microarray data to remove outliers, normalize, and filter the data from 42,921 to 20,104

probes (Supplemental Experimental Procedures), the correlation matrix was obtained by computing the signed pairwise Pearson correlations between all probes across all birds. The correlation matrix was transformed using a power function $((1 + \text{correlation}) / 2)^\beta$ to form the adjacency matrix, a matrix of network connection strengths. β was determined empirically using the scale-free topology criterion (signed network: $\beta=14$; unsigned: $\beta=6$; Zhang and Horvath, 2005). The network is “weighted” because connection strengths can take on any value between 0 and 1, in contrast to “unweighted” networks where connections are binary. Connectivity (k) is defined for each probe as the sum of its connections to all other probes. The intramodular connectivity (k/N , Table S2) of each probe is the sum of its connections to other probes in its module. Intramodular connectivity in VSP ($k/N.V$) was computed based on the co-expression relationships in VSP of probes grouped by their area X module assignments. See Supplemental Experimental Procedures for details on the scale-free topology criterion and its biological relevance, differential connectivity, signed vs unsigned networks, and *FOXP2* neighborhood analysis.

Module Definition

WGCNA identifies modules of densely interconnected probes by correlating probes with high topological overlap (TO), a biologically meaningful measure of similarity that is highly effective at filtering spurious or isolated connections (Yip and Horvath, 2007). The TO matrix was computed based on the adjacency matrix (Supplemental Experimental Procedures) and average linkage hierarchical clustering was performed using $1 - \text{TO}$ as the distance metric. Modules were defined using a

dynamic tree cutting algorithm to prune the resulting dendrogram (Supplemental Experimental Procedures; Langfelder et al., 2007).

Relating Network Structure to Singing

Expression values within each module were summarized by computing module “eigengenes” (MEs): the 1st principal component of each module obtained via singular value decomposition. We defined the module membership (MM) of individual probes as their correlations to the MEs, such that every probe had a MM value in each module.

To discover any significant relationships between gene expression perturbations within modules and traits, we computed the correlations between MEs and phenotypic measures, including age, acoustic features, number of motifs sung, and whether the bird sang or not (Figure 3B). P-values were obtained via the Fisher transformation of each correlation; modules with correlations to singing traits that had p-values below the Bonferroni corrected significance threshold ($\alpha=1.7e-4$) are referred to as the 3 “song modules” throughout the text. We also performed the less conservative Benjamini and Hochberg (1995) FDR procedure and found significant correlations to singing for the black and salmon modules. P-value corrections were performed using the results from all phenotypic measures listed above, not just those highlighted in Figure 3B.

Visualization and Functional Annotation

Lists of unique gene annotations from each module were used for all module enrichment calculations using Fisher's exact test, functional annotation studies in DAVID and Ingenuity, and when generating VisANT visualizations (Figures 6D-F and

S6, Supplemental Experimental Procedures; Hu et al., 2004).

Data Accessibility

Raw and processed microarray data, and behavioral data for each bird are available at <http://www.ncbi.nlm.nih.gov/geo> (Accession GSE34819).

Results

Prior to network construction, we defined gene significance measures (GS, Supplemental Experimental Procedures) for each probe to relate expression variability to trait variability across all birds ($n=26$), e.g. to the act of singing (referred to as GS.singing.X when measured in area X and GS.singing.V when measured in VSP, see Experimental Procedures for explanation of “probe” vs. “gene”). In area X, after false discovery rate (FDR) correction, 2,659 probes representing 1,364 known genes were significantly correlated to the act of singing ($q<0.05$; GS.singing.X), and 3,709 probes (1,825 known genes) to the number of motifs sung (GS.motifs.X; motifs are neuroethologically relevant sequences of song notes, Hahnloser et al., 2002), with 1,132 genes common to both. In sharp contrast, 0 probes in the VSP had significant GS.singing.V or GS.motifs.V scores (Table S2). We observed small differences in probe expression values in the singing vs non-singing birds: in area X, only 177 probes (~0.9% of the total) showed >100% up- or downregulation, 65 probes >200%, 3 probes >1000%. In the VSP, only 17 probes showed >100% up- or downregulation (~0.08%), 6 probes >200%, and 0 probes >1000%. We also measured correlations to individual acoustic features such as Wiener entropy (a measure of width and uniformity of the power spectrum (Tchernichovski et al., 2000; GS.entropy) that are typically used to assess song (Figures 2B and S3, Table S2). GS.age was computed for each bird as a negative control. Importantly, GS results did not influence network construction in any way.

During pre-processing, all samples were hierarchically clustered to visualize inter-array correlations and remove outliers (Supplemental Experimental Procedures).

The area X vs. VSP samples segregated into 2 distinct clusters, as would be expected if tissue source influences gene expression (Figure S1A). Within area X, the singing vs non-singing birds segregated into 2 distinct sub-clusters (Figure S1B), indicating that singing is a profound regulator of gene expression in area X. Singing birds sang throughout the 2 hour recording period (Figures 2A and S2). There was a significant correlation between the number of motifs sung and Wiener entropy, replicating our prior finding of heightened vocal variability after 2 hours of singing (Figure 2B; Miller et al., 2010).

Essential network terminology

To identify ensembles of genes that were tightly co-regulated (modules) during singing, we performed WGCNA (Experimental Procedures) of the area X samples and quantitatively related the resulting modules to traits. Co-expression networks were built based exclusively on expression levels, via unsupervised hierarchical clustering on a biologically significant distance metric (topological overlap, TO; Experimental Procedures), and relationships between GS and network structure were only examined post hoc. Modules were defined as branches of the dendrogram obtained from clustering, and labeled by colors beneath the dendrogram (Figure 3A; probes outside properly defined modules were considered background and colored grey). To study module composition we defined the 1st principal component of each module as the module eigengene (ME), which can be considered a weighted average of the probe expression profiles that make up the module. Correlating MEs to traits, e.g. number of motifs sung, is an efficient way to relate expression variability within modules to trait

variability. The module membership (MM) and intramodular connectivity (kIN) of each probe were defined as the correlation of its expression profile to the ME, and the sum of its network connections with other module members, respectively (Experimental Procedures). MM and kIN are closely related; high values for either indicate tight co-expression with most other module genes, signaling increased biological importance. The Supplemental Experimental Procedures section contains further information on WGCNA methodology, definitions, and advantages.

Multiple area X co-expression modules strongly related to singing

WGCNA yielded 21 proper co-expression modules in area X (Figure 3). Correlations were computed between MEs and traits, and p-values were computed for each correlation (Experimental Procedures). After Bonferroni correction (significance threshold $\alpha=1.7e-4$), the MEs of 3 modules were significantly related to the act and/or the amount of singing (Figure 3B, Table S3); the blue module (act of singing and number of motifs), the dark green module (act of singing and number of motifs) and the orange module (number of motifs). The positive correlations of the blue module (2,013 probes representing 995 known genes) indicate upregulation of its members during singing and, in general, increased expression with more singing. In contrast, the negative correlations observed for the dark green (1,417 probes representing 824 known genes) and orange (409 probes representing 234 known genes) modules indicate significant downregulation with the act of singing (dark green only) that continued in concert with increased amounts of singing (both). Since Bonferroni correction often results in false negatives (Benjamini and Hochberg, 1995) we also

performed a less conservative False Discovery Rate (FDR) procedure (Experimental Procedures), yielding 2 additional significant ME correlations to the number of motifs sung (black and salmon modules) and 2 to Wiener entropy (blue and orange modules). There were no significant correlations to age.

These 5 “singing-related” modules contained ~83% of the probes with significant GS.motifs.X and GS.singing.X scores. Compared to the rest of the network, genes in these modules were more strongly coupled to the act and amount of singing, and to Wiener entropy (GS.singing.X, GS.motifs.X, GS.entropy.X $p < 1e-200$, Kruskal-Wallis ANOVA). The most interconnected probes within the singing-related modules were also the most tightly regulated by singing, as evidenced by the significant correlations of MM to GS.singing.X and GS.motifs.X in these modules (Figures 4A-C and S3A-F), indicating a strong relationship between importance in the network and behavioral relevance. MM-GS relationships such as these were not found in modules unrelated to singing, e.g. the dark red and turquoise modules, indicating that connectivity, and likely the biological functions in those modules, is relatively unspecialized with respect to vocal-motor behavior in area X, at least after 2 hours of singing.

Gene significance of area X song module genes is not preserved in VSP

We performed a series of comparisons between area X and the VSP to test the hypothesis that area X singing-related network structure was specific to vocal-motor function, and not due to motor function in general. We note that the region of outlying striato-pallidum selected for our analysis, the VSP, is not transcriptionally ‘muted’ during singing, rather, it exhibits immediate early gene (IEG) activation thought to reflect non-

vocal movements that co-occur with singing (Feenders et al., 2008). To test whether single probes exhibited similar relationships to singing in both regions, we compared GS scores from area X to those measured in the VSP. As noted above, no probes had significant GS values for the amount or act of singing in the VSP, in contrast to thousands in area X. We compared GS.motifs.X and GS.singing.X within each module to GS.motifs.V and GS.singing.V for the same probes in the VSP and found weak correlations overall, especially for genes in the song modules (Figures 4D-F and S3G-L). Thus, genes whose area X expression is tightly coupled to singing have a very different relationship, or none at all, to this behavior in the VSP.

Area X-specific co-expression patterns correspond to singing

Next, we compared co-expression relationships within each area X module to the co-expression relationships between the same probes in the VSP, assigning each module a preservation score based on statistical comparisons of module composition and structure (Table S3; Langfelder et al., 2011). Area X modules were preserved to varying degrees in the VSP, with the blue, dark green, and orange song modules being the least preserved, and the modules most unrelated to singing (e.g. dark red and turquoise) being the most preserved. The song modules were effectively non-existent outside of area X, and there was a significant relationship between the strength of ME-singing correlations (Figure 3B) and module preservation ranks (Figures 4G-H), revealing a direct link between singing-relatedness and area X specific network structure in the basal ganglia.

Area X-specific co-expression patterns do not correspond to gene expression levels

To test whether the regional differences in singing-related network structure were simply due to differences in gene expression levels, we began by computing correlations between the expression values for each probe in area X and VSP. There was remarkable similarity overall ($cor=0.98$, $p<1e-200$). Inspection of individual modules revealed a range of strong correlations between area X and VSP expression values (0.94-0.99; Figures 5A-E). In contrast, we observed a weaker overall correlation between area X and VSP network connectivity ($cor=0.61$, $p<1e-200$), especially within the 3 song modules (Figures 5F-J; blue, dark green, orange: mean $cor=0.23$; all other modules: mean $cor=0.49$).

Activity in certain area X neurons increases during singing (Hessler and Doupe, 1999). One possibility for why the song modules were observed in area X but not VSP is that this increase in neuronal firing leads to increased gene expression levels only in area X. To test this, we computed the normalized median gene expression levels in both brain regions for each bird. In non-singers, levels were higher in VSP than in area X (Figure 5K). This difference disappeared in singing birds; gene expression levels in area X and VSP became very similar (Figure 5L). These results imply that the area X-specific song modules cannot be accounted for by higher (or lower) area X gene expression levels compared to VSP during singing. Rather, as revealed here by WGCNA, the relevance of transcriptional activity in these regions to singing is determined more by region-specific co-expression relationships, which comprise 'molecular microcircuitry' that arises during a specific behavior (singing) within a specific

brain region (area X) supporting that behavior. In line with the idea that mere neural activity levels do not account for the song-specialized gene modules, we previously found that activation of the IEG *Synaptotagmin 4* (*Syt4*), is not achieved by overall depolarization of neurons but rather requires the patterned activation underlying singing (Poopatanapong et al., 2006).

In silico validation of singing-driven co-expression networks

The new relationships we uncovered between gene co-expression patterns and singing are substantiated by the presence of previously identified area X singing-regulated genes in the song modules (e.g. *EGR1*, Jarvis and Nottebohm, 1997; and *FOS*, Kimpo and Doupe, 1997: blue module; *FOXP2*, Teramitsu and White, 2006: dark green/orange modules; by convention, gene symbols are capitalized and italicized and are not meant here to denote the human form, Kaestner et al., 2000). Consistent with prior reports, *EGR1* (Jarvis and Nottebohm, 1997) and *FOXP2* (Teramitsu and White, 2006; Teramitsu et al., 2010) were up and downregulated by song, respectively. The lack of correlation between *GAPDH* and singing-related probes validates its use as a control gene in area X under these conditions (Figure 3A). We compared our results to 2 prior studies which used microarrays to examine individual fold changes in gene expression in area X during singing, one of which also performed post hoc clustering (Warren et al., 2010; Wada et al., 2006). Going further, we examined GS scores, MM and KIN.X for these genes in our data.

Wada et al. (2006) identified 33 genes whose expression levels differed in singing vs. non-singing birds, 31 of which were regulated in area X. 29/31 were in our

network (1 was not on the array, 1 was filtered out in pre-processing; Table S2); 19/29 were in the blue song module ($p=8.9e-14$, Fisher's exact test; Table S2). In both studies, these 19 genes were upregulated by singing, as were probes representing 2 genes Wada et al. (2006) found to be regulated in other song nuclei, but not area X; *BDNF* and *SYT4* (8/8 *SYT4* and 2/4 *BDNF* probes had positive GS.motifs.X). Compared to the rest of the network, these 29 genes (170 probes total) had greater increases in expression in singing vs non-singing birds ($p=3.5e-27$, Kruskal-Wallis), and higher GS.motifs.X ($p=3.5e-35$) and GS.singing.X ($p=3.5e-32$). Wada et al. (2006) divided the genes they found into groups based on peak time of expression and regulation pattern. We found significant changes for multiple metrics across these groups in our data (Figure S4).

Warren et al. (2010) revisited singing driven gene regulation in area X and found 474 known genes (represented by 807 probes) that were regulated over the course of 0.5-7 hours of singing. 300 of these genes were in our network, with subsets enriched in the 3 song modules (blue: 71 genes, with, e.g., *SHC3*, *SMEK2*, *NTRK2* having the highest GS.motifs.X, $p<4e-28$; orange: 17 genes, e.g. *CSRNP3*, *SCN3B*, *PLCB1*, $p<3e-6$; dark green: 38 genes, e.g. *BSDC1*, *VLDLR*, *RORA*, $p<5e-5$; Fisher's exact test; Table S2), and in 1 other module (yellow: 104 genes, $p<5e-7$; Table S2). Compared to the rest of the network, probes for all 300 genes had greater expression increases ($p=1.9e-12$, Kruskal-Wallis test; 882 probes total), higher GS.motifs.X ($p=7.8e-11$) and GS.singing.X ($p=2.7e-11$; Table S2). These genes were also more interconnected in their respective modules throughout the network (kIN.X, $p=4.2e-4$), especially in the blue song module ($p=3.8e-14$). A separate aspect of the study revealed enrichment for the functional

annotation term “ion channel activity” in 49 genes posited to have undergone positive selection in zebra finches, which are also suppressed in the auditory forebrain during song perception. 42/49 were in our network (114 probes; Table S2), with 6 in the orange song module ($p < 3.3e-4$, Fisher's exact test). One of the ion channel genes, *TRPV1* (dark green/salmon modules) was highly connected and strongly suppressed by singing in our data, and thus selected for validation in area X *in vivo* (see below and Table S2).

Singing-related modules contain human FOXP2 transcriptional targets

We previously showed that FoxP2 mRNA and protein are lower in area X following 2 hours of undirected singing compared to non-singing, with the magnitude of downregulation correlated to singing (Miller et al., 2008; Teramitsu and White, 2006; Teramitsu et al., 2010). This finding was reproduced here; expression levels for all 12 *FOXP2* probes in the network were negatively correlated with the number of motifs sung (Figure S5). Although our study used an indirect approach, i.e. a behavioral paradigm in which the birds' natural singing behavior significantly alters FoxP2 levels within area X (Miller et al., 2008; Teramitsu and White, 2006; Teramitsu et al., 2010), we predicted that this paradigm coupled with WGCNA would reveal FoxP2 transcriptional targets in area X singing-related modules. To test this, we screened the network for direct FOXP2 targets previously identified by 3 studies. Of 175 targets found in human fetal basal ganglia (Spiteri et al., 2007), 56 were in our network (149 probes total; Table S2). These had relatively high MM in the orange song module ($p = 0.05$, Kruskal-Wallis; Table S2) which contained genes that were downregulated with continued singing, including 9/12 probes for *FOXP2*. Of 302 targets found by a second study in SY5Y cells (Vernes et al.,

2007), 119 were in our network (246 probes total; Table S2). Interestingly, these targets showed the opposite regulatory pattern, displaying high MM in modules upregulated with singing (blue: $p=9e-4$; black: $p=8.6e-3$; Table S2), but low MM in the orange module ($p=9.6e-5$; Table S2). The comparison of GS scores from these 2 groups of genes reiterated their contrary regulation during singing (GS.motifs.X scores were more negative in fetal brain targets, $p<0.04$; Table S2). These differences may be attributed to the different tissue types used in each study.

11 targets found by both studies were in our network. In line with our prediction, probes representing these 11 targets had strong relationships to singing (29 probes total; absolute values of GS.motifs.X, $p=0.037$; GS.singing.X, $p=0.017$, Kruskal-Wallis; Table S2), with a trend for greater expression increases in singing vs non-singing birds ($p=0.064$), compared to the rest of the network. Compared to the rest of the module, targets in the dark green song module (*GBAS* and *VLDLR*, 7 probes total) had high KIN.X and strong negative correlations to GS.motifs.X while showing no difference in expression levels (Figure 6A-C). This reinforces our finding that the connectivity of genes supersedes expression levels in dictating specification of networks for vocal behavior.

More recently, Vernes et al. (2011) performed a large scale-chromatin immunoprecipitation analysis of all known promoters and expression profiling to identify direct *Foxp2* targets in embryonic mouse brain. 557 of their putative 1,164 targets were present in our network, with 22 genes among the 300 closest network neighbors of *FOXP2* ($p<0.04$, Fisher's exact test). These included *NTRK2* and *YWHAH*, which the authors validated as direct targets. In our network, *NTRK2*, a blue song module

member, was the 3rd closest neighbor of *FOXP2* (probeID=2758927) and is part of a canonical network involved in post-translational modification and cellular development, growth, and proliferation that also contains many other close network neighbors of *FOXP2* (Figures 6D and 6F; Table S2). It was also found to be regulated during singing in area X by Warren et al. (2010). *YWHAH*, a gene involved in presynaptic plasticity, was in the blue song module, strongly upregulated during singing, and within the 300 closest network neighbors of *FOXP2* (Table S2). 264 genes were deemed “high confidence” targets by the authors; 95 of these were in our network, including 14, 6, and 4 genes in the blue, dark green, and orange song modules, respectively. Compared to the rest of the network, these 95 genes had relatively high blue MM and low dark green and orange MM ($p < 1e-3$, Kruskal-Wallis test), a pattern similar to what we observed for *FOXP2* targets identified in SY5Y cells (Supplemental Experimental Procedures; Vernes et al., 2007).

Overall, the findings by Vernes et al. (2011) indicate that in embryonic brain, *Foxp2* modulates neuronal network formation by directly and indirectly regulating mRNAs involved in the development and plasticity of neuronal connections. This is compatible with our WGCNA results emerging from adult songbird basal ganglia suggesting a role for *FoxP2* in singing-related synaptic plasticity via its high interconnectedness with genes linked to MAPKK binding, NMDA receptors, actin/cytoskeleton regulation, and tyrosine phosphatase regulation (see “Biological significance of singing-related modules” below).

We also found interesting overlaps between our results and those of 2 additional studies that identified direct and/or indirect *FOXP2* targets. The first study identified

genes with differing expression levels in human neural progenitor cells transfected with either the human or the chimpanzee version of *FOXP2* (Konopka et al., 2009). 24 such genes were in our network, and showed high kIN.X in their respective modules compared to the rest of the network (61 probes total; $p=0.03$, Kruskal-Wallis; Table S2). Those in the orange module had especially high kIN.X, compared to the rest of the module (*CDCA7L*, *RUNX1T1*: $p=2.7e-3$; Table S2). We observed a similar trend for those in the blue module (*B3GNT1*, *HEBP2*, *NPTX2*, *TAGLN*: $p=0.074$), but not in modules unrelated to singing that also contained many of these genes (turquoise, $p=0.9$; yellow, dark red, $p=0.76$). The second study identified 34 genes whose striatal expression levels were altered as a result of two human-specific amino-acid substitutions introduced into the endogenous *Foxp2* locus of mice (Enard et al., 2009). 13/34 genes were in our network (36 probes), including 3 in the song modules (*ELAVL1*: blue, *HEXDC* and *YPEL5*: dark green; Table S2). *YPEL5* was highly connected in the dark green module and strongly suppressed by singing in our data, and was selected for validation in area X *in vivo* (Figure 8, Table S2). In summary, comparison of our WGCNA results with the literature identified song module genes co-regulated with *FoxP2* that are common between songbird basal ganglia and mammalian tissues and, by extension, identified new genes and pathways (see below) that may be critical for speech.

Biological significance of singing-related modules

We used the functional annotation tools available through the Database for Annotation, Visualization and Integrated Discovery (DAVID ver. 6.7, Huang et al., 2009)

to characterize biological functions represented in the area X modules (Experimental Procedures). Many functional terms were enriched only in 1 of the singing-related modules, with the majority of these in the blue module; the most significant having to do with actin binding/regulation, MAP kinase activity, or proteasome activity (enrichment threshold = $p < 0.1$). See Table S4 for all enriched terms in these modules.

To identify the most singing-relevant functions, we defined a measure of term significance (TS) as the absolute value of the product of the mean MM and GS.motifs.X for genes annotated with the term, scaled by $1 - \text{the term's } p\text{-value}$. The mean MM, GS.motifs.X, differential connectivity (kIN.diff), and clustering coefficient of genes annotated by terms with the highest TS scores were compared to the rest of the module, allowing us to hone in on particularly tight-knit, behaviorally-relevant, biological pathways/functions in the singing-related modules (Supplemental Experimental Procedures). For example, 11 genes in the blue module (*ARC*, *CABP1*, *CNN3*, *DLG1*, *DLG2*, *DLGAP2*, *FREQ*, *HOMER1*, *IFNGR1*, *NLGN1*, *NTRK2*) were annotated by the term “GO:0014069~postsynaptic density” (Table S4). Probes representing these genes in the blue module had high MM and GS.motifs.X (27 probes total; mean MM=0.804, GS.motifs.X=0.682), and the term “GO:0014069~postsynaptic density” had an enrichment p -value of 0.059. Thus TS for this term = $0.804 \times 0.682 \times (1 - 0.059) = 0.516$ (7th highest of 402 enriched blue module terms; Tables S2, S4). Compared to the rest of the module, probes for the 11 genes annotated with this term had higher average MM ($p=6.2e-7$, Kruskal-Wallis test), GS.motifs.X ($p=6.8e-5$), kIN.diff ($p=4.7e-6$), and clustering coefficient ($p=5.2e-5$).

Other top ranked blue module terms included “GO:0031434~mitogen-activated

protein kinase kinase binding” and “IPR019583:PDZ-associated domain of NMDA receptors”, as well as others involving actin, cytoskeleton, and tyrosine phosphatase regulation. Genes associated with these synapse related functions in the blue module were also some of *FOXP2*'s closest neighbors, i.e. genes with which it had high TO (Figures 6D-F, Table S2, Supplemental Experimental Procedures). This may imply a role for *FoxP2* in the suppression of synaptic plasticity, since blue module genes (whose levels increased with singing in these experiments) in high TO with *FOXP2* (which decreased with singing) are good candidates for repressed transcriptional targets. Each of the song modules was enriched for astrocytic markers with developing astrocytes most enriched in the blue module ($p=7.5e-6$, Fisher's exact test) and mature astrocytes in the orange module ($p=4e-3$; Cahoy et al., 2008). This observation is consistent with the recent realization that astrocytes are involved in the regulation of neuronal functions, including behavior (Halassa and Haydon, 2010).

We screened the modules for genes associated with Parkinson's disease (Supplemental Experimental Procedures), since it is a basal ganglia based disorder with a vocal component and found enrichment in the black singing-related module (Figure S6). Another module that was moderately singing-related was also enriched for Parkinson's disease associated genes, as well as autism susceptibility genes (purple module, $p=2.7e-4$, $p=0.05$, respectively, Table S2).

Biological significance of other modules

The unique presence of the song modules in area X implies that the biological pathways they represent are co-regulated in patterns specific to area X during learned

vocal-motor behavior. Conversely, functions in modules found in both area X and VSP during singing may typify more general striato-pallidum-wide regulatory networks. To test this, we examined biological functions represented in the dark red, turquoise and pink modules; the 3 most preserved in VSP (Figures 4G-H, Table S3). The turquoise module was the largest in the network (4,616 probes representing 2,743 known genes; Table S2). It was the only module enriched for many functional terms related to hormone binding, morphogenesis, neurogenesis, and development, implicating it in steroid sensitivity and the ongoing neurogenesis known to occur throughout the adult songbird striatum (Table S4; Nottebohm, 2004; Kim et al., 2004).

The turquoise, dark red and pink modules were enriched for neuron and oligodendrocyte gene markers (turquoise: genes >10 fold enriched in oligodendrocytes, $p=0.05$, dark red: genes >20 fold enriched in neurons, $p=0.03$, Fisher's exact test; Table S2; Cahoy et al., 2008), and markers of striatal and pallidal neurons (pink: $p<0.02$; Table S2), consistent with the mixed striatal and pallidal nature of what was formerly known as the avian 'striatum' (Farries and Perkel, 2002; Reiner et al., 2004). These findings are congruent with the idea that the preserved modules represent functions common across the striato-pallidum.

Hub genes and biological pathways in singing-driven co-expression networks

Given the large number of genes in the song modules, we sought to identify the potentially most important genes for further study. We used 2 basic approaches (Figure 7); both began by restricting further analysis to the singing-related modules. In one approach, we then focused on song module genes with high GS.motifs.X and MM, i.e.

genes highly interconnected within their module (hub genes) and strongly coupled to singing, and screened them for enriched functions and biological features. The other approach is exemplified above in the “Biological significance of singing-related modules” section where we functionally annotated the singing-related modules, then prioritized enriched functional terms based on TS scores (Supplemental Experimental Procedures; Table S4), highlighting sets of tightly interconnected singing-related genes that were both important in the module and shared an enriched common feature.

We used these approaches to select pathways in which to test for the presence of constituent proteins in area X. The importance of studying molecules in the context of biological pathways, rather than simply validating mRNA expression, is underscored by our finding that gene co-expression relationships, rather than expression levels per se, determine molecular microcircuitry underlying vocal-motor-specific behavior. As our focus was on the protein level, area X tissue was isolated from singing and non-singing birds at 3 (rather than 2) hours following either time from the 1st motif or lights-on, respectively, to allow for potential translation of mRNA changes (see Supplemental Experimental Procedures for description of tissue processing methods).

WGCNA identified very-low density lipoprotein receptor, *Vldlr*, a member of the Reelin signaling pathway, as a highly connected member of the dark green song module (mean $GS.motifs.X = -0.78$, $MM = 0.82$; Table S2). *Vldlr* was also identified in the literature as a human *FOXP2* target (Spiteri et al., 2007; Vernes et al., 2007). In mammals, the Reelin pathway is critical to neuronal migration during development of the neocortex and cerebellum and to regulation of NMDA receptor-mediated synaptic plasticity in the adult hippocampus (Herz and Chen, 2006). Reelin binds to *Vldlr* on

migrating neurons and radial glial cells. While this pathway is well-established in cortex-containing structures, less is known about the role of these molecules in the basal ganglia of any species. In songbirds, Reelin is expressed in cortical HVC and striato-pallidal area X of adults, but behavioral regulation had not been examined (Balthazart et al., 2008).

In line with behavioral activation of this pathway, expression of Reelin protein was significantly higher in singing vs. non-singing birds (Figure 8A). We also detected Vldlr protein expression in area X (Figure S7A). Since in mammals, binding of Reelin to Vldlr results in the activation of the cytoplasmic adapter protein disabled 1 (Dab1) by tyrosine phosphorylation, we tested for singing-driven regulation of Dab1. As expected, we detected a significant increase in phosphorylated forms of Dab1 in area X of singers relative to non-singers (Figure 8A). *Dlgap2* (aka *PSD95*; blue module; mean GS.motifs.X=0.65, MM=0.82; Table S2) binds Vldlr to the NMDA receptor, activating downstream molecules such as the cAMP responsive element modulator (Crem). *CREM* (blue module; mean GS.motifs.X=0.83, MM=0.95) shares high TO with *FOXP2* (Figures 6D,F; Table S2), implicating FoxP2 in regulation of synaptic plasticity through indirect connections with the Reelin signaling pathway. As noted above, tyrosine phosphorylation and NMDA receptor related functional terms stood out in the blue module, and *DLGAP2* was one of 11 blue module genes annotated by “GO:0014069~postsynaptic density” (Table S4).

A second biological pathway containing yippee-like protein 5 (Ypel5) was selected for further study because of Ypel5's identification as a putative target of the partially humanized Foxp2 (Enard et al., 2009), its GS.motifs.X score (mean of 3 probes

= -0.71) and MM in the dark green module (mean=0.86; Table S2). “PIRSF028804: protein yippee-like” and “IPR004910: Yippee-like protein” had the highest TS scores in the dark green module (Table S4). We viewed this as a rigorous test of the predictive power of WGCNA because of the relative lack of information about this molecule in vertebrates (Hosono et al., 2010). In immunohistochemical analyses, we observed signals for Ypel5 protein in area X (Figure 8B), as well as for its binding partner, Ran Binding Protein in the Microtubule Organizing Center (Hosono et al., 2010), also in the dark green module (*RANBPM* aka *RANBP9*, data not shown). In line with its strong GS.motifs.X score, Ypel5 was behaviorally regulated, with lower protein levels observed in area X of birds that sang more motifs (Figure 8B). Our results for both Reelin and Ypel5 demonstrate expression of multiple members of their respective signaling pathways in area X, with behavioral regulation of each.

As further validation, we detected protein signals within area X consistent with expression of Transient Receptor Potential Vanilloid Type 1 (Trpv1), a capsaicin receptor. We selected Trpv1 for validation because of its high MM and GS.motifs.X, and its identification as an ion channel positively selected for in the songbird lineage (Figure S7B; Warren et al., 2010). *TRPV1* is in the dark green and salmon singing-related modules (1 probe in each; dark green: MM=0.85, GS.motifs.X=-0.77; salmon: MM=0.81, GS.motifs.X=-0.51; Table S2), and has been linked to endocannabinoid signaling pathways in the mammalian basal ganglia (Musella et al., 2009; Maccarrone et al., 2008). Cannabinoid exposure during zebra finch development interferes with song learning (Soderstrom and Tian, 2004), potentially through synaptic plasticity mechanisms such as modulation of glutamatergic synapses onto medium spiny neurons

in area X (Thompson and Perkel, 2010) and altered area X FoxP2 expression (Soderstrom and Luo, 2010). In keeping with its strong GS.motifs.X score, we observed lower levels of Trpv1 signal in birds that sang more motifs (Figure S7B). These findings provide additional biological and literature-based validation of our WGCNA.

Discussion

This study represents the first identification of basal ganglia gene co-expression networks specialized for vocal behavior, and the first use of WGCNA to link co-expression modules to a naturally occurring, procedurally learned behavior. We found ~2,000 genes within the song-specialized striato-pallidal area X, but not in VSP, that were significantly coupled to singing, most of which were members of one of 5 distinct singing-related modules. The 3 song modules (blue, dark green, orange; Figure 3) were unique to area X, and a given module's singing-relatedness was highly predictive of its preservation outside of area X, i.e. the more related to singing, the less preserved (Figure 4). The VSP is active during singing, as indicated by IEG expression (Feenders et al., 2008), and we found gene expression levels in VSP and area X to be remarkably similar during singing (Figure 5). Thus, the regional differences we observed in network structure are likely not due to differences in expression levels, and the singing-related modules in area X are likely not a general product of neural activity, but instead reflect area X specific singing-driven gene regulation patterns.

We predict that WGCNA-type approaches applied to expression data from other song nuclei would likewise reveal song-regulated gene ensembles not found in neighboring tissue, e.g. HVC vs. surrounding cortex. The degree to which such hypothetical song modules would conform with the area X co-expression patterns described here, or whether they would represent the same biological pathways, is an open question. Since the different song nuclei apparently support distinct aspects of singing behavior, one might predict that singing-related co-expression patterns would also be distinct, or would at least relate to different song features, e.g. HVC modules

might relate to measures of syllable sequencing (Hahnloser et al., 2002).

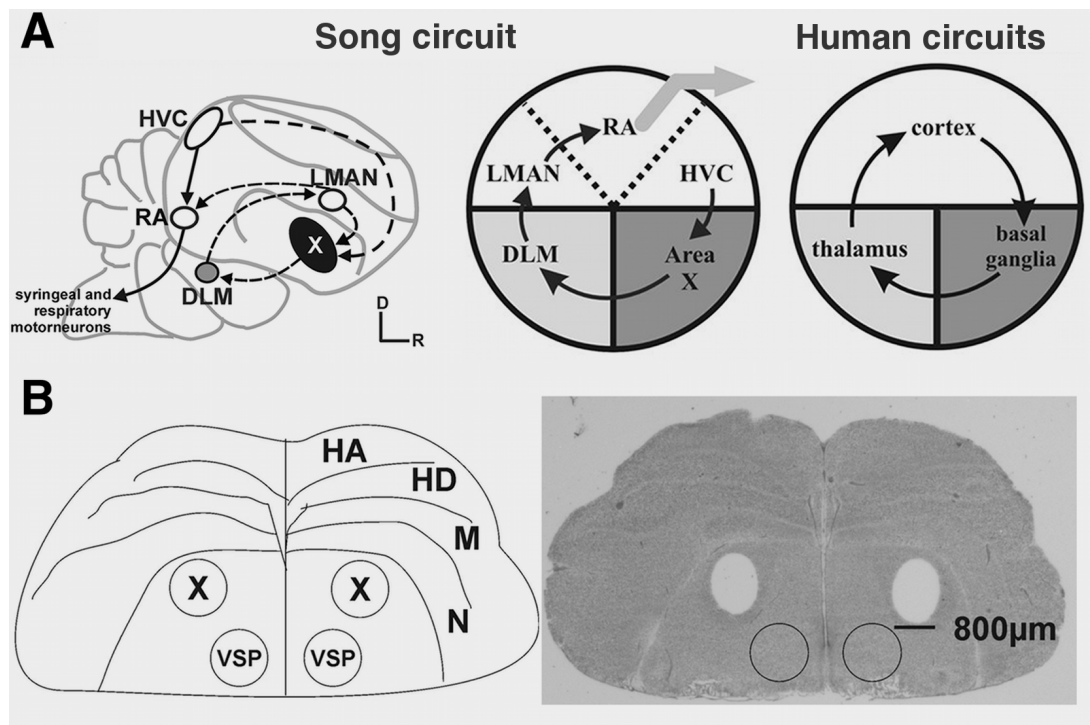
Prior microarray studies of area X gene regulation were based on singling out differentially expressed genes in singing versus non-singing birds, then placing them in groups based on the timing of their expression changes. Our approach differed in that we arranged genes into groups based only on their expression patterns, then related them to singing post-hoc. This resulted in modules that contained >1,000 genes previously unknown to be regulated by vocal behavior. The overlap of our findings with those of prior studies is dominated by genes in the blue module, which contained genes with the largest singing-driven increases in expression. This may imply that differential expression approaches are less effective at identifying gene ensembles, especially downregulated ones, with more nuanced regulation patterns. We predict WGCNA-type approaches will be more effective at uncovering biological functions vital to vocal-motor behavior that do not contain genes with massive expression perturbations.

We verified our hypothesis that targets of *FOXP2* in human tissue and cell lines would be important members of area X specific singing-related modules (Figure 6). Future studies could narrow the search for genes that interact with *FoxP2* in a vocal-motor context using our results as a guide, beginning by screening for genes with high TO with *FOXP2* that also have high singing-related GS and connectivity. We also found enriched functional categories that were unique to the singing-related modules, and described a method for prioritizing biological functions and pathways for future investigation, based on testing metrics of network importance and behavioral significance for genes annotated with significantly enriched terms. Combining this method of ranking enriched biological functions by their importance in singing-related

co-expression networks with screens for FoxP2 targets, as described above, could prove fruitful for elucidating the molecular underpinnings of learned vocal-motor behavior in songbirds and humans.

We used the WGCNA area X network results and literature sources to identify novel pathways regulated by vocal behavior in area X, and demonstrated behaviorally-driven changes in protein levels in the Reelin signaling pathway and additional molecules (Figures 8, S7). Finally, enrichment for Parkinson's disease and autism genes in the song and non-song modules (Figure S6) supports the use of songbirds not just as a model for speech, but as a model for exploring pathways in motor disorders with a vocal component.

Figure 1

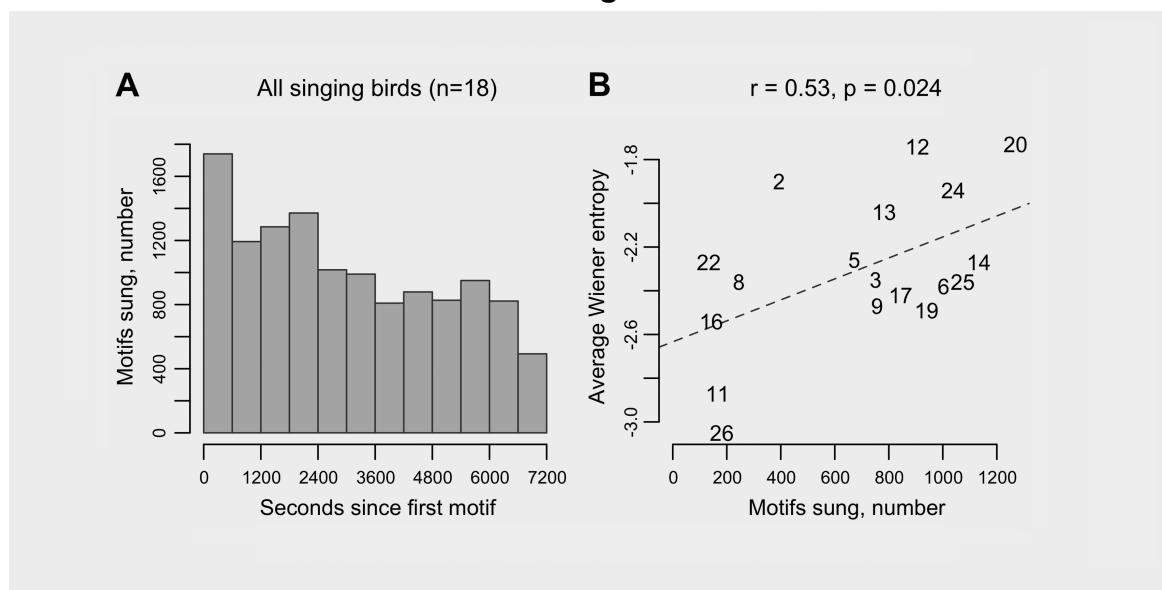


Neuroanatomical overview. (A) Schematic comparison of avian and human cortico-basal ganglia loops. Left, composite sagittal view of songbird telencephalon highlights song control nuclei. Auditory input (not shown) enters the song circuit at cortical HVC, the neurons of which contribute to 2 pathways, the vocal motor pathway (plain arrows) and the anterior forebrain pathway (stippled arrows). The latter includes basal ganglia nucleus area X and rejoins the vocal motor pathway via projections from the cortical lateral magnocellular nucleus of the anterior nidopallium (LMAN) to the robust nucleus of the arcopallium (RA). Middle, songbird cortico-basal ganglia circuitry is further simplified to illustrate song-specialized sub-regions that are embedded within similar brain areas in the human brain (Right). Cortex is in white, basal ganglia dark gray and thalamus light gray. Adapted from Teramitsu et al. (2004). (B) Striato-pallidal brain regions that gave rise to the oligoarray data consist of area X and VSP. Left, line

drawing of a coronal section through anterior zebra finch brain shows anatomical borders and highlights area X, observable in the Nissl-stained section. Right, bilateral tissue punches of equivalent size were taken from area X (holes) and VSP (circles).

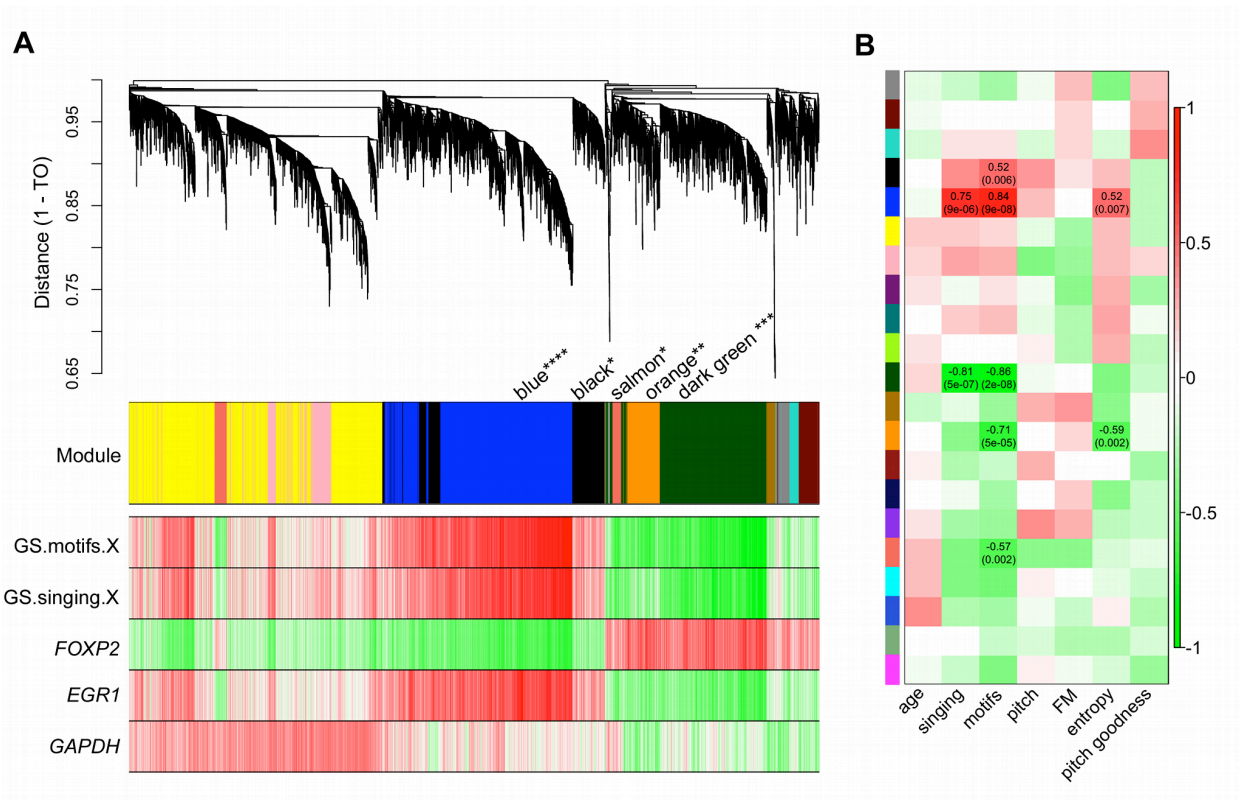
Abbreviations: D-Dorsal, HA-Hyperpallium apicale, HD–hyperpallium densocellulare, M–mesopallium, N–nidopallium, R-Rostral, X–song control area X, VSP-ventral striato-pallidum. Adapted from Miller et al. (2008).

Figure 2



Song patterns that emerged from the behavioral paradigm. (A) Histogram shows number of song motifs produced in 600 s bins for the 18 singing birds in the microarray study. (B) Birds who sang the most motifs exhibited greater acoustic variability. Individual bird identifier numbers are shown for the singing birds. Number of motifs sung was positively correlated with mean Wiener entropy, for which scores closer to 0 represent more disorder across the width and uniformity of the power spectrum (Tchernichovski et al., 2000). The dashed line represents the linear regression of Wiener entropy on number of motifs, with the Pearson correlation coefficient r and p-value (based on Fisher's z transformation) shown at top. See also Figure S2, Table S1.

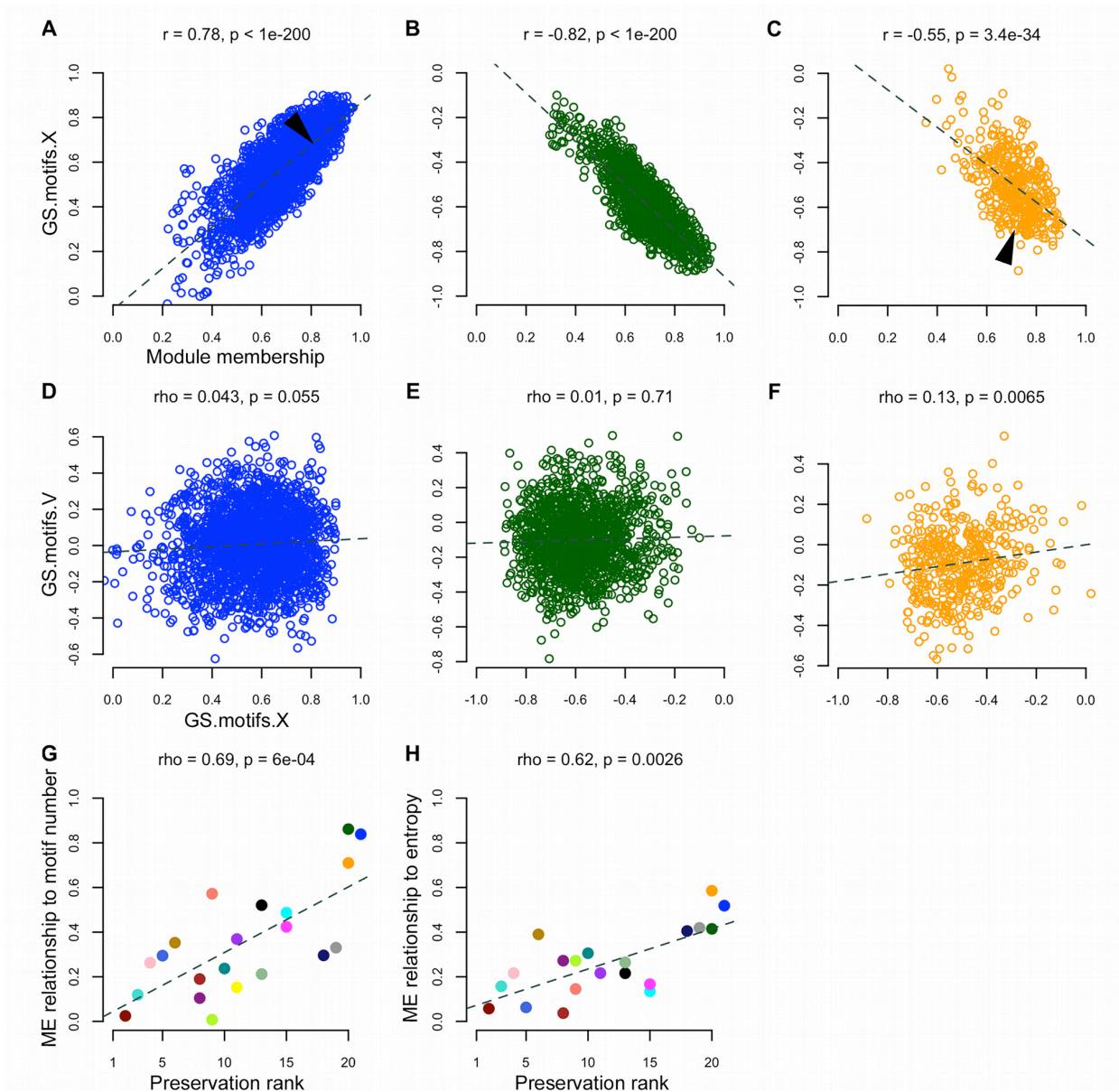
Figure 3



Relationships between network modules and behavioral traits. (A) Dendrogram of the subset of the area X network that includes the blue, dark green, orange, black, and salmon singing-related modules. ‘Leaves’ along ‘branches’ represent probes. The y-axis represents network distance as determined by 1 - TO, where values closer to 0 indicate greater similarity of probe expression profiles across samples. Color blocks below denote modules. Beneath, additional bands indicate positive (red) and negative (green) correlation (see scale bar in B). The top 2 bands show correlations to the number of motifs sung and the act of singing for probes in the dendrogram. The bottom 3 bands show the degree of correlation of these probes to the *EGR1*, *FOXP2* and *GAPDH* probes with the most significant GS.motifs.X scores, respectively. ****passed Bonferroni

for correlation to act of singing and number of motifs, and FDR for correlation to mean Wiener entropy; ***passed Bonferroni for correlation to act of singing and number of motifs, **passed Bonferroni for correlation to number of motifs and FDR for correlation to mean Wiener entropy; *passed FDR for correlation to number of motifs. (B) Colors to the left represent the 21 proper modules in the network. For each module, the heatmap shows ME correlations to traits. Numbers in each cell report the correlation coefficients and Student asymptotic p-value (parentheses) for significant ME-trait relationships for the 5 singing-related modules as indicated by asterisks in (A). Scale bar, right, indicates the range of possible correlations from positive (red, 1) to negative (green, -1).

Figure 4



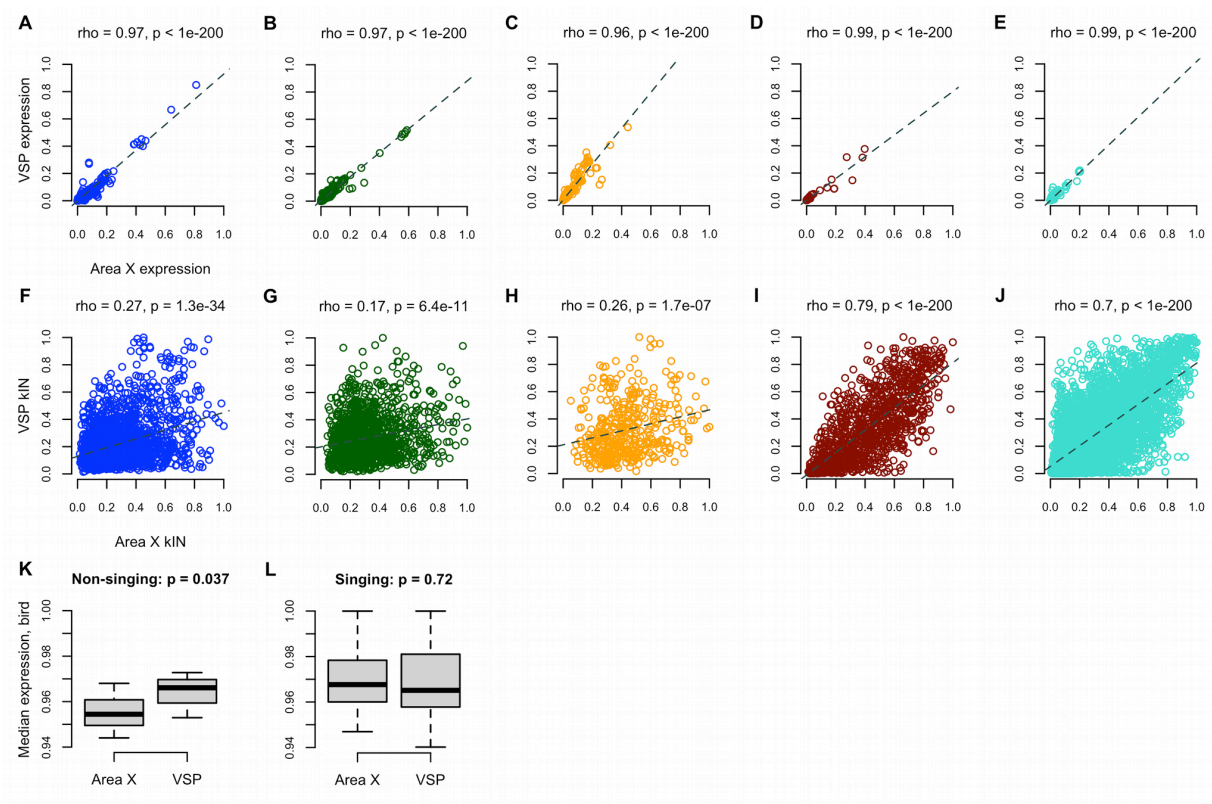
Module membership predicts relationship to singing in area X. (A-C) Area X GS scores for the number of motifs sung are plotted as a function of MM for probes in the blue (left), dark green (center) and orange (right) song modules. Each dot represents one probe. Dashed lines represent the linear regression of GS.motifs.X on MM in each module, with the Pearson correlation coefficient r and p-value (based on Fisher's z transformation) shown at top. Arrows indicate approximate locations of the *EGR1* (blue

module) and *FOXP2* (orange module) probes shown in Figure 3A.

(D-F) GS scores arising from the VSP (V) plotted as a function of the values in area X for the number of motifs sung. Each dot represents one probe. Dashed lines represent the linear regression of GS.motifs.V on GS.motifs.X in each module, with the Spearman rank correlation coefficient *rho* and p-value shown at top.

(G-H) The magnitude of ME-motifs (left) and ME-entropy (right) relationships in area X (absolute values of correlations represented in Figure 3B heatmap) plotted as a function of the degree of preservation of each module across brain regions. Each circle represents a module, colored accordingly, e.g. the blue, dark green, and orange song modules (upper right) had the strongest ME-correlations and were the least preserved in the VSP. Dashed lines represent the linear regression of ME-motifs and ME-entropy correlations on preservation rank, with Spearman's *rho* and p-value shown at top. The purple and yellow modules overlap in the right panel. See also Figure S3.

Figure 5

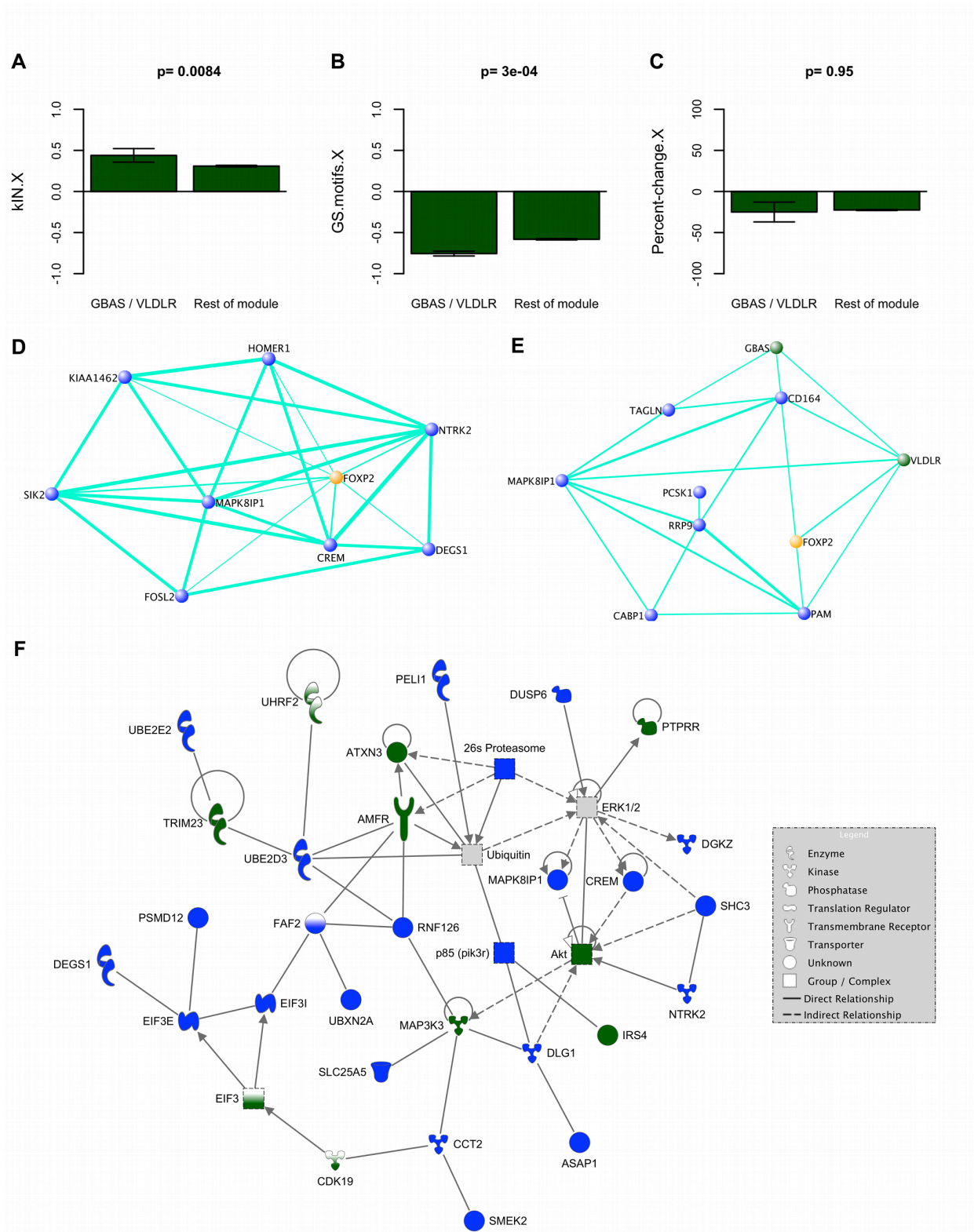


Gene co-expression levels, rather than individual expression levels, distinguish area X song modules.

(A-E) Probe normalized median expression levels in the VSP are plotted as a function of levels in area X for 5 illustrative modules, revealing extremely strong correlations, whereas intramodular connectivity values (kIN, Table S2; F-J) were much less correlated, especially in the song modules. The dark red and turquoise modules were unrelated to singing and the most preserved in VSP (Table S3).

(K-L) Box and whisker plots show birds' normalized median gene expression levels grouped by brain region for each singing state. Whiskers extend to the most extreme data points, box edges represent the 1st and 3rd quartiles, horizontal lines inside each box represent the median. Kruskal-Wallis rank sum test p-values are shown.

Figure 6



Behavioral regulation of gene expression coupled with WGCNA captures genes co-

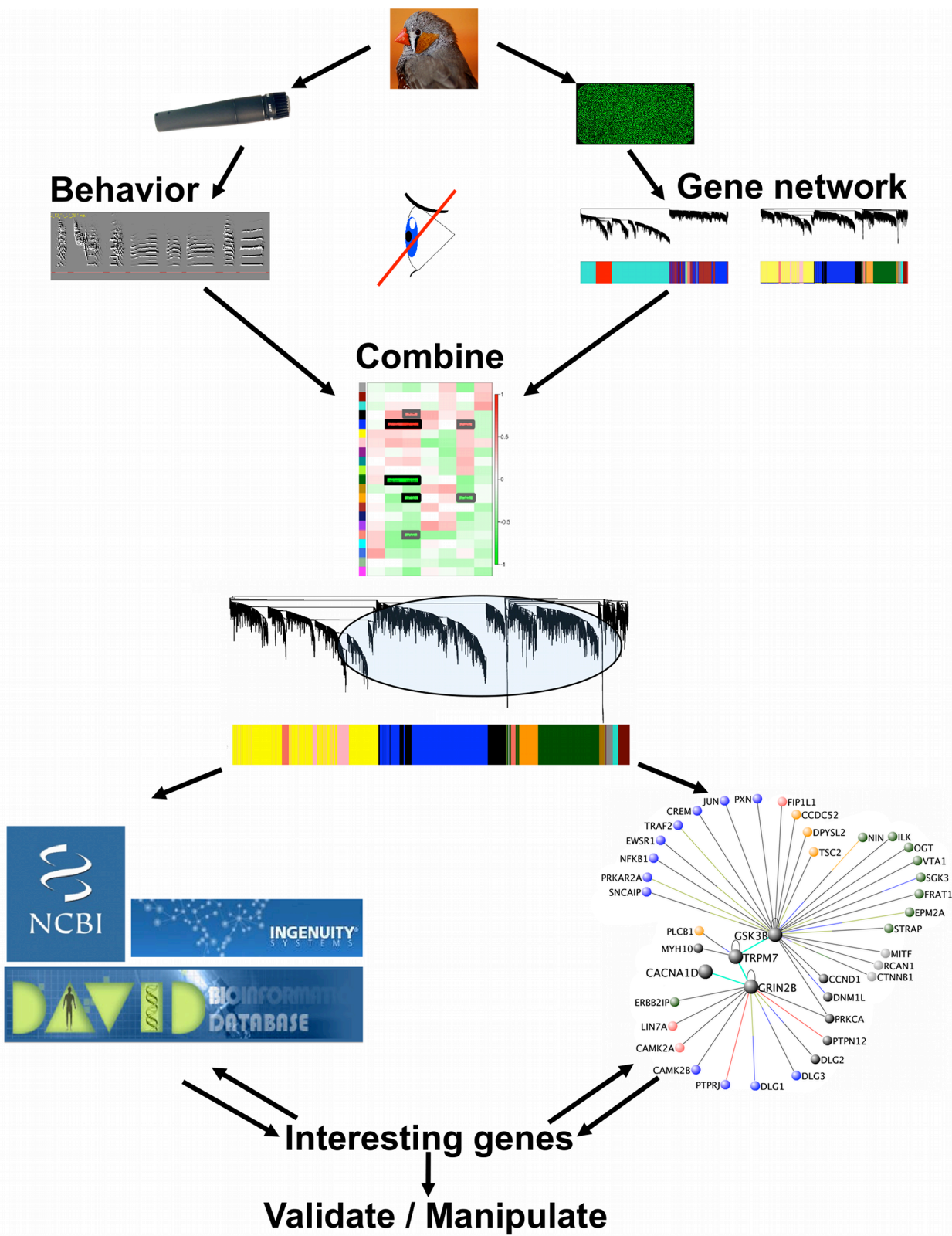
regulated with FOXP2. (A-C) Barplots show intramodular connectivity (left), GS in area X for number of motifs (middle) and expression level percent-change in singing vs. non-singing birds (right), for the dark green module. Left bars in each plot represent values for 2 direct human FOXP2 targets, *GBAS* and *VLDLR* (Spiteri et al., 2007; Vernes et al., 2007), right bars represent the rest of the probes. Error bars = 95% confidence intervals. Kruskal-Wallis p-values are shown.

(D-E) VisANT visualizations highlight co-expression relationships among *FOXP2* and subsets of its closest 300 network neighbors. TO was computed in an unsigned version of our network using the *FOXP2* probe with the most significant GS.motifs.X score. D) Relationships among the most densely interconnected genes within the 20 closest *FOXP2* neighbors (MM.blue>0.9 for all). E) The most densely interconnected genes within the 20 direct human FOXP2 (Spiteri et al., 2007; Vernes et al., 2007) targets displaying the highest TO with *FOXP2*. Nodes represent genes; node color, module assignment; edges, network connections; edge width, connection strength (thicker = stronger). Weak connections omitted for clarity.

(F) Canonical network involved in post-translational modification and cellular development, growth, and proliferation. All but 3 genes (*CDK19*, *FAF2*, *UHRF2*) were within the 300 closest *FOXP2* neighbors. Connections in this graph denote biological interactions (direct = solid line; indirect = dashed) in the Ingenuity Knowledge Base (Ingenuity® Systems, www.ingenuity.com). Genes or complexes with one color had ≥ 1 probe assigned to a song module and are colored accordingly. Genes that are half white also reflect song module membership, but were outside the 300 closest *FOXP2* neighbors. The EIF3 gene group has members in both blue and dark green modules.

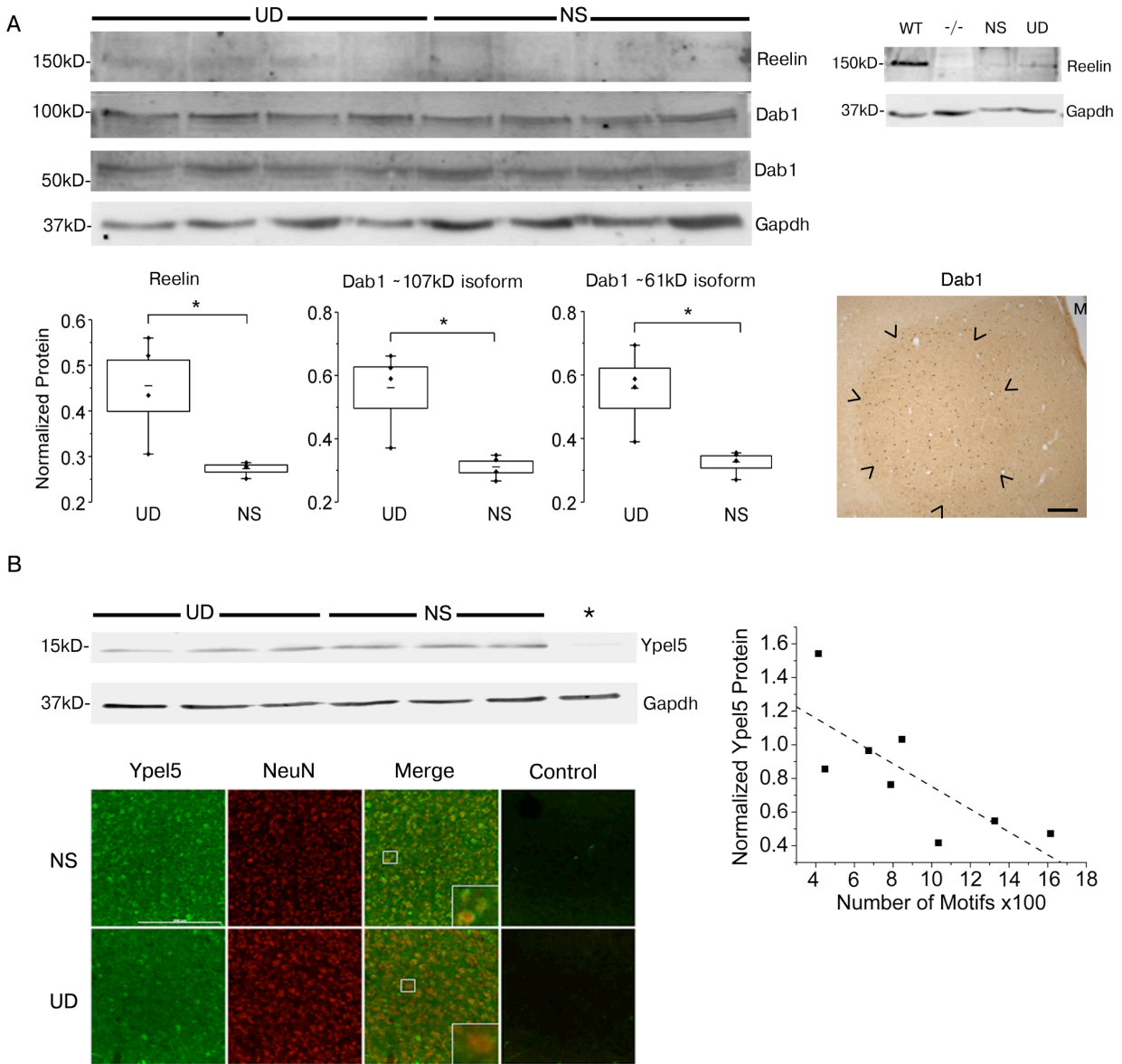
The ubiquitin and ERK1/2 complexes (grey) interact with song module genes and their enriched functions (Table S4). While *FOXP2* does not appear here, its strong connections to these genes predicts that it interacts with them. See also Figure S5.

Figure 7



Application of WGCNA to identify novel pathways in learned vocalization. Schematic of the use of WGCNA to select relevant molecules and pathways for further study. Top) Singing data (left) and gene expression data (right) were gathered from the same birds. Network construction was blind to the behavioral analysis. Middle) Co-expression network structure was then related to song analysis results to identify gene modules important for the behavior. Bottom) Focusing on singing-related modules, gene ontology and functional enrichment analyses were carried out to identify functions and pathways relevant to singing (left). Concurrently, the most important molecules populating the song modules were identified via network metrics (right). The results from each of these approaches were cross-referenced to further prioritize behaviorally relevant biological pathways. Images courtesy of Maurice van Bruggen (zebra finch, <http://creativecommons.org/licenses/by-sa/3.0/deed.en>) and Iain Fergusson (microphone, <http://creativecommons.org/licenses/by/3.0/deed.en>), DAVID and Ingenuity logos used with permission.

Figure 8



Behavioral regulation of hub genes and pathways in area X. (A) Top left) Immunoblot of area X protein from 4 undirected singing (UD) and 4 non-singing (NS) birds shows bands for Reelin (~150kD) and phosphorylated forms of the Dab1 protein (~107kD, ~61kD). Top right) Reelin protein is detected in brain extracts from a wildtype mouse (WT), whereas this band is absent in a reeler mutant mouse (-/-), confirming antibody

specificity. A band of similar size is observed in zebra finch area X samples from an NS and a UD bird. Bottom panels: Box and whisker plots show levels of Reelin protein (left) and of phosphorylated Dab1 isoforms (middle and right) as a function of singing. All 3 proteins are higher in area X of UD relative to NS birds (Mann-Whitney U 2-tailed test, $p=0.03$). Middle of each box represents the mean; top and bottom, standard error; whiskers, upper and lower 95% confidence intervals. Data from each bird is shown by individual points. At right, an immunohistochemical section at the level of area X (arrowheads) from a singing bird shows enhanced signals for Dab1 protein within the nucleus relative to outlying VSP. Scale bar = 100 μm . See also Figure S7. (B) Top left) Immunoblot of area X protein from 3 undirected singing (UD) and 3 non-singing (NS) birds shows bands at the predicted molecular weight for Ypel5 (~13kD) which are not apparent in the preadsorption control (*), indicating antibody specificity. Right) Quantification of signals from these and additional UD singers revealed a negative correlation between Ypel5 and the amount of singing (Spearman $\rho = -0.76$; $p=0.03$, $R^2 = -0.77$). Bottom, Photomicrographs of area X from a representative NS (top) and UD (bottom) bird. Immunofluorescent signals for Ypel5 (green) and the neuronal marker NeuN (red) are shown, as well as a no-primary antibody control (Control). All images were obtained at the same exposure. Qualitatively, more cell bodies appear labeled by the anti-Ypel5 antibody in the NS compared to the UD, most noticeable in the merged images where NeuN signals dominate in the UD bird. Scale bar = 200 μm . Insets of boxed areas in the merged images suggest that Ypel5 and NeuN are co-expressed within area X neurons, but in different subcellular regions.

Acknowledgements

We thank Peter Langfelder and Michael Oldham for advice on microarray pre-processing and network analysis, Jason Howard and Erich Jarvis for the arrays through a partnership with Agilent Technologies, Patty Phelps, Sarah Bottjer and Erica Sloan for material support, Felix Schweizer and Grace Xiao for statistical advice, and 4 anonymous reviewers for insightful commentary. Supported by NIH grants F31 MH082533 (ATH) and R01 MH070712 (SAW).

References

- Lieberman, P. (2006). *Toward an evolutionary biology of language* (Cambridge: Harvard University Press)
- Jarvis, E.D. (2004). Learned birdsong and the neurobiology of human language. *Ann. NY Acad. Sci.* *1016*, 749-777.
- White, S.A. (2010). Genes and vocal learning. *Brain and Language* *115*: 21-28.
- Teramitsu, I., Kudo, L. C., London, S. E., Geschwind, D. H. & White, S. A. (2004). Parallel FoxP1 and FoxP2 expression in songbird and human brain predicts functional interaction. *J. Neurosci.* *24*, 3152-63.
- Warren, W.C., Clayton, D.F., Ellegren, H., Arnold, A.P., Hillier, L.W., Kunstner, A., Searle, S., White, S., Vilella, A.J., Fairley, S., *et al.* (2010). The genome of a songbird. *Nature* *464*, 757-762.
- Zhang, B., and Horvath, S. (2005). A general framework for weighted gene co-expression network analysis. *Statistical Applications in Genetics and Molecular Biology* *4*.
- Oldham, M.C., Konopka, G., Iwamoto, K., Langfelder, P., Kato, T., Horvath, S., and Geschwind, D.H. (2008). Functional organization of the transcriptome in human brain. *Nat. Neurosci.* *11*, 1271-1282.
- Zhao, W., Langfelder, P., Fuller, T., Dong, J., Li, A. and Horvath, S. (2010). Weighted Gene Coexpression Network Analysis: State of the Art, *J. Biopharm. Stats.* *20*: 2, 281-300.
- Miller, J.E., Spiteri, E., Condro, M.C., Dosumu-Johnson, R.T., Geschwind, D.H., and White, S.A. (2008). Birdsong decreases protein levels of FoxP2, a molecule required for human speech. *J. Neurophysiol.* *100*, 2015-2025.
- Teramitsu, I. and White, S.A. (2006). FoxP2 regulation during undirected singing in adult songbirds. *J. Neurosci.* *26*, 7390-4.
- Teramitsu, I., Poopatanapong A., Torrisi, S., White, S.A. (2010). Striatal FoxP2 is actively regulated during songbird sensorimotor learning. *PloS One* *5*, e8548.
- Jarvis E.D., Nottebohm, F. (1997). Motor-driven gene expression. *Proc. Natl. Acad. Sci. USA* *94*, 4097-102.
- Jarvis E.D., Scharff C., Grossman M.R., Ramos J.A., Nottebohm F. (1998). For whom the bird sings: context-dependent gene expression. *Neuron* *21*, 775–788.

- Miller, J.E., Hilliard, A.T., and White, S.A. (2010). Song practice promotes acute vocal variability at a key stage of sensorimotor learning. *PLoS One* 5, e8592.
- Haesler, S., Rochefort, C., Georgi, B., Licznarski, P., Osten, P., and Scharff, C. (2007). Incomplete and inaccurate vocal imitation after knockdown of FoxP2 in songbird basal ganglia nucleus area X. *PLoS Biol.* 5, 2885-2897.
- Feenders, G., Liedvogel, M., Rivas, M., Zapka, M., Horita, H., Hara, E., Wada, K., Mouritsen, H., and Jarvis, E.D. (2008). Molecular mapping of movement-associated areas in the avian brain: A motor theory for vocal learning origin. *PLoS One* 3, e1768.
- Hahnloser, R.H.R., Kozhevnikov, A.A., and Fee, M.S. (2002). An ultra-sparse code underlies the generation of neural sequences in a songbird. *Nature* 419, 65-70.
- Tchernichovski, O., Nottebohm, F., Ho, C.E., Pesaran, B., and Mitra, P.P. (2000). A procedure for an automated measurement of song similarity. *Anim. Behav.* 59, 1167-1176.
- Benjamini, Y. and Hochberg, Y. (1995). Controlling the false discovery rate: A practical and powerful approach to multiple testing. *J. Royal Stat. Soc. Series B (Methodological)* 57, 289-300.
- Langfelder, P., Luo, R., Oldham, M.C., Horvath, S. (2011). Is my network module preserved and reproducible? *PLoS Comp. Biol.* 7, e1001057.
- Hessler, N.A., Doupe, A.J. (1999). Singing-related neural activity in a dorsal forebrain-basal ganglia circuit of adult zebra finches. *J. Neurosci.* 19, 10461-81.
- Poopatanapong, A., Teramitsu, I., Byun, J.S., Vician, L.J., Herschman, H.R., White, S.A. (2006). Singing, but not seizure, induces synaptotagmin IV in zebra finch song circuit nuclei. *J. Neurobiol.* 66, 1613-29.
- Kimpo, R.R., Doupe, A.J. (1997). FOS is induced by singing in distinct neuronal populations in a motor network. *Neuron* 18, 315-25.
- Kaestner, K.H., Knochel, W., Martinez, D.E. (2000). Unified nomenclature for the winged helix/forkhead transcription factors. *Genes Devel.* 14, 142:6.
- Wada, K., Howard, J.T., McConnell, P., Whitney, O., Lints, T., Rivas, M.V., Horita, H., Patterson, M.A., White, S.A., Scharff, C., *et al.* (2006). A molecular neuroethological approach for identifying and characterizing a cascade of behaviorally regulated genes. *Proc. Natl. Acad. Sci. USA* 103, 15212-7.
- Spiteri, E., Konopka, G., Coppola, G., Bomar, J., Oldham, M., Ou, J., Vernes, S.C., Fisher, S.E., Ren, B., and Geschwind, D.H. (2007). Identification of the transcriptional targets of FOXP2, a gene linked to speech and language, in developing human brain.

Am. J. Hum. Gen. 81, 1144-1157.

Vernes, S.C., Spiteri, E., Nicod, J., Groszer, M., Taylor, J.M., Davies, K.E., Geschwind, D.H., and Fisher, S.E. (2007). High-throughput analysis of promoter occupancy reveals direct neural targets of FOXP2, a gene mutated in speech and language disorders. Am. J. Hum. Gen. 81, 1232-1250.

Vernes, S.C., Oliver, P.L., Spiteri, E., Lockstone, H.E., Puliyadi, R., Taylor, J.M., Ho, J., Mombereau, C., Brewer, A., Lowy, E., et al. (2011). Foxp2 regulates gene networks implicated in neurite outgrowth in the developing brain. PLoS Genetics. 7:e1002145.

Konopka, G., Bomar, J.M., Winden, K., Coppola, G., Jonsson, Z.O., Gao, F.Y., Peng, S., Preuss, T.M., Wohlschlegel, J.A., and Geschwind, D.H. (2009). Human-specific transcriptional regulation of CNS development genes by FOXP2. Nature 462, 213-289.

Enard, W., Gehre, S., Hammerschmidt, K., Holter, S.M., Blass, T., Somel, M., Bruckner, M.K., Schreiweis, C., Winter, C., Sohr, R., et al. (2009). A humanized version of Foxp2 affects cortico-basal ganglia circuits in mice. Cell 137, 961-971.

Huang, D.W., Sherman, B.T., Lempicki, R.A. (2009). Systematic and integrative analysis of large gene lists using DAVID Bioinformatics Resources. Nature Protoc. 4(1):44-57.

Cahoy, J.D., Emery, B., Kaushal, A., Foo, L.C., Zamanian, J.L., Christopherson, K.S., Xing, Y., Lubischer, J.L., Krieg, P.A., Krupenko, S.A., et al. (2008). A transcriptome database for astrocytes, neurons, and oligodendrocytes: a new resource for understanding brain development and function. J. Neurosci. 28, 264–278.

Halassa, M.M., Haydon, P.G. (2010). Integrated brain circuits: astrocytic networks modulate neuronal activity and behavior. Ann. Rev. Physiol. 72, 335-55.

Nottebohm, F. (2004). The road we travelled – Discovery, choreography, and significance of brain replaceable neurons. Ann. NY Acad. Sci. 1016, 628-658.

Kim, Y.H., Perlman, W.R., Arnold, A.P. (2004). Expression of androgen receptor mRNA in zebra finch song system: developmental regulation by estrogen. J Comp Neurol. 469, 535-47.

Farries, M.A., and Perkel, D.J. (2002). A telencephalic nucleus essential for song learning contains neurons with physiological characteristics of both striatum and globus pallidus. J. Neurosci. 22, 3776-3787.

Reiner, A., Perkel, D.J., Bruce, L.L., Butler, A.B., Csillag, A., Kuenzel, W., Medina, L., Paxinos, G., Shimizu, T., Striedter, G., et al. (2004). Revised nomenclature for avian telencephalon and some related brainstem nuclei. J. Comp. Neurol. 473, 377-414.

Herz, J. and Chen, Y. (2006). Reelin, lipoprotein receptors and synaptic plasticity. *Nat. Rev. Neurosci.* 7, 850-859.

Balthazart, J., Voigt, C., Boseret, G., Ball, G.F. (2008). Expression of reelin, its receptors and its intracellular signaling protein, Disabled1 in the canary brain: Relationships with the song control system. *Neuroscience* 153, 944–962.

Hosono, K., Noda, S., Shimizu, A., Nakanishi, N., Ohtsubo, M., Shimizu, N., and Minoshima, S. (2010). YPEL5 protein of the YPEL gene family is involved in the cell cycle progression by interacting with 2 distinct proteins RanBPM and RanBP10. *Genomics* 96, 102-111.

Musella, A., De Chiara, V., Rossi, S., Prosperetti, C., Bernardi, G., Maccarrone, M., Centonze, D. (2009). TRPV1 channels facilitate glutamate transmission in the striatum. *Mol. Cell. Neurosci.* 40, 89-97.

Maccarrone, M., Rossi, S., Bari, M., De Chiara, V., Fezza, F., Musella, A., Gasperi, V., Prosperetti, C., Bernardi, G., Finazzi-Agrò, A., et al. (2008). Anandamide inhibits metabolism and physiological actions of 2-arachidonoylglycerol in the striatum. *Nat. Neurosci.* 11, 152-9.

Soderstrom, K., Tian, Q. (2004). Distinct periods of cannabinoid sensitivity during zebra finch vocal development. *Br. Res. Devel. Br. Res.* 153, 225-232.

Thompson, J.A. and Perkel, D.J. (2010). Endocannabinoids mediate synaptic plasticity at glutamatergic synapses on spiny neurons within a basal ganglia nucleus necessary for song learning. *J. Neurophysiol.* 105, 1159-69.

Soderstrom, K., and Luo, B. (2010). Late-postnatal cannabinoid exposure persistently increases FoxP2 expression within zebra finch striatum. *Dev. Neurobiol.* 70, 195-203.

Replogle, K., Arnold, A.P., Ball, G.F., Band, M., Bensch, S., Brenowitz, E.A., Dong, S., Drnevich, J., Ferris, M., George, J.M., et al. (2008). The Songbird Neurogenomics (SoNG) Initiative: community-based tools and strategies for study of brain gene function and evolution. *BMC Genomics* 9, 131.

Li, X., Wang, X.J., Tannenhauser, J., Podell, S., Mukherjee, P., Hertel, M., Biane, J., Masuda, S., Nottebohm, F., Gaasterland, T. (2007). Genomic resources for songbird research and their use in characterizing gene expression during brain development. *Proc. Natl. Acad. Sci. USA* 104, 6834-9.

Langfelder, P., Horvath, S. (2008). WGCNA: an R package for weighted correlation network analysis. *BMC Bioinformatics* 9, 559.

Yip, A.M., and Horvath, S. (2007). Gene network interconnectedness and the

generalized topological overlap measure. *BMC Bioinformatics* 8, 22.

Langfelder, P., Zhang, B., & Horvath, S. (2007). Defining clusters from a hierarchical cluster tree: the Dynamic Tree Cut package for R. *Bioinformatics* 24, 719-720.

Hu, Z., Mellor, J., Wu, J., DeLisi, C. (2004) VisANT: an online visualization and analysis tool for biological interaction data. *BMC Bioinformatics* 5, 17.